

INVESTIGATION OF CARBON FLUX AND SULPHIDE OXIDATION KINETICS DURING PASSIVE BIOTREATMENT OF MINE WATER

Report to the
Water Research Commission

by

Rob van Hille and Neehal Mooruth
Department of Chemical Engineering
University of Cape Town

WRC Report No. 2139/1/13
ISBN 978-1-4312-0491-5

January 2014

Obtainable from

Water Research Commission
Private Bag X03
GEZINA, 0031

orders@wrc.org.za or download from www.wrc.org.za

DISCLAIMER

This report has been reviewed by the Water Research Commission (WRC) and approved for publication. Approval does not signify that the contents necessarily reflect the views and policies of the WRC, nor does mention of trade names or commercial products constitute endorsement or recommendation for use

EXECUTIVE SUMMARY

BACKGROUND

The impact of acid rock drainage (ARD) on South Africa's already threatened water resources is a serious concern. While acid waters emanating from groundwater rebound through the Witwatersrand gold basins has received the majority of the media attention and elicited the strongest response from the authorities, ARD from diffuse sources, primarily associated with coal mining, is likely to impact a far larger area. The traditional chemical and physical interventions are not particularly well suited to these discharges.

There has been a certain amount of research aimed at developing passive and semi-passive systems, specifically suited to the South African context and some of these have been evaluated at demonstration scale, with varying degrees of success. Typically, the components of these processes that target sulphate salinity make use of biological sulphate reduction, often utilising complex organic carbon sources to provide the electron donor. The sulphide product is highly toxic and presents a significant risk to the environment and human health and needs to be carefully managed. The most attractive option is the partial oxidation of sulphide to elemental sulphur, which is stable and has commercial value.

A promising approach to achieving partial oxidation of sulphide to sulphur involves using sulphide oxidising microbes in a floating biofilm. A linear flow channel reactor has been developed at tested and fundamental aspects of the chemistry, microbiology and engineering have been reported (Van Hille *et al.*, 2012 (WRC report 1834/1/12)). The organic carbon flux through the integrated process was identified as having a significant impact overall performance and required further investigation. In addition, a more comprehensive understanding of oxygen mass transport into the biofilm would facilitate further process optimisation.

RATIONALE

The preceding research identified that efficient sulphide oxidation, with the formation of elemental sulphur as the desired product, was dependent on the diffusion of sulphide from the bulk solution and oxygen from atmosphere into the reaction space within the biofilm. There is a limited reaction space where the pH and redox potential are conducive to the partial oxidation of sulphide. In addition the reaction stoichiometry is critical. Too much oxygen or too little sulphide and the reaction proceeds to complete oxidation to sulphate. The partial pressure of oxygen in the atmosphere cannot be controlled so the system depends on the control of oxygen penetration into the biofilm. This is dependent on the structure of the biofilm, which is influenced by its organic carbon content. With the current process flowsheet the provision of organic carbon is dependent of the performance of the upstream sulphate reduction unit. Sustainable performance is dependent on the hydrolysis of the complex organic carbon at a rate sufficient to sustain effective sulphate reduction and provide overflow carbon to the sulphide oxidising unit. The rationale for the research described in this report is to provide a better understanding of the overall carbon flux across the system and the effect this has on biofilm development and the control of oxygen penetration into the reaction zone.

OBJECTIVES AND AIMS

AIMS

The primary aim of the research was to characterise the carbon flux through an integrated sulphate reduction/sulphide oxidation process and determine its effect on the recovery of sulphur in the floating sulphur biofilm. The second aim was to investigate oxygen mass transfer to the biofilm and use this information to inform optimal management of the system.

METHODOLOGY

Two packed bed columns were used to investigate the sulphate reduction efficiency and carbon flux. The effect of packing material and supplementation with simple organic carbon was investigated.

A series of linear flow channel reactors (LFCRs) were used to investigate the effect of residence time and acetate supplementation on sulphide oxidation rate and elemental sulphur yield. The oxygen mass transfer into the biofilm was investigated in a scaled-down reactor, using a dissolved oxygen microprobe. The composition and internal structure of the floating sulphur biofilm was analysed using scanning electron microscopy and elemental analysis. The structure of the biofilm informed the interpretation of the data.

RESULTS AND DISCUSSION

The experimental data allowed the specific aims to be addressed and provided significant insights into the performance of the integrated system.

Aim 1

The packing material and packing configuration had a significant effect on void volume and subsequent hydraulic residence time. Column 1 had a greater proportion of leaf mulch and dry sewage sludge, resulting in a smaller void volume (7.58 l) and lower residence time (1.75 days), while Column 2, which was packed primarily with wood chips, grass and wet sludge had a greater void volume (14.38 l) and residence time (3.33 days).

Of the individual packing material the greatest amount of organic carbon was liberated from the dry sludge, primarily as acetic acid, while butyric acid was liberated from the wood chips after approximately three weeks. Very little organic carbon was liberated from the grass. The results suggested organic carbon liberation would not be sufficient to sustain efficient sulphate reduction in the columns for a prolonged period.

Aim 2

Both packed bed columns showed similar levels of performance over the first two months, with sulphate removal efficiencies of between 50 and 75% (feed sulphate concentration 2 g/l). The performance of Column 2 (molasses supplementation) deteriorated after four months and failed completely within five months, while Column 1 (acetate supplementation) showed sustained sulphate reduction (70-90%) for 12 months. Volatile fatty acids (VFAs) were detected in the column effluents at decreasing concentrations for the first two months, after which no VFAs were detected, despite supplementation of the feed, indicating reduced hydrolysis of the packing material. The failure of Column 2 could be attributed to carbon deficiency.

In the absence of VFAs in the feed to the LFCRs a complete biofilm did not form and performance was poor. Supplementation of the reactor feed with acetate was required for efficient performance. A minimum acetate concentration of 100 mg/l was required. The absence of soluble organic carbon had a profound effect on the microbial community, which lacked many of the heterotrophic organisms required for biofilm development.

Aim 3

The performance of the sulphate reducing community was not negatively affected by catechol or gallic acid (low molecular weight phenolic compounds) at concentrations up to 100 mg/l, although complete inhibition was observed with both compounds at 1000 mg/l. The concentration of these compounds is highly unlikely to reach inhibitory levels within a packed bed reactor.

Aim 4

The mass transfer of oxygen into the reaction zone within the biofilm was shown to be significantly inhibited as the biofilm developed and more sulphur was deposited, although the rate depended on the operating conditions, particularly hydraulic residence time (HRT). The calculated mass transfer coefficient was shown to decrease by almost three orders of magnitude, from 1.64×10^{-4} m/s to 3.63×10^{-7} m/s over a five day period of biofilm development (one day HRT). From a performance perspective, the rate of sulphide oxidation peaked after two to three residence times and then decreased significantly, due to oxygen limitation. However, inhomogeneity in biofilm structure and uncertainty over a porosity factor precluded the development of an accurate mass transfer model.

GENERAL

The experiments showed that efficient sulphide oxidation was possible within the floating sulphur biofilm in the LFCR, provided the feed was supplemented with organic carbon. A hydraulic residence time between one and two days was optimal. In order to sustain optimal performance the biofilm would need to be harvested every two to three residence times. Under these conditions sulphide oxidation rates of up to 5.5 mmol/l.day could be achieved, with at least 75% of the oxidised sulphide reporting to the biofilm as elemental sulphur. Conservatively, this represents a sulphur recovery of 13.5 g/m².day, for the current reactor configuration.

CONCLUSIONS

The experimental programme illustrated that organic carbon liberation from packed bed reactors is unlikely to be sufficient to sustain efficient levels of sulphate reduction beyond the short term, once the readily labile organic carbon has been liberated. Supplementation with relatively significant (1 g/l) concentrations of readily usable organic carbon, such as acetate, was needed to sustain sulphate reduction. While the majority of the sulphate reduction ($\pm 75\%$) was reliant on the acetate, continued hydrolysis of the lignocellulose was observed. Despite this, the VFA concentration in the effluent from the packed bed reactors was negligible after the first four months. Therefore, further organic carbon supplementation (> 100 mg/l acetate) of the feed to the LFCR was necessary for biofilm development and efficient sulphide oxidation.

Under optimal conditions the biofilm formed within 12 hours, following which the oxygen mass transfer into the liquid was significantly reduced (k_f from 1.65×10^{-4} m/s to 2.35×10^{-6} m/s between 24 and 48 hours). The reduced mass transfer prevented complete sulphide oxidation, so the majority of the sulphide was oxidised to sulphur within the biofilm. The HRT and sulphide loading affected the rate of formation and structure of the biofilm, influencing performance. Optimal performance was achieved at an HRT between one and two days. Harvesting of the biofilm would be required every two to three residence times to maintain optimum sulphide oxidation rates.

RECOMMENDATIONS FOR FUTURE RESEARCH

The current research illustrated that floating sulphur biofilm could achieve efficient sulphide oxidation and sulphur recover, using the linear flow channel reactor. However, the current packed bed sulphate reducing reactor could not provide the necessary organic carbon to sustain biofilm regeneration in the long term. Therefore, the design of systems that integrate the floating sulphur biofilm unit into the overall process will need to be reconsidered, in order to ensure the required carbon flux. In addition, an effective method for biofilm harvesting and sulphur recover needs to be developed.

ACKNOWLEDGEMENTS

The authors would like to thank the Reference Group of the WRC Project K5/2139//3 for the assistance and the constructive discussions during the duration of the project:

Dr J Burgess	Water Research Commission
Prof J Maree	Tshwane University of Technology
Mr N Lesufi	Chamber of Mines
Mr P Günther	Anglo American
Dr R Heath	Golder Associates
Mrs R Mühlbauer	BHP Billiton / Anglo American
Ms K Slatter	Anglo Platinum
Mr J Beukes	Coaltech

TABLE OF CONTENTS

EXECUTIVE SUMMARY.....	I
ACKNOWLEDGEMENTS	IV
TABLE OF CONTENTS	V
LIST OF FIGURES	VII
LIST OF TABLES	XI
LIST OF ABBREVIATIONS.....	XII
1 INTRODUCTION AND OBJECTIVES	1
1.1 Biological sulphate reduction.....	1
1.1.1 Bioreactor configurations for sulphate reduction	1
1.1.2 Effect of pH, redox potential and temperature	1
1.1.3 Direct organic substrates	4
1.1.4 Indirect organic substrates.....	4
1.1.5 Sulphate reducing bacteria	8
1.2 Sulphide chemistry and biological sulphide oxidation	11
1.3 Biofilms.....	11
1.3.1 Biofilm structure	12
1.3.2 Floating biofilms.....	12
1.3.3 Mass transport and transfer limitations.....	14
1.4 Research motivation.....	15
2 MATERIALS AND METHODS	17
2.1 Microbial cultures	17
2.2 Batch digestion reactors.....	17
2.3 Packed column reactors.....	18
2.4 Linear flow channel reactors.....	18
2.5 Analytical techniques.....	22
2.5.1 pH	22
2.5.2 Sulphide	22
2.5.3 Chemical oxygen demand	22
2.5.4 Anions	22
2.5.5 Sulphur	23
2.5.6 Volatile fatty acids.....	23
2.5.7 Phenolic compounds	23
2.5.8 Microsensor measurements	23
2.5.9 Scanning electron microscopy.....	24
2.5.10 Elemental composition analysis.....	24
3 EXPERIMENTAL PROCEDURES.....	26
3.1 Characterisation of packing materials	26
3.1.1 Chemical oxygen demand	26
3.1.2 Batch tests to assess digestibility	26
3.2 Contribution of elemental sulphur to chemical oxygen demand value	26
3.3 Effect of phenolic compounds on sulphate reduction	27
3.4 Packed column studies	27
3.4.1 Preparation of packed columns	27
3.4.2 Determination of void volume and hydraulic residence time	28
3.4.3 Inoculation protocol.....	28
3.4.4 Column feed composition	28
3.4.5 Operation and monitoring	29
3.5 Linear flow channel studies	29
3.5.1 Standard operation of the linear flow channel reactors	29

	3.5.2	Determination of the oxygen mass transfer coefficient in the biofilm.....	30
4		RESULTS, TREATMENT OF RESULTS AND DISCUSSION	31
	4.1	Characterisation of packing materials	31
	4.1.1	Chemical oxygen demand	31
	4.1.2	Digestibility of the packing materials.....	31
	4.2	Effect of phenolic compounds of sulphate reducing performance.....	35
	4.2.1	Catechol	35
	4.2.2	Gallic acid	37
	4.3	Packed column performance.....	40
	4.3.1	Overall performance	40
	4.4	Linear flow channel studies	50
	4.4.1	Definition of pseudo-steady-state	50
	4.4.2	Summary of the reactor hydrodynamics	50
	4.4.3	Overall performance and species balance	52
	4.4.4	Sulphide oxidation rate	54
	4.4.5	Relationship between residence time and sulphur yield.....	57
	4.4.6	Relationship between residence time and complete oxidation of sulphide...	59
	4.4.7	Carbon species material balance	60
	4.4.8	Floating sulphur biofilm analysis.....	61
	4.4.9	Analysis of biofilm structure	62
	4.4.10	Conceptual model for biofilm formation and maturation	68
	4.4.11	Dissolved oxygen profiles through the floating biofilms	70
	4.4.12	Measurement of oxygen mass transfer coefficient	72
5		CONCLUSIONS	75
6		RECOMMENDATIONS.....	75
7		LIST OF REFERENCES	77

LIST OF FIGURES

Figure 1: Potential-pH diagram for a sulphur/water system and 298.15K.....	11
Figure 2: Simplified schematic diagram of the LFCR with an FSB and air penetrating the FSB (left image). The right hand image shows an expanded view of the air-liquid interface, rotated 90° to the right, showing the bulk gas layer, laminar gas film, FSB layer and bulk liquid layer. The trend in dissolved oxygen concentration gradient across all layers is shown. The figure is not to scale.....	15
Figure 3: Example of a reactor used for the batch digestions reactions showing the overall dimensions and location of the sampling ports.....	17
Figure 4: Example of a packed bed column reactor showing the overall dimensions and location of the feed and effluent ports.....	18
Figure 5: Schematic of the top view of the entire LFCR, divided into three sections, showing the specific dimensions and spacing of the holes for placement of the cylindrical baffles ..	19
Figure 6: Schematic drawing of the front and rear wall of the LFCR, showing the position of the three possible inlet/outlet ports for liquid and the gas inlet/outlet.....	20
Figure 7: Schematic diagram showing the location of the 15 sampling ports in the front wall.....	21
Figure 8: Schematic representation of the packed column reactors, showing dimensions, packing arrangements and relative mass fractions	27
Figure 9: pH data of batch bioreactors in VFA liberation kinetics study.....	31
Figure 10: Volatile fatty acids cumulative concentration within bioreactor 1 containing 20 g of wood chips	32
Figure 11: Volatile fatty acids cumulative concentration within bioreactor 2 containing 20 g of grass.....	33
Figure 12: Volatile fatty acids cumulative concentration within bioreactor 3 containing 20 g of dry sewage sludge	34
Figure 13: Volatile fatty acids cumulative concentration within bioreactor 4 containing 20 g of spent brew malt	34
Figure 14: Effect of increasing concentrations of catechol (0-1000 mg/l) on the rate of sulphide generation in batch sulphate reduction tests.....	36
Figure 15: Solution pH measured in the batch sulphate reducing reactors subjected to increasing concentrations (0-1000 mg/l) of catechol.....	37
Figure 16: Solution redox potential (mV) measured in the batch sulphate reduction reactors challenged with increasing concentrations (0-1000 mg/l) of catechol.....	37
Figure 17: Effect of increasing concentrations of gallic acid (0-1000 mg/l) on the rate of sulphide generation in batch sulphate reduction tests.....	38

Figure 18: Solution pH measured in the batch sulphate reducing reactors subjected to increasing concentrations (0-1000 mg/ℓ) of gallic acid	39
Figure 19: Solution redox potential (mV) determined in the batch reactors challenged with increasing concentrations of gallic acid	39
Figure 20: Redox potential and sulphide concentration measured in the effluent from Column 1 ..	40
Figure 21: Solution pH in the effluent from the packed column reactors	41
Figure 22: Sulphate concentration in the effluent from the packed column reactors	41
Figure 23: Sulphate removal efficiency, based on measurement of effluent sulphate concentration	42
Figure 24: Redox potential and sulphide concentration measured in the effluent from Column 2 ..	43
Figure 25: Volatile fatty acid concentrations detected in the effluent from Column 1. No VFAs were detected after day 129	44
Figure 26: Volatile fatty acid concentrations detected in the effluent from Column 2. No VFAs were detected after day 111	44
Figure 27: Relationship between the pH and sulphide concentration in the effluent from Column reactor 1. Dotted line represents pH and solid line sulphide concentration.....	45
Figure 28: Colloidal sulphur concentration in the effluent from the column reactors. Circles represent Column 1 data and crosses Column 2	46
Figure 29: Acetic acid balance in Column 1. The discrepancy between the calculated acetic acid required to achieve the measured sulphate reduction and the acetate supplied in the feed represents acetate equivalents liberated from the packing material.....	47
Figure 30: Acetic acid required to achieve the observed sulphate reduction in Column 2 and the measured concentration in the effluent. The sum represents the amount of acetic acid equivalents liberated from the packing material and molasses feed	48
Figure 31: Chemical oxygen demand values of effluent samples from Column 1 and Column 2 over the period January to April 2012. Filtered and unfiltered samples were analysed	49
Figure 32: Relationship between measured colloidal sulphur, measured COD and theoretical contribution to total COD from colloidal sulphur for effluent from Column 1.....	50
Figure 33: Schematic representation of fluid flow regime in the LFCR with various types of flow being displayed accordingly. The sinking influent (green arrows), entrance dead zone (red arrows), laminar parabolic flow (black arrows) and back corner dead zone (orange, maroon, blue arrows) are displayed. The smaller pink arrows represent the movement of fluid in the y-direction due to displacement from below	51
Figure 34: Example of a phenolphthalein tracer experiment showing discolouration of the indicator by the introduction of sulphuric acid into an alkaline solution. The relative density difference between the acid and alkaline solutions were similar to the sulphide feed and bulk liquid during LFCR operation.....	52

Figure 35: Mean daily sulphide oxidation rates across the LFCR for experimental runs 8 and 9. Experiments run at a 4 day HRT and sulphide loadings of 33.6 and 29.7 mmol/d respectively	55
Figure 36: Mean daily sulphide oxidation rates across the LFCR for experimental runs 13, 14 and 16. Runs 13 and 14 were performed at a 1 day HRT and sulphide loadings of 122.8 and 111.5 mmol/d respectively, while runs 16-(1) and 16-(2) were consecutive, separated by a biofilm harvest. Sulphide loading rates were 98.9 and 111.9 mmol/day respectively	56
Figure 37: Feed and effluent sulphide and colloidal sulphur concentrations (mM) for the duration of experimental run 14.....	56
Figure 38: Feed and effluent sulphide and colloidal sulphur concentrations (mM) for the duration of experimental run 10.....	57
Figure 39: Relationship between sulphur yield and residence time for the series of LFCR experiments. The two points in the bottom left quadrant were omitted when determining the relationship	58
Figure 40: Relationship between residence time and complete oxidation of sulphide to sulphate. The sulphate produced value excludes the oxidation of colloidal sulphur in the reactor feed	60
Figure 41: Relative proportion of elemental sulphur (○) versus organic carbon (×) and inorganic salts in the FSBs harvested at the end of each experimental run	62
Figure 42: Rhombic sulphur crystals attached to the underside of the biofilm showing evidence of chemical sulphide oxidation.....	63
Figure 43: Cross-sectional SEM of part of the biofilm sampled from experimental run 12 (two day residence time). The biofilm thickness is annotated on the image. Discrete layers are clearly visible, as are areas of dense sulphur deposition (bright white).....	64
Figure 44: Cross-sectional SEM images of biofilm sampled from experimental runs 14 (a) and 16 (2) (b) showing discrete layers and areas of dense sulphur deposition	64
Figure 45: Cross-sectional SEM illustrating how parallel layers within the biofilm could be held together by EPS strands. The strands are between 1-2 µm long.....	65
Figure 46: Cross-sectional SEM image of biofilm sampled from experimental run 8 (four day residence time) showing porous structure. The biofilm is inverted with the lower edge representing the upper surface.....	66
Figure 47: Relationship between FSB thickness and residence time, with the maximum thickness achieved at residence times between one and two days	66
Figure 48: Scanning electron micrographs of the underside of the biofilm showing (a) the immobilisation of cells within the EPS matrix and (b) morphological diversity	67
Figure 49: Scanning electron micrographs of the biofilm from (a) run 12 and (b) run 13, showing the presence of pod-shaped macrostructures.....	67

Figure 50: Scanning electron micrograph showing the topography of an individual pod (main image). The insert is a density scatter image of the same pod clearly showing the presence of sulphur granules within the pod	68
Figure 51: Conceptual model of floating sulphur biofilm formation. The upper image (1) describes the first 12 hours. The inset image at the top right illustrates the colloidal sulphur layer. The middle image (2) depicts the processes occurring during the establishment of pseudo-steady-state, while the lower image depicts the process occurring during the formation of a new layer	69
Figure 52: Photograph illustrating the apparatus used to determine the DO profile through the biofilm. The newly formed and mature biofilm (five day old) sections are clearly visible	71
Figure 53: Dissolved oxygen profile through the FSB, as a function of position and time. Data from experimental run 13 (one day RT).....	71
Figure 54: Dissolved oxygen profiles through the FSB operated at a one day residence time, measured on days 1-5.....	73
Figure 55: Calculated oxygen diffusion coefficients in the FSB as a function of biofilm age for experimental runs 11-15.....	74
Figure 56: Summary of operating conditions and overall performance of the integrated system under optimised conditions. The relatively low total sulphur species removal is due to the persistence of colloidal sulphur and sulphate in the effluent from the SRB column.....	76

LIST OF TABLES

Table 1: Comparison of active and passive biological sulphate reducing systems	3
Table 2: Diversity and morphological features of cellulolytic microbes (Lynd <i>et al.</i> , 2002; Roman, 2004)	7
Table 3: Morphological and physiological characteristics of selected genera and strains of sulphate reducing bacteria (Adapted from Dworkin <i>et al.</i> , 2006).....	10
Table 4: Composition of synthetic ARD feed. Feed was adjusted to pH 6.1-6.5 with NaOH	28
Table 5: Summary of experimental conditions during LFCR channel experiments	29
Table 6: Summary of density and COD of dried organic packing materials	31
Table 7: Summary of results from the batch digestability tests. Total VFA and soluble COD data represent final values at the end of the experiment.....	32
Table 8: Summary of overall performance and distribution of sulphur species for the biological LFCR experiments	53
Table 9: Acetate material balance for the LFCR experimental runs 11-16	61
Table 10: Elemental composition of the FSB from experiments 8 to 16 (2). The sulphur content represents elemental sulphur and excludes sulphate salts	62
Table 11: Exponential functions fitted to the dissolved oxygen concentration data for days 1-5. In addition, the goodness of fit and respective functions' derivatives are presented, as well as the calculate diffusion and local mass transfer coefficients.....	72

LIST OF ABBREVIATIONS

AD	anaerobic digestion
ARD	acid rock drainage
BESA	bromoethane sulphonic acid
BSR	bacterial sulphate reduction
CeBER	Centre for Bioprocess Engineering Research
COD	chemical oxygen demand
CSTR	continuous stirred tank reactor
DF-PBR	down-flow packed bed reactor
DO	dissolved oxygen
DOC	dissolved organic carbon
DPBR	degrading packed bed reactor
EPS	extracellular polymeric substance
FSB	floating sulphur biofilm
GAA	Golder Associates Africa
GC	gas chromatography
HPLC	high performance liquid chromatography
HRT	hydraulic residence time
LFGR	linear flow channel reactor
PBS	phosphate buffered saline
PSS	pseudo-steady-state
PVC	polyvinyl chloride
RDD	relative density difference
SCOD	soluble chemical oxygen demand
SEM	scanning electron microscopy
SEM-EDX	scanning electron microscopy energy dispersive X-ray spectroscopy
SRB	sulphate reducing bacteria
SRBR	sulphate reducing bioreactor
TCOD	total chemical oxygen demand
UASB	up-flow anaerobic sludge blanket
UF-PBR	up-flow packed bed reactor
VFA	volatile fatty acid

1 INTRODUCTION AND OBJECTIVES

The research presented in this report focuses primarily on the organic carbon flux through an integrated semi-passive process for treating acid rock drainage (ARD), specifically on the effect this has on the performance of the sulphate reducing and downstream sulphide oxidation units. The second major focus is the relationship between oxygen mass transfer into the floating sulphur biofilm and sulphide oxidation efficiency and how operational factors such as hydraulic residence time and availability of organic carbon affect this. A brief literature review, providing context and discussing relevant components of the research is presented below.

1.1 Biological sulphate reduction

For many years sulphate reducing bioreactors (SRBRs) were treated as black boxes, with limited fundamental understanding of the complex chemical and biological processes which occurred within the reactor. This began to change in the late 20th century (Sheoran *et al.*, 2010), resulting in a better understanding of the effect of pH, redox, metal concentration, sulphate concentration, hydraulic residence time, organic substrate loading and most importantly microbial community structure and activity. Sulphate reducing prokaryotes inhabit a variety of environments, such as wetland sediments, cattle rumens and geothermal vents. They may be either heterotrophic or autotrophic and reduce a sulphate ion to sulphide if there is a suitable electron donor available. The organic substrate (electron donor) is oxidised and the sulphate ion (electron acceptor) is reduced (Equation 1).



The energy released is used by the microbe for metabolic activity, growth and development (Sheoran *et al.*, 2010). The sulphide can react with dissolved metals to form metal sulphides or remain in solution.

1.1.1 Bioreactor configurations for sulphate reduction

A variety of reactor configurations have been investigated for application in active systems. These include continuous stirred tank reactors (CSTRs), upflow anaerobic sludge bed reactors (UASBs) and upflow or down flow packed bed reactors. The most common passive reactor configuration is an upflow or down flow packed bed reactor (UF/DF-PBR). The major difference between passive treatment systems and active treatment systems is that passive systems have no mixing or temperature control.

The current study is restricted to a passive system, so active systems will not be discussed in detail. The majority of recent studies on passive treatment have used a packed bed reactor configuration. Typically, the sulphate reduction rate achieved in passive systems is significantly lower than that in active processes, a maximum sulphate reduction rate of 0.31 g/l.day reported (Table 1). The performance of passive treatment systems is heavily reliant on the following parameters: organic substrate and sulphate loading rates, pH/redox potential, metal concentration, temperature and residence time.

1.1.2 Effect of pH, redox potential and temperature

The correct environmental conditions, such as pH, redox potential and temperature are necessary for the biological sulphate reduction process to occur effectively. The majority of known sulphate reducing species are inhibited at low pH, although exceptions exist. Elliot and associates (1998) showed that some sulphate reducers are capable of biological sulphate reduction under acidic conditions (pH 3.25) and achieved a sulphate removal of 38.3%, although the sulphate removal fell

to 14.4% at pH 3. Johnson and Hallberg (2003) and Dopson and Johnson (2012) conducted several studies into the microbial diversity of acidophilic microorganisms and described an acidophilic sulphate reducing consortia, capable of sulphide generation at low pH conditions in a laboratory reactor. These studies represent the exception and the majority of sulphate reducers thrive in pH range from pH 5-8. Outside this range the rate of microbial sulphate reduction decreases rapidly (Sheoran *et al.*, 2010).

An anoxic environment, with a redox potential lower than -100 mV, is essential for treating sulphate rich waters (Sheoran *et al.*, 2010; Cocos *et al.*, 2002). Once sulphate reduction is initiated, the sulphide products help to drive the redox potential down further, with efficiently operating systems typically showing a redox potential below -350 mV.

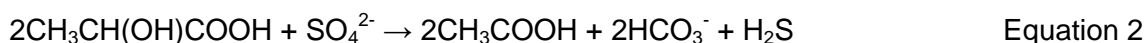
Sulphate reducing species have been identified in environments across a wide range of temperatures (-5°C to 75°C). They may be classified as mesophiles (< 40°C), thermophiles (40-60°C) and extreme thermophiles (> 60°C) based on optimum growth temperatures. Typically, the rate of sulphate reduction increases with temperature to a maximum, then decreases rapidly once the optimum is exceeded. Moosa and co-workers (2002) reported an increase in sulphate reduction rate with an increase in temperature from 20°C to 35°C while a further increase to 40°C resulted in complete inhibition of the mixed SRB culture. At low temperature (< 10°C) the sulphate reduction rate decreases by 50% from an optimum temperature of 20°C. However, some passive bioreactors have been operated successfully between 2°C and 16°C over a period of 32 months (Sheoran *et al.*, 2010). In general the performance of a passive sulphate reducing bioreactor is reduced at low temperatures. However, the sub-optimum temperature also affects the rate of hydrolysis of complex organic substrates. Therefore, the biological sulphate reduction process could be further hampered by lack of soluble chemical oxygen demand (SCOD), due to the hydrolysis reactions being extremely slow.

Table 1: Comparison of active and passive biological sulphate reducing systems

Reactor	Temperature (°C)	Carbon source	SO ₄ concentration (g/l)	SO ₄ reduction rate (g/l.day)	Conversion (%)	COD:SO ₄	Reference
Active	35	Acetate	1.0	0.77	80-90	n.d.	Moosa <i>et al.</i> (2002)
CSTR	-	Tannery effluent	1.8	0.25	60-80	0.1	Boshoff <i>et al.</i> (2004)
CSTR	-	Tannery effluent	1.8	0.60	80	0.56	Boshoff <i>et al.</i> (2004)
UASB	30	Acetate, propionate, butyrate	1.2	0.81	68	0.5	Ormil <i>et al.</i> (1996)
UASB	20	Primary sewage sludge	1.5	1.74	93	1.75	Poinapen <i>et al.</i> (2009)
UASB	35	Primary sewage sludge	1.8	2.42	92	1.45	Poinapen <i>et al.</i> (2009)
UASB	35	Molasses	2.2	1.86	80	15	Annachhatre and Sookrakoolvait (2001)
UF-PBR	25	Lactate	3.8	0.46	82	1.88	Jong and Parry (2003)
Passive							
PBR	25	Whey, cow manure	0.90	0.003	27	n.d.	Christensen <i>et al.</i> (1996)
UF-PBR	25	Mushroom compost, wastepaper sludge, oak chips	0.13	0.102	79	n.d.	Chang <i>et al.</i> (2000)
UF-PBR	25	Wood chips, sawdust	0.24	0.12	32	n.d.	Waybrant <i>et al.</i> (2002)
DF-PBR	25	Wood chips, manure, primary sewage sludge	1.09	0.013	1.8	n.d.	Molwantwa <i>et al.</i> (2010)
Batch	-	Wood chips, leaf compost, poultry manure	3.39	0.06	>95	n.d.	Zagury <i>et al.</i> (2006)
DF-PBR	-	Wood chips, primary sewage sludge, molasses	1.73	0.31	23.5	0.75 (SCOD)	Coetser <i>et al.</i> (2005)

1.1.3 Direct organic substrates

Direct organic substrates are compounds that do not require prior processing by other microorganisms and can be utilised immediately by sulphate reducers. These substrates are generally alcohols (ethanol and methanol), organic acids (acetate, lactate, formate) or sugars (glucose and sucrose) (Sheoran *et al.*, 2010). Lactate is theoretically the superior electron donor with respect to its thermodynamic and kinetic properties and amount of biomass and energy produced, compared to acetate, ethanol or methanol. The complete oxidation of one mole of lactate results in the production of three moles of bicarbonate alkalinity (Equations 2 and 3) (Tsukamoto and Miller, 1999; Sheoran *et al.*, 2010; Nagpal *et al.*, 2000; Liamleam and Annachatre, 2007).



The major disadvantages of utilising lactate or ethanol are that most sulphate reducers can only partially oxidise them to acetate and very few sulphate reducers are capable of utilising acetate alone (Sheoran *et al.*, 2010). Another significant factor with lactate is competition for substrate by lactate fermenters reactions (Oyekola, 2008). The most significant disadvantage of direct organic substrates is the cost of the electron donor and BSR treatment processes have been largely confined to niche applications as a consequence (Hulshoff Pol *et al.*, 1998). Tsukamoto and Miller (1999) found that methanol was a more efficient electron donor than lactate in the bioreactor column setup. However, methanol is considerably more expensive than lactate. The choice of organic substrates is of critical importance in a sulphate reduction bioreactor. Hence, many passive SRBRs are designed to utilise indirect, waste organic substrates that are cheap, easily accessible and can be broken down into VFAs. In order for passive treatment to be a viable, long-term, sustainable solution for ARD treatment, the organic substrate has to be a readily available waste material.

1.1.4 Indirect organic substrates

Sulphate reducing bacteria (SRB) are unable to utilise indirect (complex) organic substrates as electron donors, therefore prior decomposition by other microorganisms is required. There is a wide variety of substrates that can be utilised, such as composts (spent mushroom/leaf compost), agricultural by-products (cow, horse, poultry, sheep manure or molasses), cellulosic wastes (grass cuttings, wood chips, straw, hay, sawdust or leaf mulch) and sewage waste (sewage sludge or digested sludge). In order to sustain an SRB community there has to be a sustained release of organic acids from the complex substrates. Therefore, the selection and characterisation of substrates is critical.

1.1.4.1 Characterisation of organic wastes

A number of studies (Christensen *et al.*, 1996; Gibert *et al.*, 2004; Cocos *et al.*, 2002; Sheoran *et al.*, 2010) have concluded that individual waste carbon sources do not promote significant activity of SRB. As a result, a more reactive mixture containing more than one organic carbon source is preferred. The performance of reactors packed with these mixtures is influenced by several factors, such as the degree of liberation of dissolved organic carbon (DOC) and nutrients (N, P). Chang and co-workers (2000) showed better sulphate reduction in reactors packed with spent mushroom compost, spent oak from shiitake farms and wastepaper sludge, than those packed with oak chips or organic rich soil. Their results showed that raw oak contained chemicals that inhibited sulphate reduction. These were hydrophobic in nature and degraded over time. Furthermore, it was determined that biologically or chemically treated/degraded organic substrates

are better electron donors for sulphidogenesis than unaltered substrates such as oak chips or organic rich soil.

Gibert and associates (2004) characterised the composition of lignocellulosic and organic wastes and found that sheep manure had a greater biodegradable fraction (by 20%) than oak leaves. Moreover, sheep manure had a lower lignin and cellulose content, by 7% and 33% respectively. While lignocellulosic wastes (oak leaves) have a greater carbon content and volatile solids fraction, the carbon to nitrogen ratio was lower than organic waste (sheep and poultry manure), which is preferable for long-term BSR. Similarly, compost has a higher lignin and cellulose content with an extremely low biodegradable fraction. As a result, biological sulphate reduction was only observed after the addition of a soluble carbon source such as sodium acetate.

Therefore, waste organic substrates such as sewage sludge, manure or digested sludge are ideal for biological sulphate reduction as these contain more labile and easily biodegradable carbon. In addition, these substrates have a higher nitrogen and phosphorus content than lignocellulosic wastes, which is preferable for long term operation of SRBR. However, only a fraction of the organic wastes are bioavailable for the process of biological sulphate reduction, consequently they are depleted fairly rapidly. Therefore lignocellulosic wastes need to be utilised for long term operation (> 1 year) of a passive SRBR, as they generally have a higher carbon content and the potential to release DOC over a longer period (Waybrant *et al.*, 2002; Cocos *et al.*, 2002; Gibert *et al.*, 2004). However, the primary disadvantage of lignocellulosic wastes is the high lignin, cellulose and hemicelluloses content. These are not easily hydrolysable and ideally need to undergo pre-treatment via biological or chemical methods.

Some studies have shown promising results where sulphidogenesis using cellulosic wastes is supplemented with easily assimilated electron donors (Christensen *et al.*, 1996; Nagpal *et al.*, 2000; Dvorak *et al.*, 1992; Coetser *et al.*, 2005; Molwantwa *et al.*, 2010). The hydrolysis of lignocellulosic material is the rate limiting step with regard to biological sulphate reduction. Therefore, if the rate of hydrolysis can be improved it would greatly improve the performance of a passive SRBR. Nevertheless, all lignocellulosic wastes are not the same, so the data and observations are specific to the substrates utilised and sulphate loading to the reactor.

1.1.4.2 Indirect substrate hydrolysis

Anaerobic digestion (AD) is comprised of four sequential bio-chemical processes. These are hydrolysis, followed by acidogenesis, acetogenesis and methanogenesis. Many studies have concluded that the hydrolysis step is the least well defined and generally also the rate limiting step (Vavilin *et al.*, 2008; Appels *et al.*, 2008). The hydrolysis step breaks down insoluble organic material and high molecular weight compounds, such as carbohydrates, polysaccharides, lipids and proteins into soluble monosaccharides and long chain fatty acids. Thereafter these components are further metabolised into VFAs, by the process of acidogenesis, performed by acidogenic (fermentative) bacteria. This is generally considered the quickest step in the AD process (Vavilin *et al.*, 2008). The third stage, acetogenesis, is where the VFAs and alcohols are digested further by acetogens to produce acetic acid, CO₂ and H₂. The final stage, methanogenesis results in methane production.

Therefore, in order to promote biological sulphate reduction using indirect substrates the time required to hydrolyse these materials needs to be minimised. First-order kinetics can only be applied when the rate-limiting factor (in hydrolysis) is the surface area of the particulate substrate and biodegradability phenomena don't interfere. Vavilin and co-workers (2008) found kinetic coefficients of the first-order rate hydrolysis to vary greatly amongst various substrates. For crop residues it was 0.094 day⁻¹, whilst for forest soil, pig manure and cattle manure were 0.54, 0.1 and 0.13 day⁻¹ respectively. The highest was primary sludge at 0.99 day⁻¹. While these values were

highly dependent on the experimental conditions, inoculum composition and enzyme concentrations they clearly show the stark contrast between lignocellulosic wastes and organic waste materials, with primary sludge being the most ideal. Furthermore, cattle manure and pig manure contain a large proportion of lignocellulosic material, as opposed to primary sludge which has a greater carbohydrate, lipid and protein content.

Organic wastes (sewage sludge, manure)

The hydrolysis of primary sewage sludge and activated sewage sludge has been investigated by several researchers. Andreasen and associates (1997) observed that 9-16% of the total COD (TCOD) could be released as soluble COD (SCOD) during primary sludge fermentation, but this dropped to 2.5% for activated sludge. Similarly, Ucisik and Henze (2008) found that the hydrolysis of primary sewage sludge yielded approximately 16% SCOD, but only between 1.93-5.6% for activated sludge, in a semi-continuous reactor over a period of five days. Furthermore, there was a 4.4 fold increase in the production of VFAs from primary sewage sludge relative to activated sludge, with a higher proportion of acetate being formed from primary sewage sludge hydrolysis (50%), whilst a greater proportion of propionate (35%), butyrate (10%) and longer chain VFAs (25%) were formed from activated sludge hydrolysis. They proposed that the higher production of VFAs from primary sewage sludge was due to the higher proportion of organic constituents, in the form of proteins and carbohydrates. Additionally, the higher organic content gave rise to a higher bacterial activity and consequently a higher concentration of hydrolytic enzymes. Conversely most of the TCOD in activated sludge is in the form of polymers or large organic compounds. However, the primary reason for low SCOD liberation is the inaccessibility of the organic material due to the accumulation of cellular residues and inert materials within the activated sludge matrix. These are generally regarded as non-biodegradable. Anaerobic digestion of sewage sludge is also affected by pH, with the optimum between pH 7-11, in order to promote hydrolysis of proteins, carbohydrates and lipids to form VFAs. The alkaline pH results in the dissociation of acidic groups in the extracellular polymeric substances (EPS) and repulsion between the negatively charged EPS. Extracellular polymeric substances are largely composed of proteins and carbohydrates and thus the solubility of proteins and carbohydrates is increased due to the repulsive forces (Chen *et al.*, 2007b).

Therefore, a study comparing a passive SRBR packed with more organic waste versus one with lignocellulosic wastes is required in order to adequately evaluate the performance a SRBR over the long term. Furthermore, primary sewage sludge will be compared to activated sewage sludge to determine the biodegradability and liberation of VFAs.

Lignocellulose wastes (wood chips, grass and leaves)

The conversion of cellulosic biomass to alternative organic compounds, such as ethanol for transportation fuel or VFAs for bioreactor processes, has received substantial interest recently, as it is relatively cheap and abundant. The overriding impediment to a more widespread utilisation of this natural, sustainable resource is the inability to overcome the recalcitrance of cellulosic materials (Lynd *et al.*, 2002; Weimer *et al.*, 2009). Considerable effort has been directed toward understanding the rumen ecosystem of ruminant animals, which is arguably the most elegant system able to effectively hydrolyse and ferment cellulosic matter to produce predominantly VFAs. This is performed by the complex rumen community that has been shown to consist of bacteria, fungi and protozoa (Lee *et al.*, 2000). However, bacteria are believed to play the major role because of their numerical predominance and metabolic diversity, with fermentative bacteria being responsible for hydrolysis and acidogenesis. These bacteria produce the necessary enzymes to hydrolyse organic compounds such as cellulose, hemicellulose and others into smaller molecular carbon chain compounds (Roman, 2004).

Lignocellulosic materials are composed of lignin, cellulose and hemicelluloses, which forms a three dimensional structure that renders cellulose and hemicellulose less accessible to microbial attack, due to the physical barrier imparted by the lignin. Lignin is an aromatic polymer that provides cell walls with rigidity, in addition to making the plant resistant to enzyme, microbial or mechanical stresses. The substituents are connected by both ether and carbon-carbon linkages. It is essentially composed of three building blocks: p-coumaryl alcohol, coniferyl alcohol and sinapyl alcohol.

To achieve the complete degradation of these polysaccharides a suite of (bacterial) hydrolytic enzymes, which have been shown to target different linkages in the molecules are required (Roman, 2004). There is a distinct difference between aerobic and anaerobic microorganisms in their strategy to hydrolyse cellulose (Table 2). Aerobic cellulolytic bacteria (e.g. *Cellulomonas*, *Cytophaga* and most fungi) can generally utilise a variety of carbohydrates, proteins, lipids and cellulose. On the other hand anaerobic cellulolytic species (e.g. *Clostridium*, *Ruminococcus* and *Fibrobacter*) are more limited and are only able to grow on cellulose and its hydrolytic products. Aerobic organisms produce a vast amount of individual enzymes that have a strong synergy in the hydrolysis of cellulose. Conversely, anaerobes don't release a large amount of extracellular cellulase, but instead have a localised multi-enzyme cellulase complex on the surface of the cell or the cell-glycocalyx matrix (Lynd *et al.*, 2002). Therefore, cell attachment and adhesion to the substrate is necessary. Due to the crystalline nature of cellulose, attachment is only possible at an irregularity in the structure, where amorphous cellulose is present. This allows the adhesion and penetration of cellulolytic enzymes. There are three major types of enzymatic activities which occur synergistically and simultaneously. Endoglucanases, which hydrolyse β -1,4-bonds randomly within the cellulose molecule, producing reducing and non-reducing ends, exoglucanases, which cleave cellobiose from the non-reducing ends of the polymer and β -glucosidases, which hydrolyse cellobiose producing glucose monomers (Roman, 2004). Anaerobic cellulolytic bacteria follow a similar process except that a cellulosome allows close proximity between the bacterial cell wall and cellulose substrate to be constantly maintained during the enzymatic process.

Table 2: Diversity and morphological features of cellulolytic microbes (Lynd *et al.*, 2002; Roman, 2004)

Genus	Growth temperature	Morphology	Features of cellulases
<i>Acetovibrio</i>	Mesophile	Curved rod	Complexed
<i>Anaerocellum</i>	Thermophile	Rod	Non complexed/extracellular
<i>Butyrivibrio</i>	Mesophile	Curved rod	Non-complexed
<i>Caldicellulosiuptor</i>	Thermophile	Rod	Non complexed/extracellular
<i>Clostridium</i>	Mesophile/thermophile	Rod	Complexed
<i>Eubacterium</i>	Mesophile	Rod	
<i>Fibrobacter</i>	Mesophile	Rod	Complexed
<i>Halocella</i>	Mesophile	Rod	Non-complexed
<i>Ruminococcus</i>	Mesophile	Coccus	Complexed
<i>Spirochaeta</i>	Thermophile	Spiral	Non-complexed
<i>Thermotoga</i>	Thermophile	Rod	

Anaerobic (cellulolytic) microorganisms, possessing this cellulosome are generally found within a complex community of interacting (fermentative) anaerobic microorganisms. In an anaerobic, sulphidogenic environment, with inorganic electron acceptors (Fe^{3+} , SO_4^{2-}), cellulose is degraded to ultimately form CO_2 , H_2O and CH_4 . However, within a sulphidogenic environment methanogenesis can be inhibited by a high sulphide concentration and SRBs are able to dominate the methanogens. Furthermore, it has been shown that the degradation of lignocellulosic materials under sulphidogenic conditions is two times faster than under methanogenic conditions (Pareek *et al.*, 1998).

Recent years have witnessed an increasing interest in the enzymatic biodegradation of lignin, hemicellulose and cellulose. The most common enzymes associated with the degradation of these

compounds are lignin peroxidase, endo-xylanase and cellobiohydrolase respectively (Van Dyk and Pletschke, 2012). These enzymes are generally found in white-rot fungi such as *Phaenerochaete chrysosporium* or *Coriolus versicolor*, or in ruminant bacteria (Wan and Li, 2012). However, the biodegradation of lignin compounds also results in the production of phenolic compounds, such as catechol, phenol, gallic acid and ferulic acid, which are toxic to rumen bacteria (Jeffries, 1994; Roman, 2004).

Therefore, from a fundamental perspective the degradation of lignocellulosic materials within a passive sulphate reducing bioreactor is possible, with VFAs being generated for the BSR reaction. While this would occur at a significantly lower rate than for organic waste substrates, VFA production would last considerably longer.

1.1.5 Sulphate reducing bacteria

Until the early 1980s, it was believed that SRBs were only able to utilise electron donors such as hydrogen, ethanol, formate, lactate, pyruvate, malate and succinate for growth. These particular organisms were able to incompletely oxidise these compounds to acetate. However, Widdel (1988) isolated and characterised a large number of sulphate reducers that were able to grow on short-chain fatty acids (acetate), long-chain fatty acids and aromatic compounds, such as phenol. As a result SRB are classified into two broad groups, those that degrade organic compounds incompletely to acetate and those that completely metabolise them to carbon dioxide. Sulphate reducers use sulphate as the terminal electron acceptor and an organic compound (or H₂) as the electron donor. However, SRBs are also able to reduce other compounds such as SO₃²⁻, S₂O₃²⁻, Fe³⁺, Cr⁶⁺, Se⁶⁺ and As⁶⁺. Based on comparative 16S rRNA sequences, most sulphate reducers belong to 23 genera within the δ -proteobacterium class, followed by gram-positive SRB within the Clostridia (Muyzer and Stams, 2008). The most well characterised sulphate reducers, along with their morphological and physiological characteristics are summarised in Table 3. It is evident that the average optimum temperature is 30°C and almost every organism is able to utilise sulphate, sulphite and thiosulphate as an electron acceptor. *Desulfovibrio* and *Desulfobulbus* are unable to utilise acetate, but are able to use lactate for BSR. *Desulfovibrio sulfodismutans* is also able to grow by disproportionation of a sulphur species. It is able to utilise thiosulphate, sulphite, and elemental sulphur (Dworkin *et al.*, 2006).

Desulfobacterium, *Desulfococcus*, *Desulfosarcina* and *Desulfotomaculum* are able to use almost all organic compounds, especially longer chain fatty acids, greater than three carbons. The incomplete oxidation of even C-fatty acids yields only acetate. The odd C-fatty acids yield acetate and propionate by β -oxidation. In the case of odd C-fatty acids, propionyl-CoA and acetyl-CoA is produced, but propionyl CoA cannot be metabolised by an incomplete SRP oxidiser and therefore is excreted. If 2-methylbutyrate is used by an incomplete oxidiser, propionate is formed as well. Most complete oxidisers can degrade the propionyl residue. Therefore, SRBs are able to utilise a variety of organic compounds in addition to phenyl substituted organic acids and phenolics (Dworkin *et al.*, 2006).

Various sulphate reducing prokaryotes are able to utilise phenolic compounds as the electron donor for BSR. Harms and co-workers (1999) identified two strains m-XyS1 and o-XyS1, which showed highest similarity to *Desulfococcus multivorans* (86.9%) and *Desulfosarcina variabilis* (98.7%) respectively. Strain m-XyS1 was able to utilise m-xylene, toluene, m-methylbenzoate, benzoate and m-ethyltoluene. Strain o-XyS1 was able to degrade o-xylene, toluene, o-methylbenzoate, benzoate and o-ethyltoluene. These studies were conducted up to a loading concentration of approximately 100 mg/l of each aromatic compound and showed positive biological sulphide generation. Likewise, Schnell and co-workers (1989) showed that strain Cat2 was capable of degrading phenol, catechol, m-cresol, p-cresol and many others. However, these studies did not determine the maximum inhibitory concentration for SRBs and the process of

biological sulphate reduction. This information is crucial to the performance of an SRBR which is primarily provided with lignocellulosic materials as the organic substrate. If sufficient quantities of phenolic and aromatic compounds are produced via hydrolysis then it could inhibit the BSR process.

Table 3: Morphological and physiological characteristics of selected genera and strains of sulphate reducing bacteria (adapted from Dworkin *et al.*, 2006)

Genus	Morphology	Optimum T°C	e ⁻ acceptors	Electron donors				
				Acetate	Propionate	Lactate	C _x (x > 3)	Phenyl organic acid
<i>Desulfovibrio</i>	Vibrio	30-38	SO ₄ ²⁻ , SO ₃ ²⁻ , S ₂ O ₃ ²⁻	-	-	+	-	-
<i>Desulfobulbus</i>	Oval/rod	28-39	SO ₄ ²⁻ , SO ₃ ²⁻ , S ₂ O ₃ ²⁻	-	+	+	-	-
<i>Desulfobacter</i>	Oval/vibrio	28-32	SO ₄ ²⁻ , SO ₃ ²⁻ , S ₂ O ₃ ²⁻	+	-	-	-	-
<i>Desulfobacterium</i>	Oval	20-35	SO ₄ ²⁻ , S ₂ O ₃ ²⁻	+	+	+	+	+
<i>Desulfococcus</i>	Sphere	28-36	SO ₄ ²⁻ , SO ₃ ²⁻ , S ₂ O ₃ ²⁻	+	+	+	+	+
<i>Desulfosarcina</i>	Oval	33	SO ₄ ²⁻ , SO ₃ ²⁻ , S ₂ O ₃ ²⁻	+	+	+	+	+
<i>Desulfotomaculum</i>	Straight/curved rod	30-38	SO ₄ ²⁻ , S ₂ O ₃ ²⁻	+	+	+	+	+
<i>Desulfospira</i>	Curved rod	26-30	SO ₄ ²⁻ , SO ₃ ²⁻ , S ₂ O ₃ ²⁻	-	-	+	+	+
<i>Desulfobacula</i>	Rod	28	SO ₄ ²⁻	+	-	+	+	Toluene, p-cresol, benzoate
mXyS1	Rod	30	SO ₄ ²⁻	+	-	+	+	m-xylene, toluene
oXyS1	Rod	32	SO ₄ ²⁻	+	-	+	+	o-xylene, toluene
Cat2	Rod	28	SO ₄ ²⁻	+	-	+	+	Phenol, catechol, m-cresol, p-cresol

1.2 Sulphide chemistry and biological sulphide oxidation

The partial oxidation of sulphide to elemental sulphur, the desired product in the floating sulphur biofilm occurs within a very narrow redox potential and pH window (Figure 1).

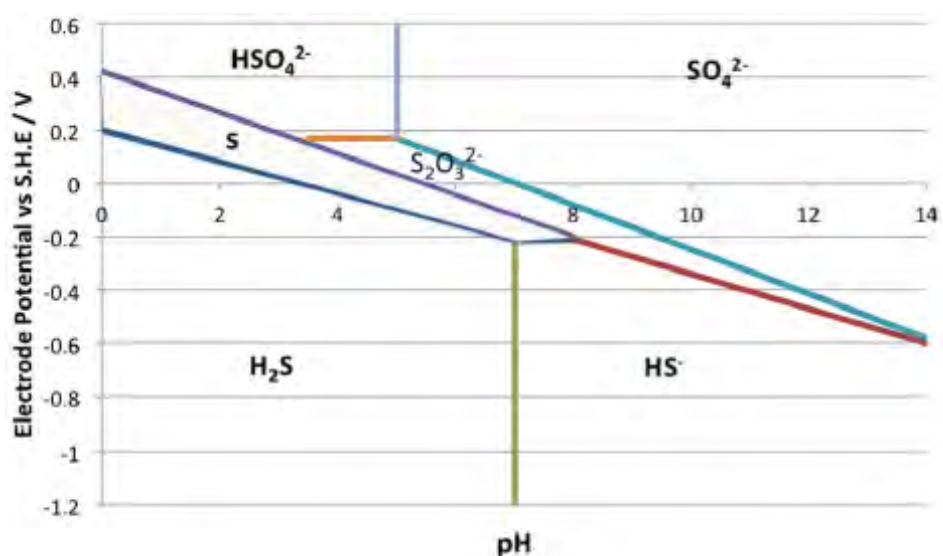


Figure 1: Potential-pH diagram for a sulphur/water system and 298.15K

In addition, the stoichiometric ratio of sulphide to oxygen needs to be maintained 2:1 in order to achieve the desired product. A stoichiometric excess of oxygen will drive the oxidation of both sulphide and elemental sulphur to completion, producing sulphate and acid. From an energetic perspective the complete oxidation of sulphide is far more favourable for sulphur oxidising microbes, so control of oxygen supply is critical.

Sulphide oxidation is a complex process, with competing chemical and biological reactions at play. In addition, these are influenced by pH, redox potential and the presence of other sulphur intermediates. The detailed chemistry will not be reviewed in this report as it has been discussed in detail, for the current experimental system, previously (Van Hille *et al.*, 2012; Mooruth, 2013). The subsequent discussion will focus on biofilms, with specific reference to floating biofilms, and the mass transport and transfer challenges associated with biofilms.

1.3 Biofilms

Since the 1980s, biofilms have become a focal point in the field of water and wastewater treatment, as well as biotechnology. A biofilm is defined as a matrix-enclosed bacterial population, adherent to each other and/or to surfaces or interfaces (Costerton *et al.*, 1995). Microbial biofilms are often involved in the biocorrosion of steel piping, due to SRBs and sulphide oxidising bacteria. Biofilms have also been identified within bioleaching systems and environments. The attachment process to the mineral sulphide surface is largely mediated by an EPS layer. The chemical reactions occur outside of the cells, but still within the EPS-generated microenvironment. Bioleaching is essentially an interfacial process that takes place within this particular microenvironment, which is created by exopolymers and ferric ions to form the EPS layer (Sand and Gehrke, 2006).

Bacteria will initiate biofilm development within an aquatic system if there are sufficient nutrients available for cell replication, as well as EPS production (Costerton *et al.*, 1995; Lazarova and Manem, 1995). Thereafter, the bacteria adhere to the surface, undergo phenotypic changes (alter many of their structural molecules) and derepress EPS synthesis (Costerton *et al.*, 1995), leading

to the development of a microcolony. The microcolony is the basic unit of biofilm growth and these combine to form a biofilm. One of the most important fundamental characteristics of bacterial biofilms is their capacity for focussed and cooperative proliferation. If a particular cell is unable to replicate, due to lack of suitable substrates, it may simply remain dormant, entrapped within the biofilm until conditions improve. Alternatively, if a neighbouring cell is able to provide the substrate, it will utilise the neighbouring cell's by-products. It is these symbiotic relationships and metabolic cooperation that produces extremely complex and heterogeneous biofilms, with vastly intricate metabolic networks (Lappin-Scott and Costerton, 1995; Costerton, 2000). Microbial growth and life within a biofilm is very different to that of planktonic life forms. Bacteria may also form biofilms as a stress response to environmental conditions. This stress could be physical forces, such as shear produced by water flow, nutrient deprivation or the presence of toxic compounds that are inhibitory to bacterial growth (Jefferson, 2004). Additionally, the biofilm matrix provides a safe-haven from predation, which is a common threat from bacterial predators such as amoebae (Costerton, 2007).

1.3.1 Biofilm structure

Biofilms form intriguing microbial systems within the aquatic environment, with characteristic internal architecture. In essence, bacteria produce EPS to facilitate attachment to the substratum, but also the formation and maintenance of the biofilm structure and resistance to environmental stresses. Previous studies (Costerton, 2007; Lawrence *et al.*, 1991; Purevdorj-Gage and Stoodley, 2004; Purevdorj-Gage, 2004; Stoodley *et al.*, 2000) have shown that biofilms are not flat, uniform structures, but rather highly complex heterogenic films, consisting of voids, channels, pores, cell clusters and layers. The biofilm may be made up of thick flat biomasses, organised mushrooms or thin filamentous streamers. It has been hypothesised and observed that the biofilm structure is not a random formation of bacterial cells, but rather an arrangement determined to maximise the influx of nutrients. It is also influenced by a diverse range of physical, chemical and environmental factors which affect the adaptation and growth of the organisms (Costerton *et al.*, 1995). Studies (Lappin-Scott and Costerton, 1995; Bowker, 2002) have shown that different populations are restricted to well-defined depth intervals within the biofilm. Therefore, the structured distribution of various microbial populations within the biofilm is dependent on their role within the general microbial community. The general principle within a microbial community is that the end products of metabolism by one population are utilised as a resource by another. Biofilms therefore may be considered as micro-ecosystems wherein different microbial strains and species efficiently work together for the general wellbeing of the bacterial community. As mentioned earlier the biofilm does consist of voids and pores which facilitate transport of nutrients and water. Therefore the internal structure of the biofilm plays a key role in the mass transport within the film. Biofilms are generally attached to a solid substrate, to provide anchor points and encourage proliferation. However, biofilms may also form on the liquid surface.

1.3.2 Floating biofilms

Most literature has focussed on biofilms which arise from colonisation of solid-liquid interfaces, such as submerged biofilms. However, there are occurrences of floating biofilms in nature. Floating biofilms have been observed on the surface of highly sulphidic tannery wastewater ponds (Molwantwa, 2007).

Floating biofilms are similar in nature to biofilms that are attached to a substrate. The air-liquid interface of an open body of water is an ideal substrate for the development of a biofilm, as there is easy access to gaseous oxygen and nutrients within the liquid medium. The air-liquid interface is an attractive site for aerobic organisms. The biofilms formed by these organisms remain at the air-liquid interface, mainly due to the hydrophobic nature of the organisms rather than their buoyancy (Spiers *et al.*, 2003). All surfaces possess physiochemical characteristics which may influence the adsorption and attachment of bacteria and inevitably the development of a biofilm. The DLVO

theory, originally formulated by Derjaguin and Landau, in 1941, and Verwey and Overbeek, in 1948, equates electrostatic forces and London-van der Waals forces active at the surface with the propensity for colloidal attraction and adhesion (Lappin-Scott and Costerton, 1995). It is generally represented by Equation 4.

$$V_T(L) = V_A(L) + V_R(L) \quad \text{Equation 4}$$

The total interaction energy (V_T) of a particle, as a function of its separation distance (L) from the substrate, is the sum of the Van der Waals attraction force (V_A) and the electrostatic interaction (V_R). The theory predicts that there are two regions where particle attraction may occur, when $L \leq 1 \text{ nm}$ or $10 \text{ nm} \geq L \geq 5 \text{ nm}$. These points in space are known as the primary and secondary minimum respectively and between these two positions the surfaces (bacterium and substratum) experience maximum repulsion (Lappin-Scott and Costerton, 1995). This electrostatic repulsion is primarily due to the fact that the substratum and bacterial cell surface are negatively charged. In this particular case the water surface is negatively charged, which is further exacerbated by the influence of the electrolytic strength of the aqueous medium. If the medium has a high concentration of cations (sodium, calcium, aluminium) and anions (acetate, sulphate, sulphide), this will cause an increase in the ionic strength of the solution, including the surface tension of the water, even though it is still 'dilute'. Weissenborn and Pugh (1996) found that there was a substantial increase in surface tension of water with sodium acetate, magnesium and sodium sulphate (dilute) solutions. This is beneficial as a high surface tension leads to an increase in bacterial adhesion, thus facilitating floating biofilm formation.

The DLVO theory is popular as a theoretical model. However, there are discrepancies between observed and predicted results. The most commonly used (alternative) theory is the surface free energy theory, for describing the surface tension of a surface. This theory is best explained in terms of system free energy. If the total free energy of the system is reduced by cell contact with a surface, then adsorption of the cell to the substratum will occur (Absolom *et al.*, 1983; Lappin-Scott and Costerton, 1995). Therefore, if the free energy function (ΔF_{adh}) decreases, then bacterial adhesion will be favoured. A thermodynamic free energy balance may be developed on the basis of interfacial free energies.

$$\Delta F_{adh} = \gamma_{bs} - \gamma_s - \gamma_{bl} \quad \text{Equation 5}$$

ΔF_{adh} is the free energy of adhesion, γ_{bs} is the interfacial free energy and γ_{bl} is the bacterial-liquid interfacial free energy. Young's equation (Equation 6) describes the relationship between contact angle and interfacial energies of the involved phases. Therefore, if the contact angle is measured then the free energy of adhesion can be determined (Lappin-Scott and Costerton, 1995).

$$\gamma_{sv} - \gamma_{sl} = \gamma_l \cos \theta \quad \text{Equation 6}$$

Absolom and co-workers (1983) were able to show that the adhesion of bacteria from aqueous suspensions to polymeric substrata followed the thermodynamic model to a considerable extent. Furthermore, the determination of the extent of adhesion of bacteria to polymeric substrata provided a method for determining the surface tension of the various bacterial species. The bacteria studied were hydrophilic, with surface tensions in the range of 0.03-0.06 N/m. The surface tension of water in contact with air is approximately 0.072 N/m at 25°C (Perry and Green, 2008). Therefore, the greater upward force of the water's surface tension, which is increased due to the high concentration of dissolved ions, should cause the bacterial floating biofilm to be supported at the air-liquid interface.

1.3.3 Mass transport and transfer limitations

The mass transport of sulphide and oxygen to and within the biofilm will play an important role in the biological oxidation of sulphide. In biofilms at steady-state, a continuity equation (Equation 7) has been found to represent a comprehensive model and provide an accurate description of the nutrient concentration profiles within the biofilm. Equation 7 equates biofilm activity with internal mass transport, assuming constant effective diffusivity and constant biofilm density (Beyenal and Lewandowski, 2002).

$$D_f \frac{d^2C}{dz^2} = \frac{\mu_{max}CX_f}{Y_x(K_s + C)}$$

Equation 7

However, due to the FSB constantly growing and the diffusivity possibly changing, due to the amount of sulphur deposited within the FSB, this equation would not be valid in representing the mass transport through a floating sulphur biofilm. Beyenal and Lewandowski (2002) described the rate of nutrient and sulphide transport to the biofilm and proposed that this may be quantified by linking the convective external mass transfer rate to the diffusive mass transport rate across the biofilm interface. Assuming there is no, or negligible, substrate consumption in the bulk solution, the flux of dissolved substrates must be conserved. Therefore, the external transfer rate ($k_1(C_b - C_s)$) and internal mass transfer rate ($D_f(dC/dz) |_{z=L_f}$) must be equal at the biofilm surface. Hence, the flux of substrates into the biofilm at the surface is:

$$N_S = k_1(C_b - C_s) = D_f \frac{dC}{dz} |_{z=L_f}$$

Equation 8

However, once again this equation is suited to a particular biofilm that is fully submerged and not at an air-liquid interface. Due to the heterogeneous nature of the FSB and the many conduits, the following proposed equation and idealistic model will represent the movement of oxygen downwards into the FSB. However, the concept behind Equation 8 will be followed. The movement of sulphide and nutrients upwards is not considered. The flux of oxygen through the laminar gas-film is represented by the right-hand side of Equation 9, which occurs over a distance of δ_G . The flux of oxygen through the FSB is represented by the equation on the left-hand side and occurs over the thickness of the FSB. This is best represented by Figure 2, which depicts the mass transport of oxygen through the floating sulphur biofilm and shows how both flux equations are equal.

$$N_{O_2} = -D_f \frac{\partial C_{O_2}}{\partial y} \dots \{FSB\}; N_{O_2} = (N_{O_2} + N_{N_2})Y_{O_2} - D_f \frac{P}{RT} \frac{\partial Y_{O_2}}{\partial y} \dots \{Gas - film\}$$

Equation 9

Mass transport within a biofilm is greatly affected by the hydrodynamics of the system. According to de Beer and co-workers (1996) the mass transfer boundary layer was parallel to the substratum at low velocities, however at higher velocities (>0.04 m/s) the boundary layer closely followed the irregular biofilm surface. In addition, the voids within the biofilm enhanced the mass transfer rate and product exchange with the bulk liquid by facilitating convection when the velocity was high enough to ensure the boundary layer was close to the biofilm surface. It was also demonstrated how an increase in the velocity decreased the mass transfer boundary layer above the voids and cell clusters. The oxygen concentration was much greater within the void at a higher velocity (de Beer *et al.*, 1996).

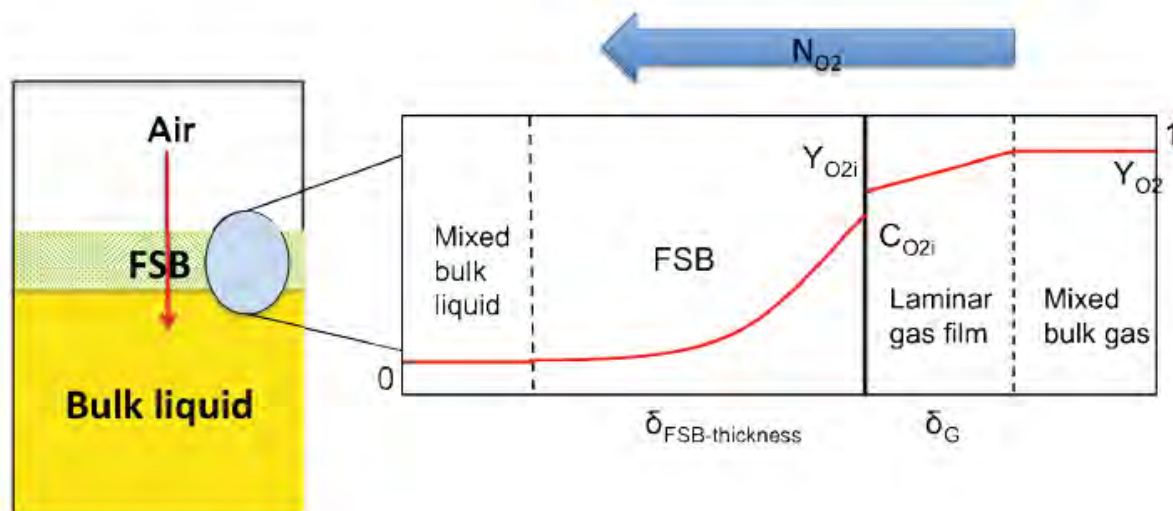


Figure 2: Simplified schematic diagram of the LFCR with an FSB and air penetrating the FSB (left image). The right hand image shows an expanded view of the air-liquid interface, rotated 90° to the right, showing the bulk gas layer, laminar gas film, FSB layer and bulk liquid layer. The trend in dissolved oxygen concentration gradient across all layers is shown. The figure is not to scale.

A biofilm consists of cell clusters and voids, which form a network of channels and allows the lateral movement of fluid within the biofilm. The oxygen distribution is strongly associated to the biofilm structure. de Beer and associates (1994) demonstrated that oxygen was supplied to the cell cluster through the cell cluster-liquid interface. The largest gradient existed at both the cell cluster-pore interface and the cell cluster-bulk liquid interface. It was also determined that the flux from the void to the cell cluster and from the bulk liquid to the cell cluster was of the same order of magnitude, provided the mass transfer boundary layer was thin. However, the conduits below the cell clusters facilitated oxygen transport in the horizontal direction.

The flow velocity at which the biofilm is cultivated also plays an important role in the internal structure of a biofilm. Beyenal and Lewandowski (2002) determined that the flow velocity affected the nutrient transport rate as well as the mechanical pliability of the biofilm structure. When the velocity was too high the biofilm increased its mechanical strength to resist shearing. As a result the density increased and ultimately led to a less porous structure, where the internal mass transfer rate was significantly reduced. Therefore, it will be the aim of this investigation to ascertain to what extent mass transport limitations affect sulphide oxidation within the floating sulphur biofilm.

1.4 Research motivation

The sulphate reducing unit of the integrated, semi-passive system is essentially a packed bed reactor loaded with a large amount of lignocellulosic materials, as the organic carbon substrate. There is limited literature covering the fundamental chemical, biochemical and microbiological reactions that occur within the reactor. In addition, the break-down and hydrolysis of complex organic substrates to sustain biological sulphate reduction over the long-term (> 6 months) has not been studied extensively. Furthermore, each investigation has been unique with respect to the substrates utilised and the ARD waters treated. Therefore, investigating the hydrolysis and release of soluble organic carbon, in the form of VFAs, over the long-term is essential to adequately assess the stability of semi-passive processes. Earlier research (Van Hille *et al.*, 2012) highlighted the importance of a consistent feed to the sulphide oxidation unit, both in terms of sulphide and organic carbon.

The preceding research identified that efficient sulphide oxidation, with the formation of elemental sulphur as the desired product, was dependent on the diffusion of sulphide from the bulk solution and oxygen from atmosphere into the reaction space within the biofilm. There is a limited reaction space where the pH and redox potential are conducive to the partial oxidation of sulphide. In addition the reaction stoichiometry is critical. Too much oxygen or too little sulphide and the reaction proceeds to complete oxidation to sulphate. The partial pressure of oxygen in the atmosphere cannot be controlled so the system depends on the control of oxygen penetration into the biofilm. This is dependent on the structure of the biofilm, which is influenced by its organic carbon content. The relationship between biofilm structure and oxygen mass transfer, particularly how it is affected by biofilm composition and operating conditions, is not well understood. A better understanding of the mechanistic relationship would facilitate further optimisation of the process.

2 MATERIALS AND METHODS

2.1 Microbial cultures

Three microbial cultures were used to inoculate the column reactors during this study. The rumen fluid was obtained directly from the Malmesbury abattoir. The second culture comprised of sludge from a batch sulphate reducing reactor, maintained on a lactate based medium, and the third was derived from washing the residual solid material from the original packed columns obtained from Golder Associates Research Laboratories (GARL).

Where linear flow channel reactors required inoculation this was achieved using stock cultures maintained in the CeBER laboratories.

2.2 Batch digestion reactors

The batch digestion reactors consisted of 1 l Schott bottles, fitted with a custom designed lid with ports for sampling and gas analysis. The contents of the reactors were agitated using a magnetic stirrer bar. An example of the reactor type is illustrated in Figure 3.

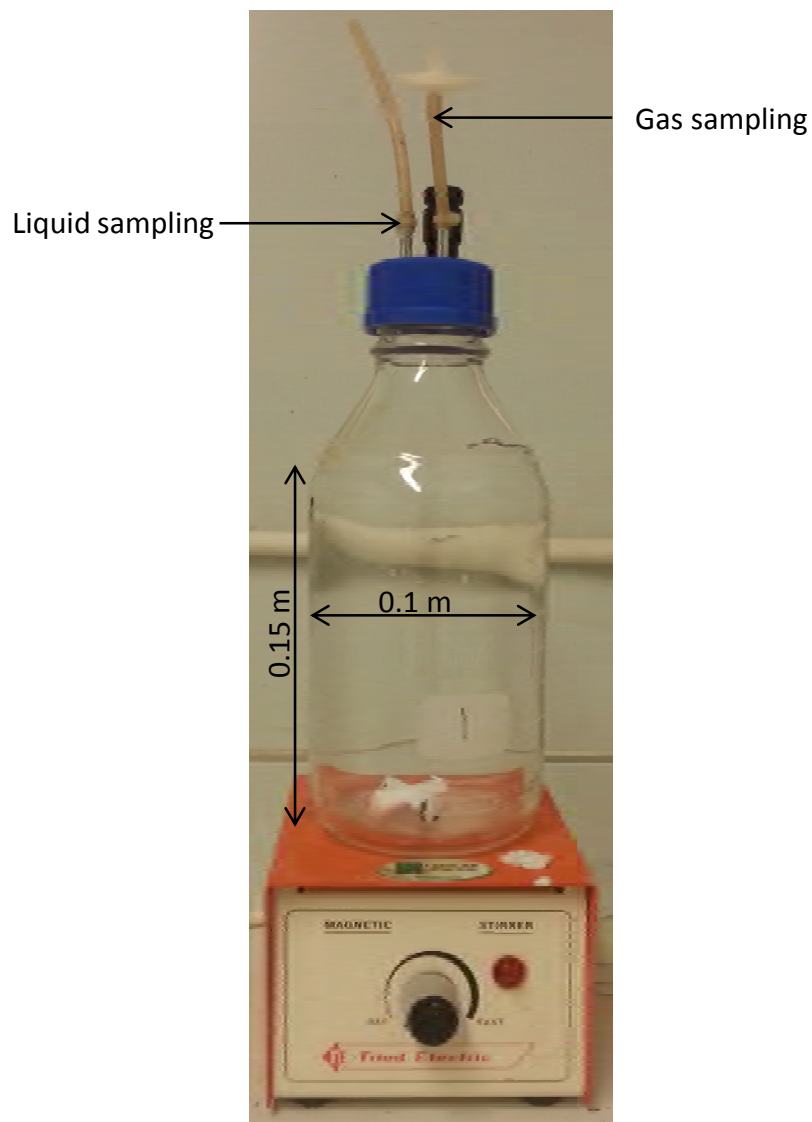


Figure 3: Example of a reactor used for the batch digestions reactions showing the overall dimensions and location of the sampling ports

2.3 Packed column reactors

The column reactors were obtained from Golder Associates Africa (GAA). They measured 1.0 m in length, with a diameter of 0.21 m and were constructed of PVC pipe. The effective liquid height in the reactor was 0.69 m, resulting in an empty volume of approximately 21.5 l. The reactors were fitted with four sample points along the length of the column. The lower port was used to pump the feed into the reactor and the uppermost port for the reactor effluent. An example of the packed column reactor is shown in Figure 4.

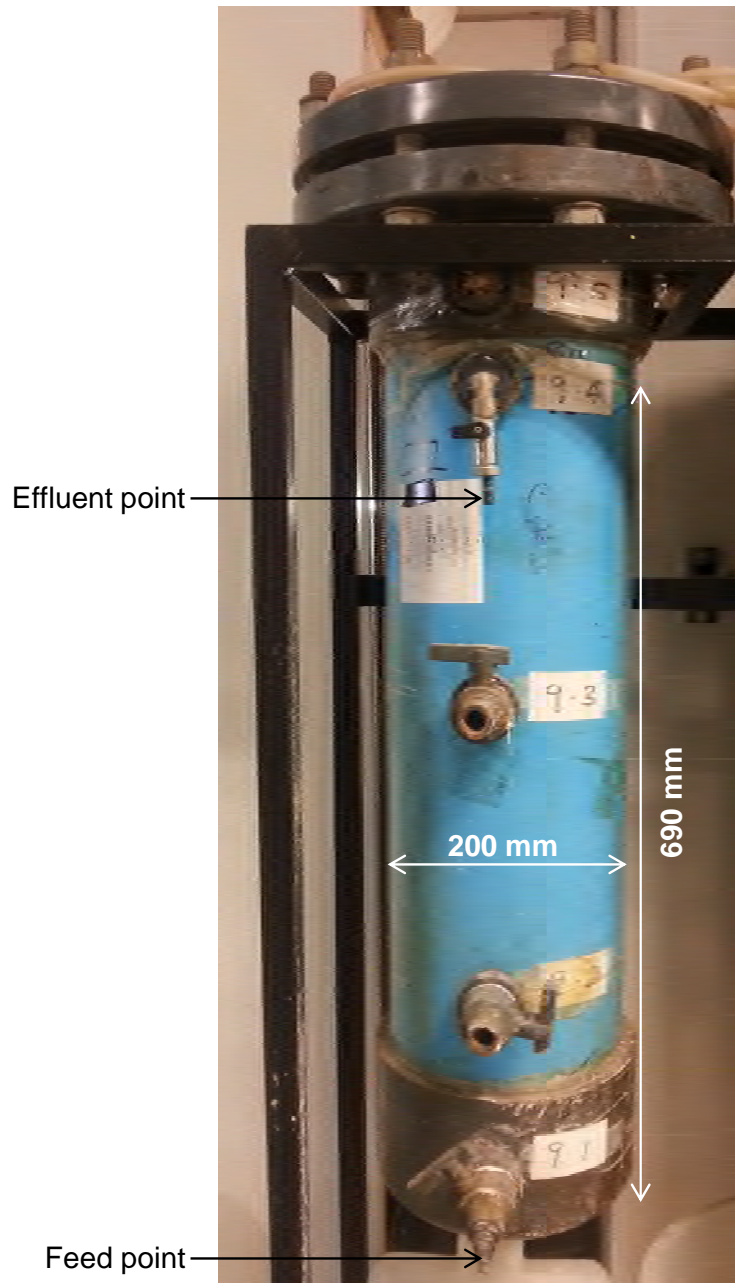


Figure 4: Example of a packed bed column reactor showing the overall dimensions and location of the feed and effluent ports

2.4 Linear flow channel reactors

Three identical linear flow channel reactors (LFCRs) were constructed. The LFCR design was based on the dimensions of the pilot reactor used at GARL during an earlier project. The reactor was constructed of Perspex, with dimensions of 0.1 m (w) × 0.15 m (h) × 2.5 m (l), giving a total

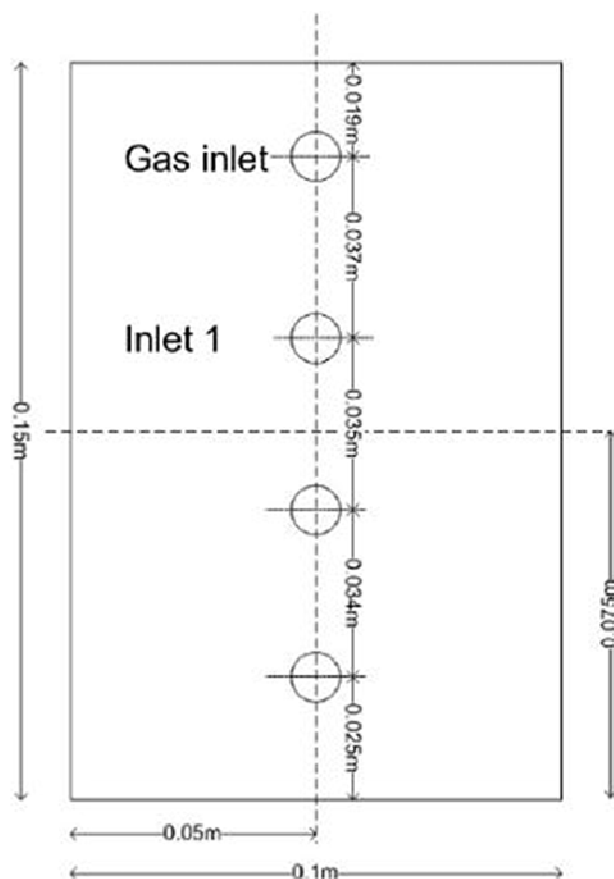


Figure 6: Schematic drawing of the front and rear wall of the LFCR, showing the position of the three possible inlet/outlet ports for liquid and the gas inlet/outlet

The side wall of the reactor has 15 sample ports at three levels (Figure 7) allowing for liquid samples to be removed along the length of the reactor at different depths. Each sample port consisted of a threaded fitting which incorporated a GC septum held in place by a hose end and nut. Samples could be withdrawn using a hypodermic needle and syringe.

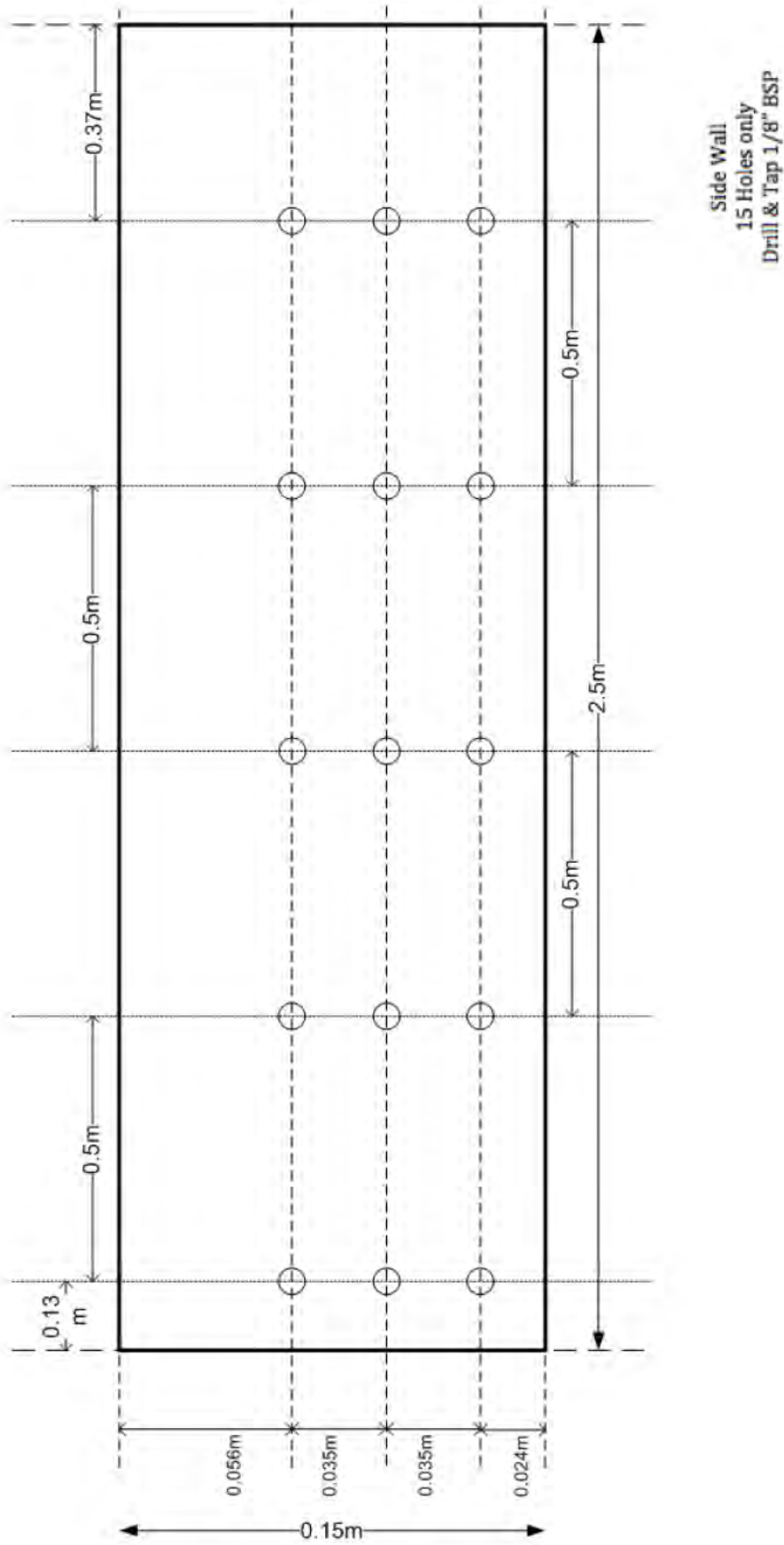


Figure 7: Schematic diagram showing the location of the 15 sampling ports in the front wall

2.5 Analytical techniques

2.5.1 pH

Solution pH values were determined using a Cyberscan 2500 micro pH meter. The meter was calibrated daily using Metrohm standard solutions (pH 4.0, 7.0 and 9.0).

2.5.2 Sulphide

Aqueous sulphide was quantified using the colorimetric N,N-dimethyl-p-phenylene diamine (DMPD) method. The principle of the method is reaction of aqueous sulphide with DMPD, catalysed by ferric ions, to produce methylene blue. An appropriate volume of sample (10-4800- μl) is added to 200 μl of 1% zinc acetate. The volume is made up to 5 ml with deoxygenated water, after which 500 μl of 0.4% N,N-dimethyl-p-phenylene diamine (in 6 M HCl) and 500 μl of 1.6% ferric chloride (in 6 M HCl) are added. The sample is mixed well and left to react for a minimum of 5 minutes after which the absorbance is read at 670 nm and the concentration determined relative to a standard curve. The assay has a maximum detection limit of just over 1 mg/l so significant dilution is required. This is typically achieved by using a small volume (20-50 μl) of sample.

2.5.3 Chemical oxygen demand

All COD measurements were carried out using the Merck reagent test protocols for high (1500-10000 mg/l) and low (100-1500 mg/l) concentrations. The method is based on the oxidation of the sample with a hot sulphuric acid solution containing potassium dichromate, with silver sulphate as the catalyst. The chloride is masked with mercury sulphate. The concentration of unconsumed yellow $\text{Cr}_2\text{O}_7^{2-}$ ions or green Cr_3^+ ions is then determined photometrically and used to quantify oxygen demand.

2.5.3.1 Low concentration range (100-1500 mg/l)

Reactors were performed in Merck COD tubes. The COD reagents (0.3 ml reagent A and 2.3 ml reagent B) were added to the reaction tube, followed by 3 ml of appropriately diluted sample (1 ml deionised water for blank). The tube was agitated to ensure good mixing and heated to 150°C for 2 hours in a heating block. Once cooled the absorbance was read at 610 nm using a Helios spectrophotometer. A standard curve (250, 500, 750, 1000, 1250 and 1500 mg/l COD) was prepared using potassium hydrogen phthalate.

2.5.3.2 High range (1500-10000 mg/l)

Reactors were performed in Merck COD tubes. The COD reagents (2.2 ml reagent A and 1.8 ml reagent B) were added to the reaction tube, followed by 1 ml of appropriately diluted sample (1 ml deionised water for blank). The tube was agitated to ensure good mixing and heated to 150°C for 2 hours in a heating block. Once cooled the absorbance was read at 610 nm using a Helios spectrophotometer. A standard curve (2500, 5000, 7500 and 10000 mg/l COD) was prepared using potassium hydrogen phthalate.

2.5.4 Anions

Dissolved anions (sulphate, chloride, nitrate and phosphate) were measured by HPLC using a Waters Breeze 2.0 system equipped with a Waters IC-Pak A HR (Anion High resolution) column and a conductivity detector. The system was run isocratically using a sodium borate-gluconate mobile phase at a flow rate of 1 ml/min. The pressure in the column did not exceed 2000 psi. Sample injection volumes of 100 μl were used. To quantify the ion concentrations standard

solutions (250, 500, 750 and 1000 mg/l) of each ion were prepared using their respective sodium salt.

2.5.5 Sulphur

Elemental sulphur was determined by reverse phase HPLC using a C18 column (Phenomenex Luna, 150 mm x 4.6 mm). The mobile phase was methanol:water (95:5) at a flow rate of 2 ml/min. The sample injection volume was 20 µl. Standards were prepared by dissolving elemental sulphur powder in chloroform. Sulphur was detected by UV. Optimisation of the technique showed maximum absorbance at 263 nm at a residence time of approximately 8.2 minutes.

2.5.6 Volatile fatty acids

A full volatile fatty acids (VFA) analysis was conducted to quantify the concentration of lactic, acetic, propionic, iso-butyric, butyric, iso-valeric and valeric acids present in the reactors. The concentration of each VFA was determined using HPLC on a Waters Breeze 2 HPLC system equipped with a Bio-Rad Organics Acids ROA column and a UV (210 nm wavelength) detector. The system was run isocratically using a mobile phase of 0.01 M H₂SO₄ at a flow rate of 0.6 ml/min. The pressure in the column did not exceed 2000 psi. Sample injection volumes of 50 µl were used. To quantify the VFA concentrations standard solutions (250, 500, 750 and 1000 mg/l for each acid) were prepared.

2.5.7 Phenolic compounds

The low molecular weight phenolic compounds (catechol and gallic acid) were quantified using HPLC (Thermo Scientific System). An Ascentis RP-Amide (C18) octadecylsilane reverse phase column (15 cm x 4.6 mm, 5 µm) was used, with mobile phase (1% glacial acetic acid) pumped through at a flow rate of 0.5 ml/min. The injection volume was 20 µl and the phenolic compounds were quantified using a UV detector (230 nm). Gallic acid had a retention time of approximately 5 minutes and catechol 11 minutes. Standard curves (0-100 mg/l) were generated for each compound.

2.5.8 Microsensor measurements

Dissolved oxygen and redox potential were determined using custom built microprobes (Unisense, Denmark).

2.5.8.1 Dissolved oxygen

A Clark-type OXY-10 glass electrode (10 µm diameter) DO microsensor, connected to a picoammeter (OXY-Meter), was used to measure *in situ* dissolved oxygen concentrations within the biofilm. A manual manipulator (MM-33) was used to lower the electrode at 5 µm steps. The output signal was sent to a laptop computer via a USB cable and recorded using the Unisense[®] SensorTrace BASIC 3.0 software.

The microsensor was calibrated in a glove box using degassed deionised water as the zero solution and oxygen saturated water as the maximum value solution. The zero solution was degassed with nitrogen for 1 hour and the saturated solution was prepared by aerating for 24 hours.

2.5.8.2 Redox potential

The redox potential through the biofilm was measured using a redox microelectrode (RD-10, 10 µm) in conjunction with a reference electrode (REF-10). The reference electrode was placed in

a sample of the bulk liquid solution taken from the vicinity of the biofilm. Both electrodes were connected to a high impedance millivolt meter (Unisense[®] pH/mV-Meter) and the output signal was sent to a laptop computer via a USB cable and recorded using the Unisense[®] SensorTrace BASIC 3.0 software. The reference electrode was a silver/silver-chloride open-ended electrode with a gel stabilised electrolyte and a tip diameter of 10 µm. The micromanipulator (MM-33) was used to lower the electrode in 5 µm intervals.

2.5.9 Scanning electron microscopy

All preparations were visualised using a FEI NOVA NANOSEM 230 with a field emission gun.

2.5.9.1 Top-view

All top-view samples were prepared by harvesting the material onto a piece of filter paper prior to fixation in a 1% glutaraldehyde solution for 1-2 days, depending on the structural integrity of the biofilm. After fixation the glutaraldehyde solution was removed and the sample washed in 1 × phosphate buffered saline (PBS) solution. This was followed by a dehydration series, using increasing concentrations of ethanol (30, 50, 75, 90, 95 and 100%) for 10 minutes at each concentration. The filter was placed in a sealed Petri dish, covered in 100% ethanol, and refrigerated (4°C) for 2-3 days prior to analysis. A portion of the sample was mounted onto an aluminium stub with carbon glue. A few drops of hexamethyldisilazane (HDMS) was added on top of the sample, which was left to dry for 3 hours prior to carbon coating using a Balzers evaporation coater.

2.5.9.2 Bottom-view

Samples where visualisation of the underside of the biofilm was desired were not harvested onto a filter paper. A portion of the biofilm was carefully removed and inverted into a Petri dish containing the glutaraldehyde. Following fixation the dehydration series was performed by removing the liquid (using a pipette) and replacing it with the next solution. The samples were mounted onto the stub using carbon tape, rather than glue to minimise damage to delicate structures.

2.5.9.3 Cross-section of biofilm

Samples for cross-sectional analysis were fixed using 1% glutaraldehyde for 2-3 days. After fixation the samples were washed with 1 × PBS and dehydrated as described above. A quickset L.R. resin was mixed and poured into a rubber mould. Once the resin had set the specimen was placed on the resin block and fresh resin was poured over to fill the mould. The resin was left to dry overnight. The block was removed from the mould and sanded down to expose the biofilm cross-section. Thereafter it was polished using a 1 µm polishing wheel and 0.05 µm silica powder suspension in order to obtain a smooth, clear finish on the resin surface. The block was washed with deionised water and sonicated for 10 minutes to remove debris from the surface. The block was mounted on a stub and coated twice with carbon (Balzers evaporation coater) to improve the conductivity of the sample. A silver dag was placed on the resin block to provide a conductive path to the aluminium stub.

2.5.10 Elemental composition analysis

The biofilm was harvested from the LFCR by skimming off the surface with a scoop. The slurry mixture was centrifuged to separate the solid and liquid fractions. The supernatant was discarded and the solid fraction dried at 37°C for 48 hours, then weighed.

2.5.10.1 Sulphur analysis

The dried biofilm was suspended in 1 l of 100% chloroform in a Schott bottle. The bottle was sealed and the suspension agitated at 50°C for 5 days to ensure complete dissolution of elemental sulphur. The mixture was cooled to 25°C in a water bath and vacuum filtered using a Durapore Millipore filtration apparatus using a hydrophobic membrane (0.45 µm). The recovered solids were dried at 37°C for 24 hours and the filtrate stored in a clean Schott bottle. The filtrate was diluted, as necessary, and the sulphur content quantified by HPLC. The recovered solids were combusted in a furnace at 450°C to determine if they contained any residual sulphur. The temperature was chosen as the boiling point of amorphous, monoclinic and rhombic sulphur is 444.6°C (Perry and Green, 2008). Any residual sulphur would be volatilised, leaving behind the carbon and inorganic matter.

2.5.10.2 Carbon and inorganic matter

After the initial combustion step the remaining material was allowed to cool to room temperature and weighed. This was further combusted at 550°C to remove the organic matter. The remaining ash was reweighed to determine the inorganic content. The residual ash was analysed by scanning electron microscopy energy dispersive x-ray (SEM-EDX) analysis to obtain a qualitative assessment of the composition of the inorganic matter.

3 EXPERIMENTAL PROCEDURES

3.1 Characterisation of packing materials

A number of complex organic carbon sources were used to pack the column reactors. To assess their potential to provide organic carbon to the sulphate reducing and sulphide oxidising communities they were characterised to determine their COD and the ease with which they could be hydrolysed under anaerobic conditions.

3.1.1 Chemical oxygen demand

The four solid complex carbon sources used in the study were wood chips (wattle and bluegum), grass, dry activated sewage sludge and leaf mulch. The leaf mulch had already undergone partial decomposition so it was not possible to obtain a representative sample for the COD analysis. Representative samples of the other materials were dried at 80°C for 48 hours and then homogenised in a laboratory mill. The density of the material was recorded and a small fraction subjected to a COD assay using the standard assay (high range).

3.1.2 Batch tests to assess digestibility

The intention of the batch tests was to assess the potential for biomass hydrolysis and volatile fatty acid liberation from the different packing materials (wood chips, grass and dry sewage sludge). The tests were designed to promote the initial stages of anaerobic digestion (hydrolysis and acidogenesis), but to prevent the subsequent utilisation of the VFAs by sulphate reducers or methanogens. The batch tests were conducted in 1 l Schott bottle reactors to which 20 g of the dried packing material was added. Aside from the three packing materials a fourth test was performed using spent brew malt, which was expected to readily liberate organic carbon. The reactors were inoculated with 10 ml of rumen fluid and 10 ml of solution sulphate reducing stock culture. No sulphate (substrate for SRB) was added to the reactors and 10 ml of a 2% bromoethane sulphonic acid (BESA) solution was added to inhibit methanogenesis. In addition, 5 ml of a concentrated sodium sulphide (10 g HS⁻/l) was added, resulting in a final sulphide concentration of 50 mg/l. This was done as it has been speculated that the hydrolysis of lignocellulosic material is promoted under biosulphidogenic conditions. The reactors were placed on magnetic stirrers in a constant environment room at 37°C and monitored for a period of 36 days. Samples (2 ml) were removed daily and analysed for pH and volatile fatty acid content.

3.2 Contribution of elemental sulphur to chemical oxygen demand value

From direct observation of the effluent from the packed columns it was clear that the effluent contained colloidal sulphur particles. The packed columns were not devoid of oxygen and contained organisms capable of sulphide oxidation so the presence of colloidal sulphur was not unexpected. Furthermore, analysis of the effluent from the demonstration scale DPBR indicated that despite a COD value of several hundred mg/l the contribution of VFAs or sugars was insignificant. Consideration of some earlier published data, in light of current work, suggests that reported COD values may also have been inflated by the contribution of colloidal sulphur.

A standard curve was generated by determining the COD value of defined masses of elemental sulphur powder. This was used in conjunction with measured colloidal sulphur concentrations in the effluent from the packed columns, to determine the contribution of the colloidal sulphur to the measured COD values.

3.3 Effect of phenolic compounds on sulphate reduction

The effect of low molecular weight phenolic compounds on sulphate reduction performance was tested in a series of batch reactors. The reactors consisted of 1 l Schott bottles, as described in 3.1.2, to which the following were added: sodium sulphate (2 g), sodium acetate (2 g), sodium sulphide (20 ml of a 1 g/l stock – final concentration 20 mg/l) and 30 ml of active sludge from a sulphate reducing reactor. The control reactors were not dosed with phenolic compounds while the experimental reactors received increasing concentrations (10, 50, 100 or 1000 mg/l) of catechol (1,2-dihydroxybenzene). The experiments were repeated with a second phenolic compound, gallic acid (3,4,5-trihydroxybenzoate). Gallic acid was selected as it is a product of wattle degradation by wattle-tannin-degrading bacteria (*Enterobacter aerogenes* or *Celluomonas*). The reactors were sampled daily and pH, redox potential and sulphide concentration measured.

3.4 Packed column studies

A pair of packed bed column reactors had been received from Golder Associates Africa and operated in the CeBER laboratories for a number of years, as part of a previous project. By the conclusion of that project the rates of organic carbon liberation and sulphate reduction within the columns had fallen significantly so the decision was taken to unpack the columns and prepare two fresh reactors for the current study. This would allow the determination of void volumes and more accurate estimation of hydraulic residence times.

3.4.1 Preparation of packed columns

Two packed bed reactors were prepared with different packing regimes. The packing in the first column consisted of a smaller proportion of lignocellulosic material (Figure 8, Column 1), while the second was packed according to a traditional degrading packed bed reactor design (Figure 8, Column 2).

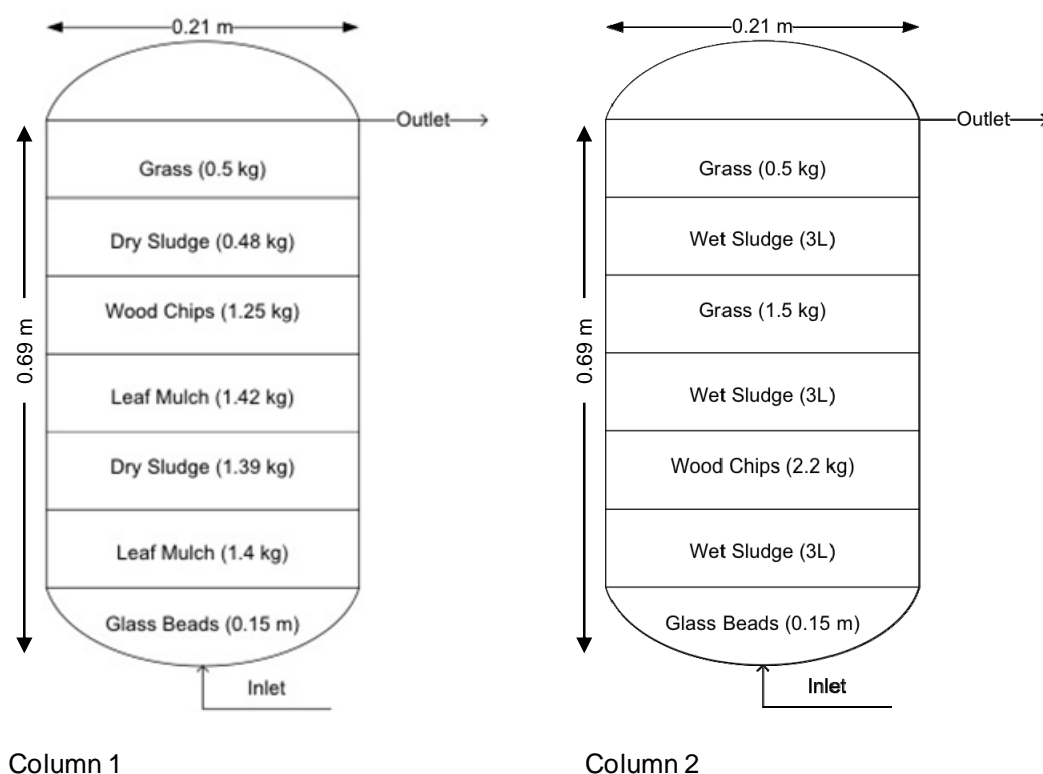


Figure 8: Schematic representation of the packed column reactors, showing dimensions, packing arrangements and relative mass fractions

The total organic carbon loading for Column 1 was 7.39 kg. The lower section of Column 1 was packed with more organic waste material, while the upper section had more lignocellulosic matter.

Column 2 was packed with more lignocellulosic and cellulosic materials, in the form of wood chips and grass. In addition, 9 l of wet primary sewage sludge was utilised. The wet sludge had a solids concentration of 9 g/l, resulting a total mass loading of 4.281 kg.

3.4.2 Determination of void volume and hydraulic residence time

The void volume and hydraulic residence time (HRT) were calculated for each column by pumping in dH₂O until water exited out the top outlet. Column 1 had a significantly smaller void volume (7.58 l) due to the smaller particle size of the leaf mulch and dry sewage sludge. Column 2 had a void volume of 14.38 l due to the larger, irregular-shaped wood chips, as well as the liquid volume associated with the primary sewage sludge. Based on a feed rate of 3 ml/min Column 1 had a HRT of 1.75 days, while for Column 2 it was 3.33 days.

3.4.3 Inoculation protocol

The packed columns were inoculated with a mixture of three microbial consortia, rumen fluid, sludge from a batch sulphate reducing reactor and cells detached from the packing material of a previous packed column. The columns were first inoculated with 15 l of rumen fluid, pumped in at a rate of 1.5 l/hr. The column effluent was recycled for a period of three days. All grass particles and partially digested grass were removed by filtering the fluid through a linen cloth to ensure that the mass of organic packing was not changed.

The second inoculum was prepared by agitating 50 ml of sludge from a BSR batch reactor in 50 ml of the bulk reactor fluid. This was mixed with 5 l of detached cell suspension, prepared by agitated washing of packing material (wood chips) from the previous DPBR column. This was pumped into the column at a rate of 1.5 l/hr, after which the columns were sealed and allowed to acclimatise for five days prior to the initiation of feeding.

3.4.4 Column feed composition

The columns were fed with a synthetic ARD stream at a flow rate of 3 ml/min. The feed composition (Table 4) was determined based on the predicted composition of a raw ARD stream from the Landau Colliery after neutralisation in a high density sludge process. The synthetic ARD feed to Column 1 was supplemented with sodium acetate (CH₃COONa) to a final concentration of 1 g/l. The feed to Column 2 was supplemented with molasses (0.075 g/l) in order to provide some soluble organic carbon to “kick-start” BSR process over the period from March 2012 to June 2012.

Table 4: Composition of synthetic ARD feed. Feed was adjusted to pH 6.1-6.5 with NaOH

Component	Concentration (mg/l)	Concentration (mM)
SO ₄ ²⁻	2000	20.8
Al ³⁺	100	3.7
Ca ²⁺	230	5.8
Fe ²⁺	35	0.6
Mg ²⁺	210	8.6
Mn ²⁺	96	1.7
Na ⁺	8	0.3

3.4.5 Operation and monitoring

Feeding of the columns was started on the 11th of December 2011. The columns were monitored regularly (typically daily) by collecting a sample of the effluent and testing for pH, redox potential, sulphide and sulphate. In addition to the routine measurements, regular analyses to determine COD, VFA concentration and colloidal sulphur were performed, while the measurement of polysulphides was performed on a smaller number of samples. During the first month sulphate reduction was erratic and a stable redox potential was not observed, particularly for Column 1. To accelerate the transition to steady state operation the columns were supplemented with additional inoculum, consisting of cell suspension from a stock sulphate reducing reactor. Column 2 received a single dose of 4 l two days after the initial inoculation, while Column 1 received 6.2 l, in smaller doses, between day 2 and day 17 post inoculation.

3.5 Linear flow channel studies

3.5.1 Standard operation of the linear flow channel reactors

The LFCRs were operated with a working liquid volume of 25 l, unless otherwise stated. The reactors were closed to the surroundings (gasket sealed lid) creating a headspace of 12.5 l. The headspace was flushed with air at a flow rate of 48 l/day, with the exit gas passing through an alkaline scrubber to recover any H₂S gas. The lid was only removed when microprobe measurements were taken. Unless otherwise stated the reactors were fed, via the uppermost inlet port, at a set flow rate and the effluent exited via the uppermost exit port. For each experiment the reactor was filled with 25 l of sulphide effluent from the packed column and was allowed to stand for 24 hours. This was to allow the microbial consortium to acclimatise to the new conditions prior to starting the experiment. The packed column effluent contained both the sulphate reducing and sulphide oxidising bacterial consortia. The FSB was only harvested from the liquid surface at the end of the experiment unless, otherwise stated. The experimental conditions are summarised in Table 5.

Table 5: Summary of experimental conditions during LFCR channel experiments

Experiment ¹	Feed rate (l/day)	HRT (days)	Duration (days)	Acetate addition ² (g/l.day)	Mean feed pH
8	6.25	4	18	0	7.80
9	6.25	4	18	0	7.70
10	12.5	2	12	0	7.50
11	12.5	2	12	0.99	7.78
12	12.5	2	14	2.26	7.79
13	25	1	10	1.17	7.67
14	25	1	10	2.24	7.89
15	25	0.5	7	0.86	8.05
16 (1)	18.75	1.5	7	1.26	7.90
16 (2)	18.75	1.5	7	1.77	7.85

¹ The numbering of experiments represents those used in Mooruth's (2013) PhD thesis. Not all experimental runs are relevant to this report.

² The initial channel volume was dosed with acetate to 1 g/l

The reactors were sampled daily from all 15 sample ports, in addition to the feed and effluent. The samples were analysed to determine pH, sulphur species and VFAs. At the end of the experiments the biofilm was harvested, dried and analysed to determine the composition. Small sections of biofilm were removed before harvesting and prepared for SEM analysis.

3.5.2 Determination of the oxygen mass transfer coefficient in the biofilm

In order to determine the change in dissolved oxygen concentration with depth and time the smaller LFCR (2.5 l) apparatus was utilised. The DO profile was measured daily for five consecutive days, to determine the change with time. The LFCR was operated at a one day residence time with an average organic loading rate of 1.77 g/l.day and sulphide loading rate of approximately 11.36 mmol/day (374 mg/day). Following the measurement of the DO profile, the headspace (1.25 l) was flushed with nitrogen for 40 minutes at 400 ml/min to deoxygenate the FSB. Thereafter the DO microprobe was lowered to a predetermined depth to measure the rate of change of the DO concentration. The working principle of the DO microprobe is based on the diffusion of oxygen through a silicone membrane to an oxygen reducing cathode. The reducing cathode is polarised against an Ag/AgCl anode. Therefore, the change in the oxygen concentration that diffused through a particular distance over a certain time period was measured. Together with the DO profile, the local oxygen mass transfer coefficient (k_f) was determined by Equation 10. The diffusivity of oxygen within the biofilm (D_f) was determined and thereafter (k_f). The depth (F_{depth}) was chosen such that the DO concentration profile decreased consistently, thus ensuring there were few or no pores or conduits to influence the movement of oxygen through the FSB. The measurements were conducted in order to determine the mass transport of oxygen from the atmosphere downwards into the FSB.

$$\frac{\partial CO_2}{\partial t} = D_f \frac{\partial^2 CO_2}{\partial y^2} \quad \text{where } D_f = k_f F_{depth}$$

Equation 10

Rasmussen and Lewandowski (1998b) proposed an alternative method to measuring the local mass transfer coefficient, utilising ferricyanide and measuring the amount of ferricyanide that diffused to the tip and had been reduced to ferrocyanide. This particular method is dependent on the fact that the ferricyanide is able to diffuse freely within the biofilm structure and that there is movement of water and pore water. Hence, it is particularly useful in determining the mass transfer coefficient of water and dissolved substrates within the FSB. However, within this particular system, the fluid velocities are significantly lower, by orders of magnitude. Furthermore, the diffusion coefficient of ferricyanide ($7.35 \times 10^{-10} \text{ m}^2/\text{s}$) in water is an order of magnitude different to that of oxygen in water ($2.38 \times 10^{-9} \text{ m}^2/\text{s}$). Therefore, the actual molecular diffusion of the ions will be significantly slower than that of oxygen. In addition, the movement of oxygen is primarily in the y-direction, from the atmosphere downwards, while the ferricyanide method relies upon the lateral and upward movement of the ferricyanide ions from the bulk solution below. Therefore, the DO microprobe method was considered more appropriate to determine the mass transfer coefficient of oxygen. Measurements were conducted in triplicate in order to obtain an accurate measurement of the mass transfer coefficient. Furthermore, Rasmussen and Lewandowski (1998a) demonstrated that the D.O. microprobe method is accurate within the concerned flow range of 0-4.1 mm/s, as the average deviation as percentage of average flux was 16-19%.

4 RESULTS, TREATMENT OF RESULTS, AND DISCUSSION

4.1 Characterisation of packing materials

4.1.1 Chemical oxygen demand

The density and COD of the three packing materials tested are summarised in the table below.

Table 6: Summary of density and COD of dried organic packing materials

Organic material	Density (g/cm ³)	COD (g/cm ³)
Wood chips	0.506	902.79
Grass	0.817	685.99
Dry activated sewage sludge	1.375	752.63

4.1.2 Digestibility of the packing materials

The data from the batch digestibility tests show that VFAs were liberated from all packing materials, with the exception of the grass. The intention of the experiment was to assess the extent to which the complex carbon sources could be hydrolysed and VFAs released. The experiments were designed in such a way that processes which would consume acetate (methanogenesis and sulphate reduction) were inhibited, but more complex VFAs could be partially oxidised to acetate.

The pH in the reactors initially increased as a consequence of the addition of sulphide (Figure 9). The extent of the increase was greatest in the reactors where the initial VFA production was lowest. This was followed by a period during which the pH decreased due to VFA generation and some oxidation of the sulphide and then a period of stability, for approximately two weeks. During this period further oxidation of the sulphide was observed, so a second spike of sodium sulphide was added, increasing the concentration to 50 mg/l. This resulted in a further increase in pH across all reactors, although the extent of the increase was lower in the reactors with the highest VFA concentrations.

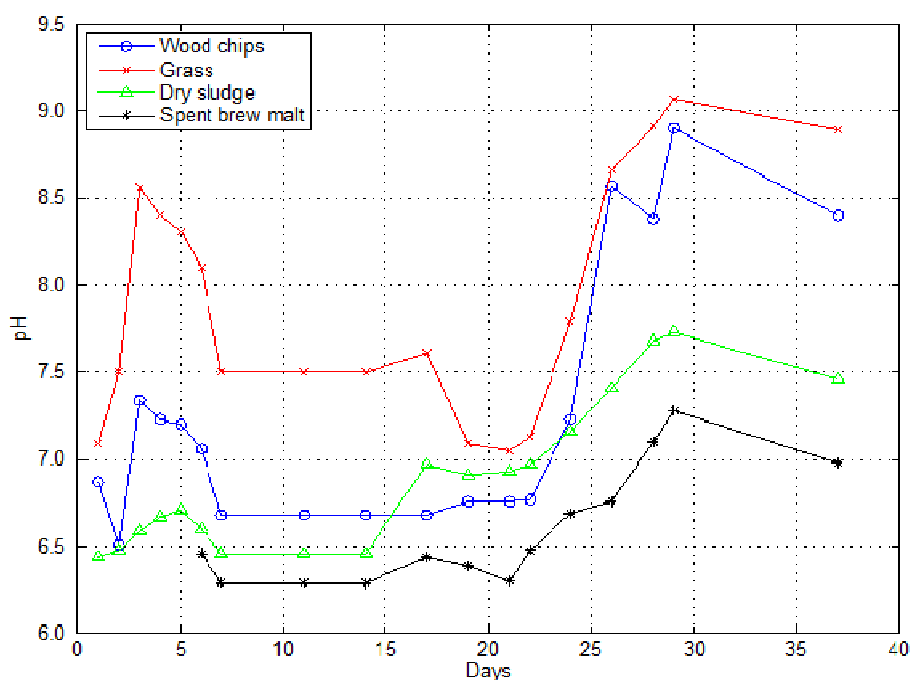


Figure 9: pH data of batch bioreactors in VFA liberation kinetics study

The greatest amount of VFA liberation occurred in the spent brew malt bioreactor (3.78 g/l), followed by the dry activated sewage sludge producing (1.96 g/l) and wood chips (1.57 g/l). The spent brew malt had been crushed and subjected to the mashing process, where it was stirred in the mash tun at 60°C for one hour. A large proportion of the sugars and complex carbohydrates would have been removed from the solids during the mash process, although some residual would remain, while the remaining complex carbohydrates could have been partially hydrolysed. The wood chips, grass and dry sludge did not undergo any pretreatment. The final VFA and soluble COD values at the end of the test are shown in Table 7.

Table 7: Summary of results from the batch digestability tests. Total VFA and soluble COD data represent final values at the end of the experiment

Substrate	Wood chips	Grass	Dry sludge	Spent brew malt
Total VFAs (g/l)	1.57	0.00	1.96	3.78
Sol COD (g/l)	2.10	1.21	2.00	3.17
Avg. VFA release rate (mg/l.day.{g of substrate})	2.18	0.00	2.72	6.09

During the initial phase of the experiment the liberation of acetic acid appeared to follow linear first order kinetics in all cases, except grass. The acetic acid liberation rate in the wood chip fed bioreactor was 66.13 mg/l.day over the first 10 days (Figure 10). Thereafter the concentration of acetic acid decreased, possibly due to the reduction of residual sulphate in the inoculum sludge.

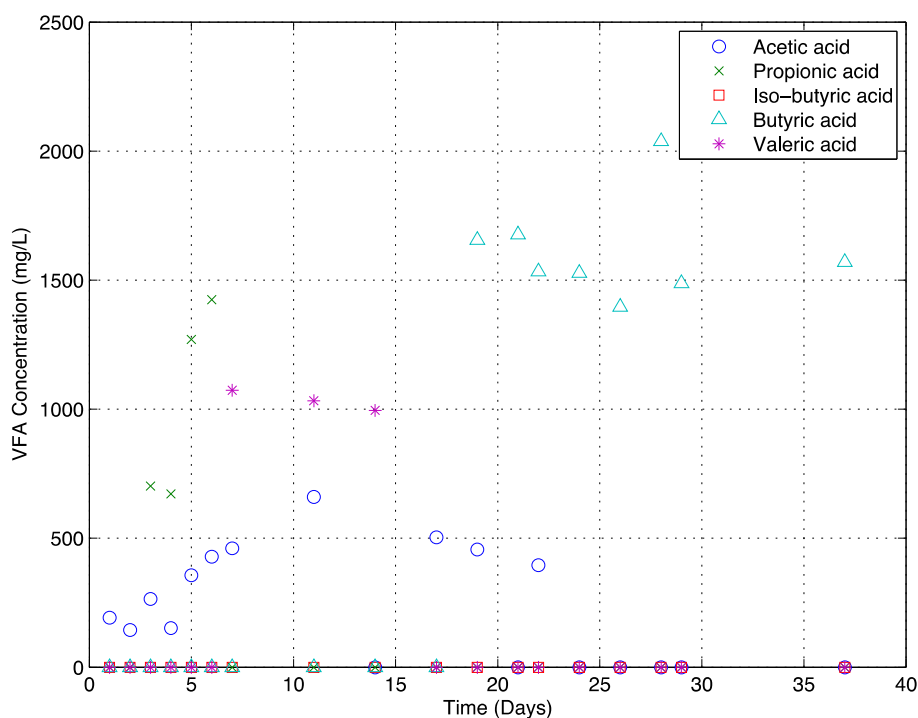


Figure 10: Volatile fatty acids cumulative concentration within bioreactor 1 containing 20 g of wood chips

Propionic acid was detected during the first week, but not thereafter and was most likely partially oxidised to acetic acid, although the acetic acid concentration did not increase to the same extent. Following that, liberation of iso-butyric acid and valeric acid took place. The valeric acid was only detected for a short period and may have been converted to butyric (C5 to C4), although this has not been reported in literature.

Hydrolysis did occur within the first six days in the grass bioreactor (Figure 11), at a rate of 134.56 mg/l.day, with valeric acid as the primary product. Valeric acid is not a typical product of cellulose fermentation, but has been shown to be produced under conditions of nitrogen limitation

(Cline *et al.*, 1958). No nitrogen compounds were added at the start of these experiments. However, the process of hydrolysis seemed to cease after day six after which the valeric acid was consumed.

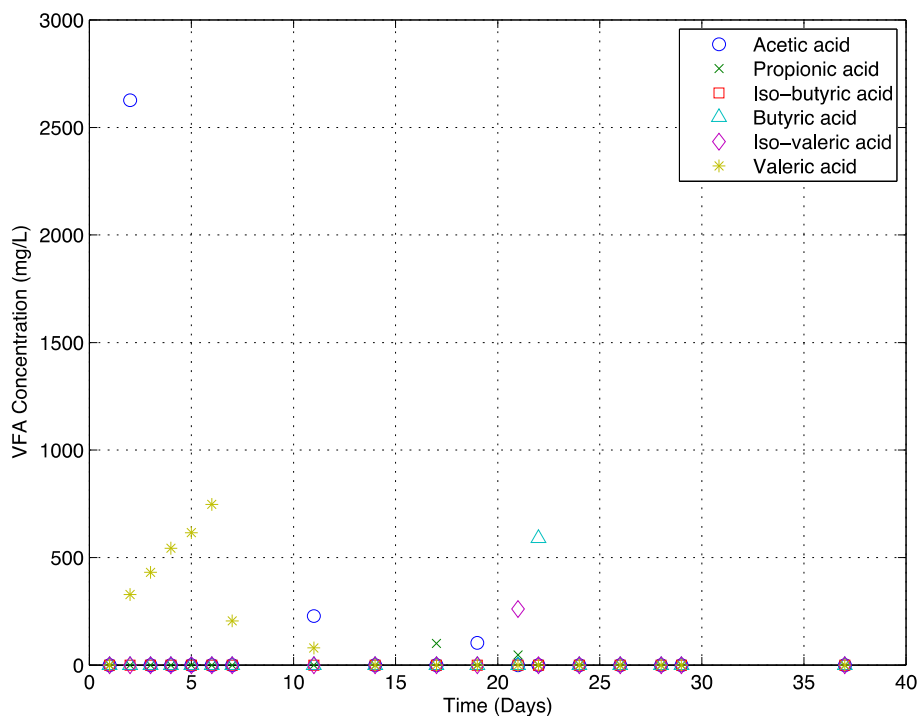


Figure 11: Volatile fatty acids cumulative concentration within bioreactor 2 containing 20 g of grass

The dry sludge fed bioreactor performed significantly better with acetic acid produced at a rate of 131.22 mg/l.day during the initial phase, whilst propionic and iso-valeric acid were produced at a rate of 52.88 and 62.94 mg/l.day respectively (Figure 12). Thereafter there appeared to be a decrease in VFA concentrations until the 1st of June when a second spike in VFA production was observed, after which the concentrations remained stable, suggesting no further liberation of VFAs or that liberation and utilisation reached a steady state. The former appears the more likely explanation as the concentration of all VFAs, except iso-butyric acid remained stable.

Acetic acid generation in the bioreactor loaded with spent brew malt also followed classic linear first order hydrolysis kinetics, with a production rate of 57.62 mg/l.day. However, the butyric and iso-butyric acid liberation did not follow a stable trend (Figure 13). Butyric and iso-butyric acid are produced primarily through the metabolism of specific amino acids, such as histidine, lysine, threonine, valine and glutamic acid (Lee, 2010). It is possible that amino acid degradation only became significant after 14 days in the batch reactors. Butyric acid can be further metabolised to acetic acid.

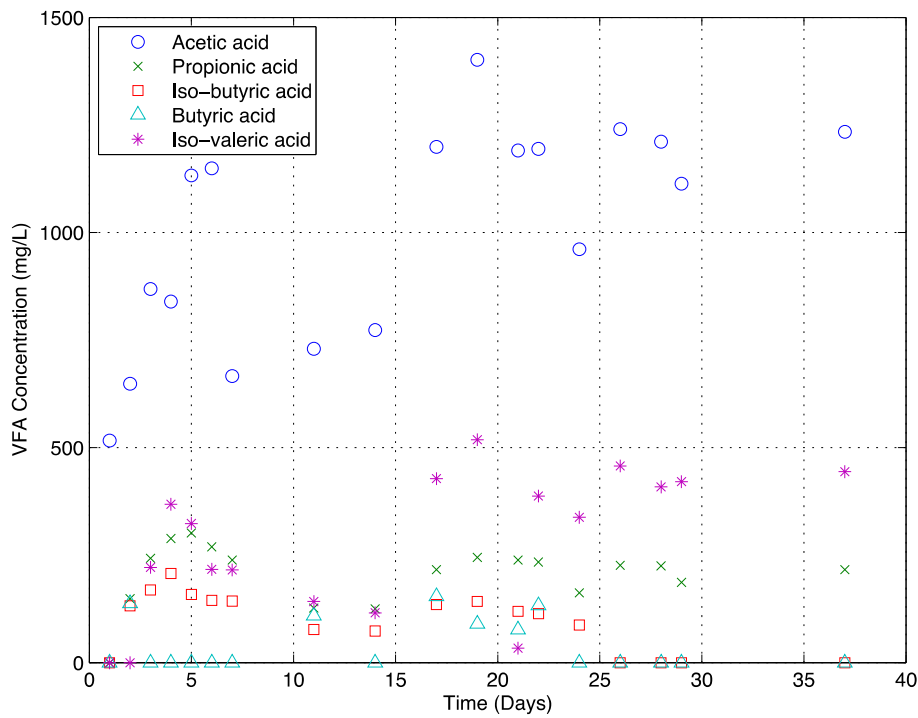


Figure 12: Volatile fatty acids cumulative concentration within bioreactor 3 containing 20 g of dry sewage sludge

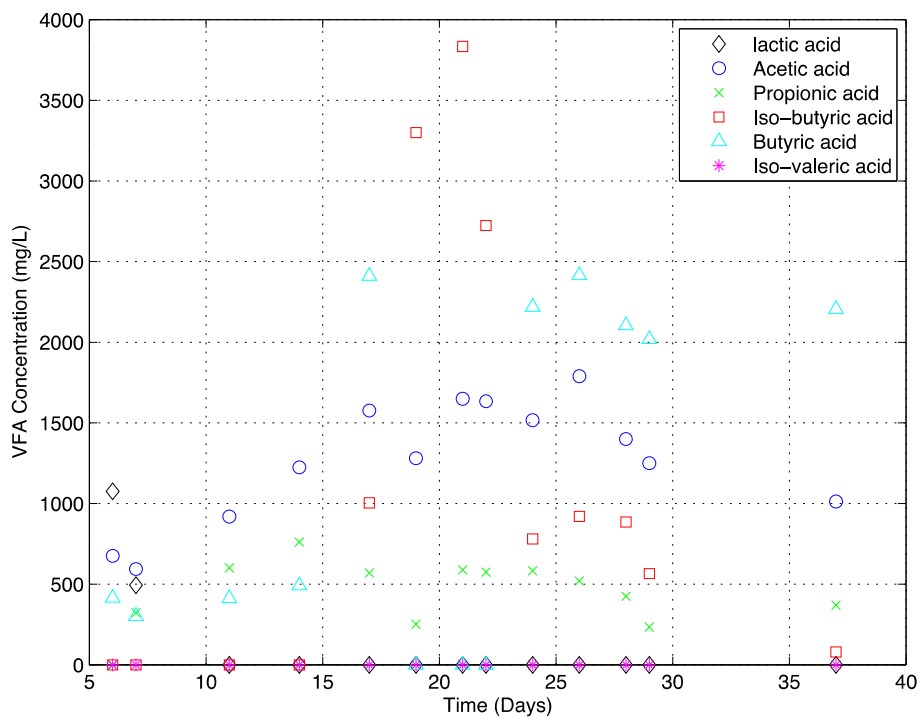


Figure 13: Volatile fatty acids cumulative concentration within bioreactor 4 containing 20 g of spent brew malt

The reactor loaded with dry activated sewage sludge managed to liberate a total of 1.96 g of VFAs, which was significantly higher (10x) than the study conducted by Chen and co-workers (2007). They showed that hydrolysis occurred at a faster rate under alkaline conditions, with the optimum at pH 10. However, no improvement was observed when the pH was increased during this study. The primary products of hydrolysis, acetic acid and iso-valeric, were similar in their study.

Whittington-Jones and co-workers (2006) demonstrated that hydrolysis and VFA production was enhanced under sulphidogenic conditions and managed to achieve a maximum hydrolysis rate of 4 g/l.day. However, their study used primary sewage sludge which has a significantly greater labile organic carbon fraction. Additionally, the experiment was only conducted for eight hours, so the rate of hydrolysis cannot be considered an accurate representation of long-term sewage sludge degradation.

The grass bioreactor reached a maximum degradation rate of 123.11 mg/l.hr within 24 hours and subsequently decreased until no VFAs were present. This indicated that the easily hydrolysable fraction was rapidly metabolised and the more complex lignocellulose was not. The average total VFA production rate was 49 mg/l.day. A substantially higher rate of VFA production, at 112.2 mg/l.day, has been demonstrated under different reactor conditions (Greben *et al.*, 2009). These results were generated using a reactor was supplied 1 kg of grass cuttings initially, with an additional 20 g added daily. When the amount of grass supplied was reduced there was a significant decline in VFA production and sulphate reduction. The system utilised in the study was an 'active' CSTR (with recycle). Therefore, grass does not appear to be a suitable substrate, due to its recalcitrant nature and low rate of hydrolysis.

The reactor loaded with wood chips showed slightly lower rates, as the average total VFA liberation rate was 43.61 mg/l.day. A study conducted by Yamashita and co-workers (2011) showed that hydrolysis of wood was slow and limiting, as the sulphate reduction rate was 0.47 g/kg wood.day. However, a second study (Roman *et al.*, 2008) managed to achieve a sulphate reduction rate of 0.243 g/kg wood.day. Assuming the VFAs liberated in the wood chip loaded reactor were metabolised completely to acetate and utilised for BSR, the theoretical sulphate reduction rate would be 3.55 g/kg wood.day. The theoretical sulphate reduction rate is significantly higher, most likely due to the higher temperature (37°C) as it has been shown that hydrolysis is significantly faster at a higher temperature. Yamashita and Roman conducted their studies at 20°C and 25°C respectively.

The batch tests showed that the complex carbon sources used to pack the columns could be partially hydrolysed under sulphidogenic conditions and that volatile fatty acids, including acetate, were liberated. However, the rate of VFA liberation was substantially slower than that required to sustain the integrated semi-passive system. A comparison of the COD liberated in the batch tests against the inherent COD of the packing materials demonstrates the very low extent of hydrolysis achieved. The data support the rationale of adding molasses or a similar simple carbon source to the system.

4.2 Effect of phenolic compounds of sulphate reducing performance

The hydrolysis of lignocellulosic materials has been shown to release aromatic compounds under methanogenic and sulphidogenic conditions (Roman *et al.*, 2008). Previous work has shown that certain SRBs are able to hydrolyse and metabolise phenolic compounds, but the impact of the low molecular weight phenolics on the BSR process has not been definitively studied. Additionally, the toxic concentration (IC₅₀) of catechol has been shown to vary from 3-2200 mg/l, depending on the microbial species and environmental conditions (Blum and Speece, 1991; Park *et al.*, 2011).

4.2.1 Catechol

Sulphide was generated at a rate of 1.45 mmol/l.day (46.4 mg/l.day) in the control reactor, reaching a maximum concentration of 10.19 mM (326 mg/l). The 10, 50 and 100 mg/l reactors achieved a sulphide generation rate of 1.05, 1.14 and 1.39 mmol/l.day (33.8, 36.5 and 44.5 mg/l.day) respectively (Figure 14). Surprisingly, there was an increase in the biological sulphate reduction rate with an increase in catechol. However, in the presence of 1000 mg/l no

BSR was observed, indicating that the tolerance of the microbial community is between 100 and 1000 mg/l. The pH (Figure 15) and redox potential (Figure 16) data were consistent with the generation of sulphide. The solution pH in the reactors loaded with 50 and 100 mg/l catechol decreased over the first three days, which could have been due to the conversion of catechol to VFAs.

An analysis of residual volatile fatty acids was conducted in order to understand the observed trends. Based on the amount of sulphide generated the theoretical acetic acid consumption was calculated. The analyses showed a greater than expected residual acetate concentration, suggesting that the microbial population either hydrolysed the phenolic compound and utilised the resulting monomers as an organic substrate for the BSR process, or converted the catechol to acetate. No VFAs other than acetic acid were detected. Schink and co-workers (2000) and Zeyaulah and associates (2009) presented metabolic pathways for the degradation of catechol, resulting in the formation of benzoyl-CoA or pyruvate/succinate respectively. Pyruvate is only formed in the presence of magnesium ions. These metabolic pathways have been observed to occur in the presence of SRPs, such as *Desulfobacterium* (Harms *et al.*, 1999; Schink *et al.*, 2000). Therefore it is likely the pyruvate was reduced to lactate, by lactate dehydrogenase, for the purposes of biological sulphate reduction.

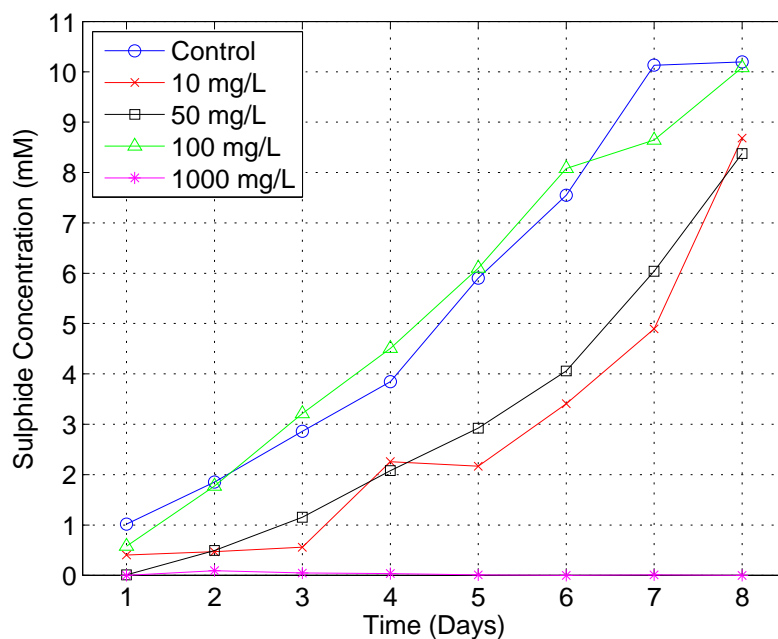


Figure 14: Effect of increasing concentrations of catechol (0-1000 mg/l) on the rate of sulphide generation in batch sulphate reduction tests

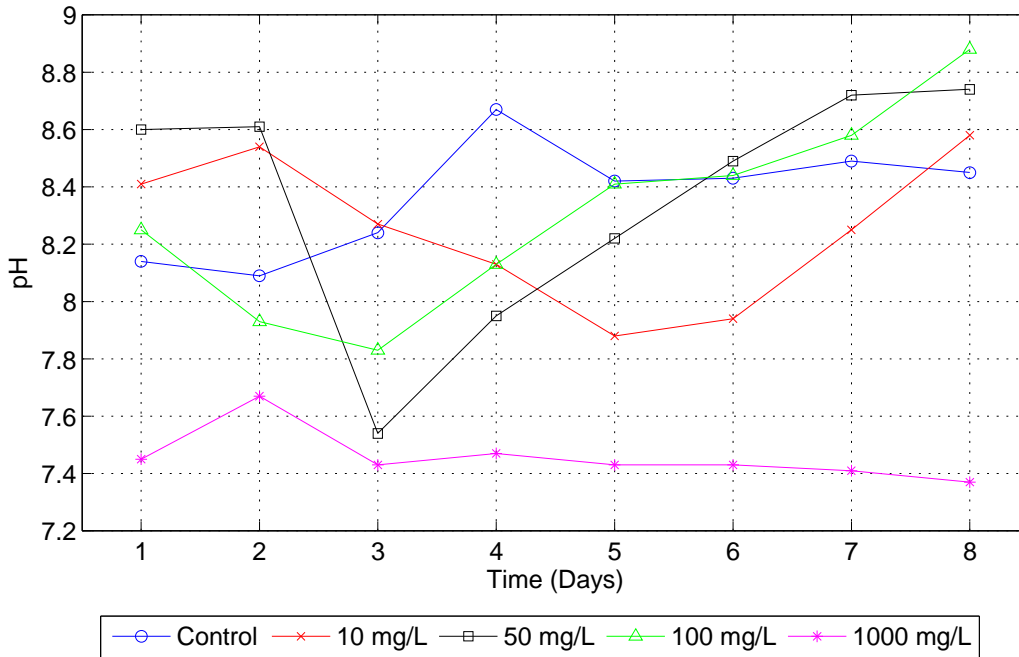


Figure 15: Solution pH measured in the batch sulphate reducing reactors subjected to increasing concentrations (0-1000 mg/l) of catechol

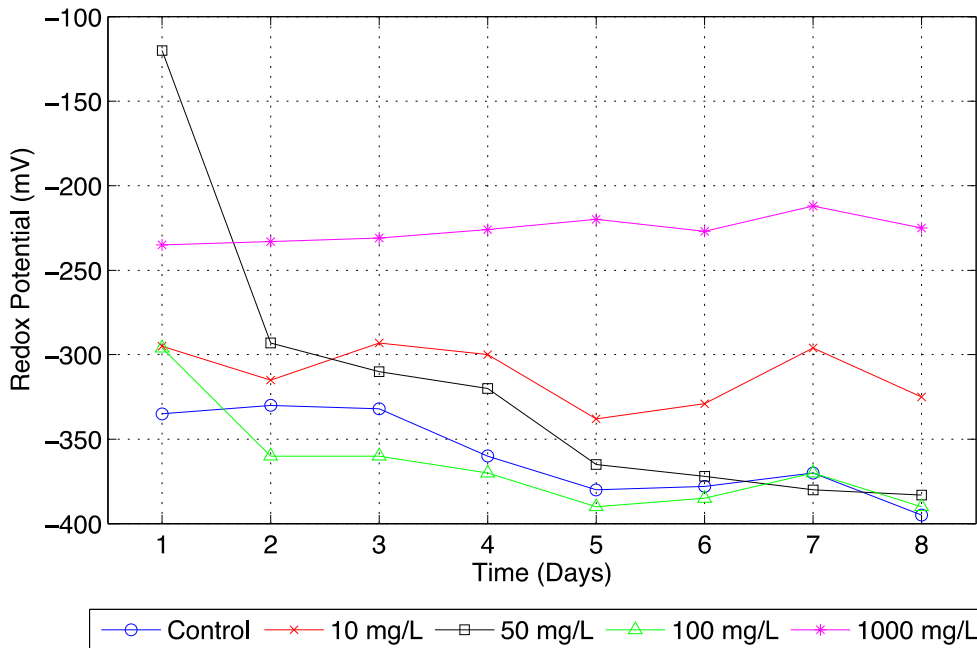


Figure 16: Solution redox potential (mV) measured in the batch sulphate reduction reactors challenged with increasing concentrations (0-1000 mg/l) of catechol

4.2.2 Gallic acid

The results for the gallic acid tests showed a similar trend to those for catechol. Sulphide was generated in the control reactor at a rate of 1.59 mmol/l.day (50.9 mg/l.day). The reactors loaded with 10, 50 and 100 mg/l gallic acid showed sulphide generation rates equivalent or even greater than the control reactor (Figure 17). This was unexpected as it was assumed that gallic acid would be more inhibitory than catechol. Once again, no sulphate reduction was observed in the presence of 1000 mg/l. The solution pH data (Figure 18) showed that the initial pH was lower, due to the

acidity of gallic acid, but increased after the first day. This may have been due to the degradation of gallic acid. However, the pH in the 1000 mg/l reactor varied significantly, despite no apparent sulphate reduction. The redox potential (Figure 19) decreased in all reactors where sulphate reduction was observed, as expected.

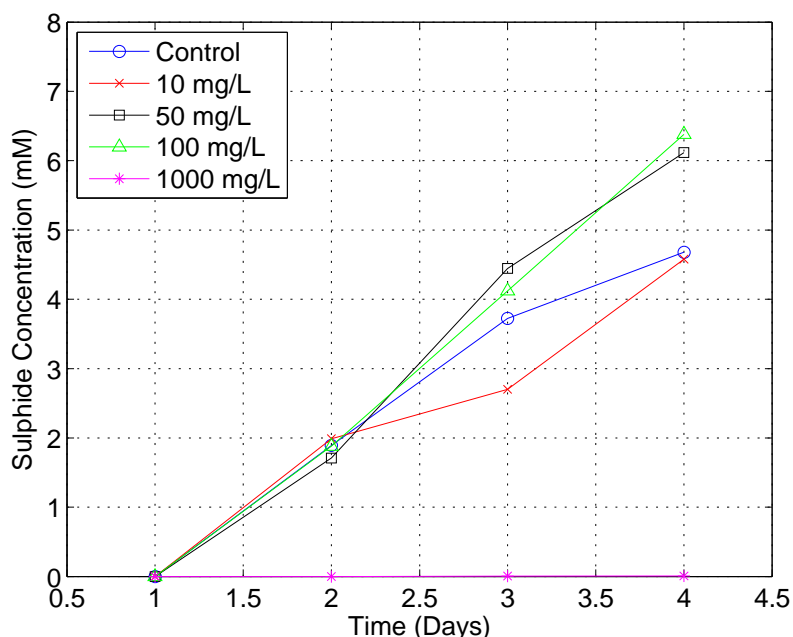


Figure 17: Effect of increasing concentrations of gallic acid (0-1000 mg/l) on the rate of sulphide generation in batch sulphate reduction tests

The analysis of residual fatty acids again showed that less acetate was consumed than was expected, based on the sulphide generation. The most likely explanation is the degradation of gallic acid and the use of the products to sustain the BSR process. The HPLC analysis indicated the presence of butyric and valeric acid peaks on day 2 (100 mg/l) and day 3 (10 mg/l). Acetic acid was the only VFA added to the reactors initially and no other VFA peaks were observed in the catechol experiment, suggesting that the butyric and valeric acid peaks were products of gallic acid metabolism. Bhat and co-workers (1998) compiled a comprehensive review of tannin degradation, illustrating a five step metabolic pathway under anaerobic conditions. Gallic acid is firstly decarboxylated to form pyrogallol and thereafter isomerised to phloroglucinol by pyrogallol-phloroglucinol isomerase. Subsequently it is converted to dihydrophloroglucinol, followed by 3-hydroxy-5-oxohexanoate that is degraded further to three molecules of acetyl CoA, or utilised directly in the citric acid cycle. In earlier studies it was shown that rumen bacteria are able to degrade gallic acid to acetate and butyrate.

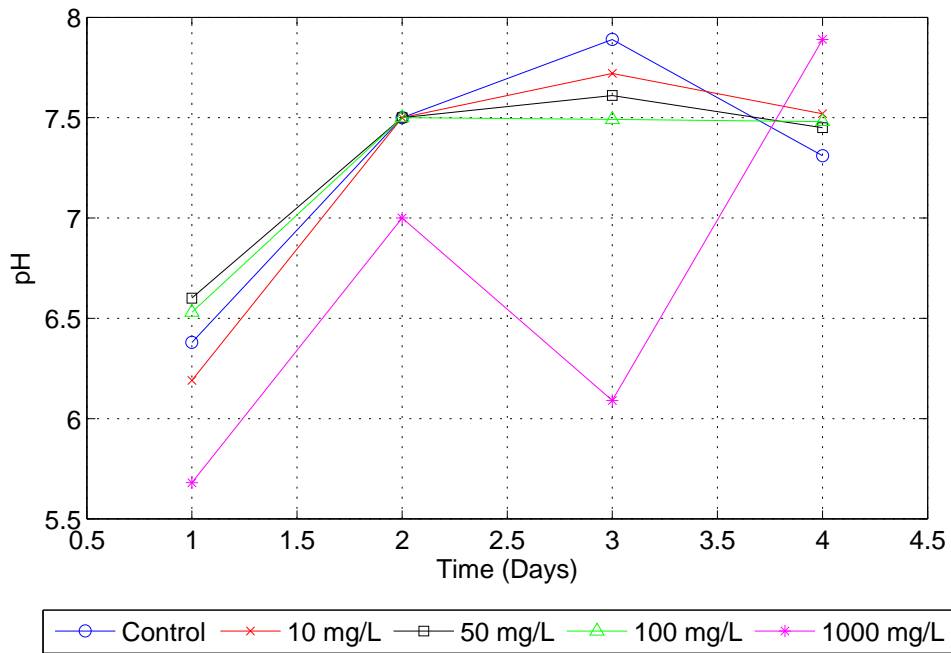


Figure 18: Solution pH measured in the batch sulphate reducing reactors subjected to increasing concentrations (0-1000 mg/l) of gallic acid

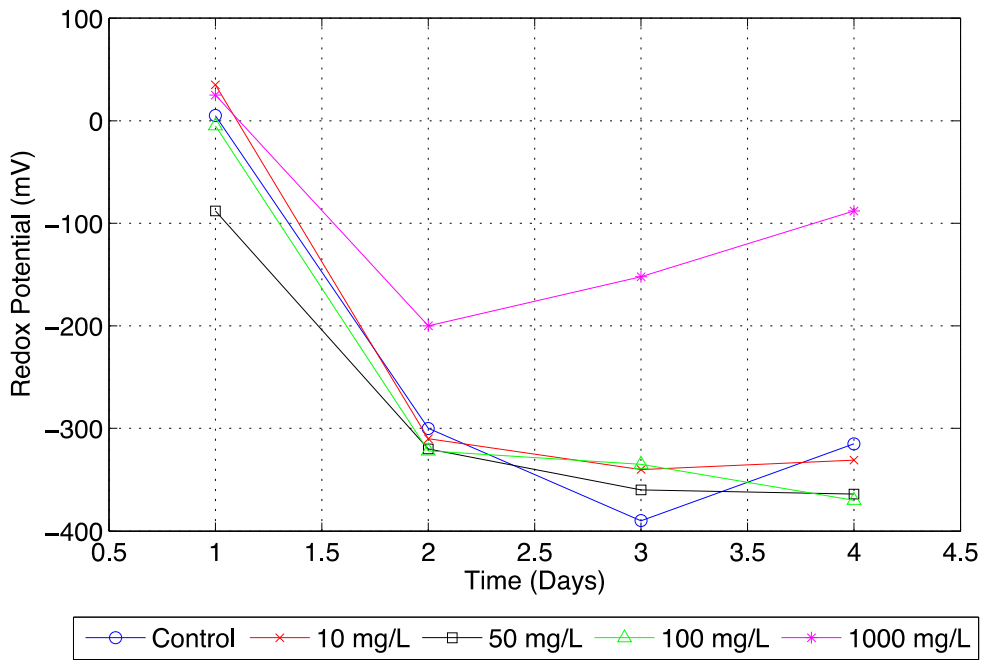


Figure 19: Solution redox potential (mV) determined in the batch reactors challenged with increasing concentrations of gallic acid

The study has shown that microbial consortium is tolerant of low molecular weight phenolic compounds, such as catechol and gallic acid, to concentrations of at least 100 mg/l. In addition, there is strong evidence to suggest that these compounds were metabolised and the products utilised as electron donors for biological sulphate reduction. While BSR was completely inhibited at 1000 mg/l with both phenolic compounds the concentration of such compounds originating from the degradation of lignocellulosic packing material is likely to be low, due to the slow kinetics and the fact that the phenolics can be degraded. Therefore, it can be concluded that inhibition of sulphate reduction in the packed bed reactors is highly unlikely.

4.3 Packed column performance

4.3.1 Overall performance

During the initial phase of the experiment the performance of the columns was unstable. No sulphide was detected in the effluent from Column 1 for the first month (Figure 20) and the redox potential fluctuated between -350 mV and -100 mV. During this unsteady state phase the pH remained relatively stable, between pH 6.5 and pH 7.5 (Figure 21). Sulphate reduction did occur in both columns (Figure 22), although the fluctuations in the effluent sulphate concentration were relatively large, representing sulphated reduction efficiencies between 21 and 94% (Column 1) and 27 and 77% (Column 2). The mean sulphate reduction efficiencies for both columns were approximately 60% during the first month. The lack of sulphide in the effluent indicated partial sulphide oxidation within the columns as well as the pH dependent speciation of sulphide species (Section 4.3.1.1.), particularly in Column 1, which was consistent with the relatively high redox potentials.

During the first month of operation the evolution of gas from Column 1 was observed. The gas was collected and analysed by gas chromatography, which confirmed a mixture of methane (70%) and carbon dioxide (30%). In an attempt to inhibit methanogenesis the sulphate concentration in the feed to Column 1 was increased to 5 g/l (Day 17) in an attempt to increase the sulphide concentration. Methanogenic organisms are more susceptible to sulphide inhibition than sulphate reducers. The increased feed concentration was maintained for one month and accounts for the significant increase in effluent sulphate concentration (Figure 22). On day 68 each column was dosed with 1 l of 2-Bromoethanesulfonic acid (BESA, 5 mM) to further inhibit the methanogenic organisms and the feed sulphate concentration was reduced back to 2 g/l in Column 1.

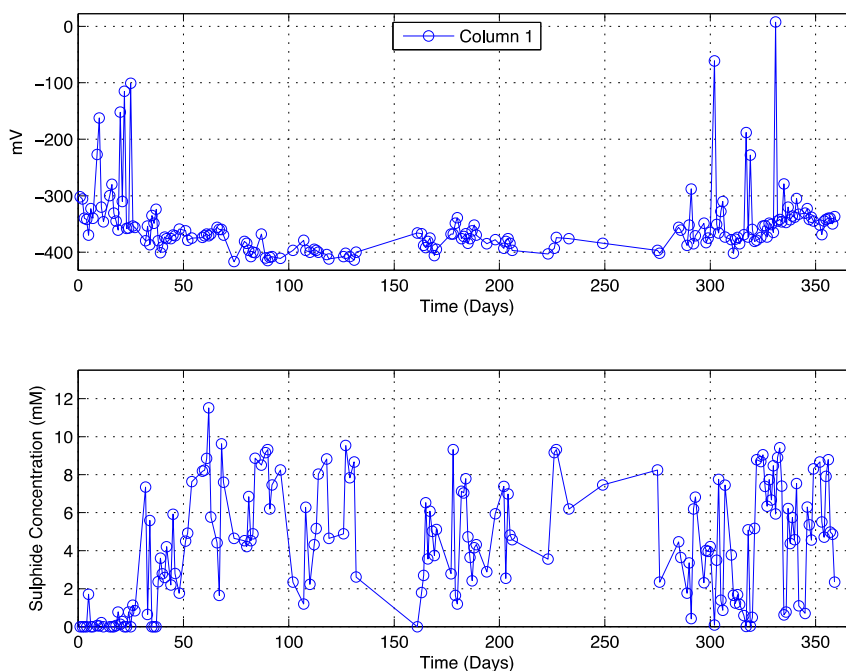


Figure 20: Redox potential and sulphide concentration measured in the effluent from Column 1

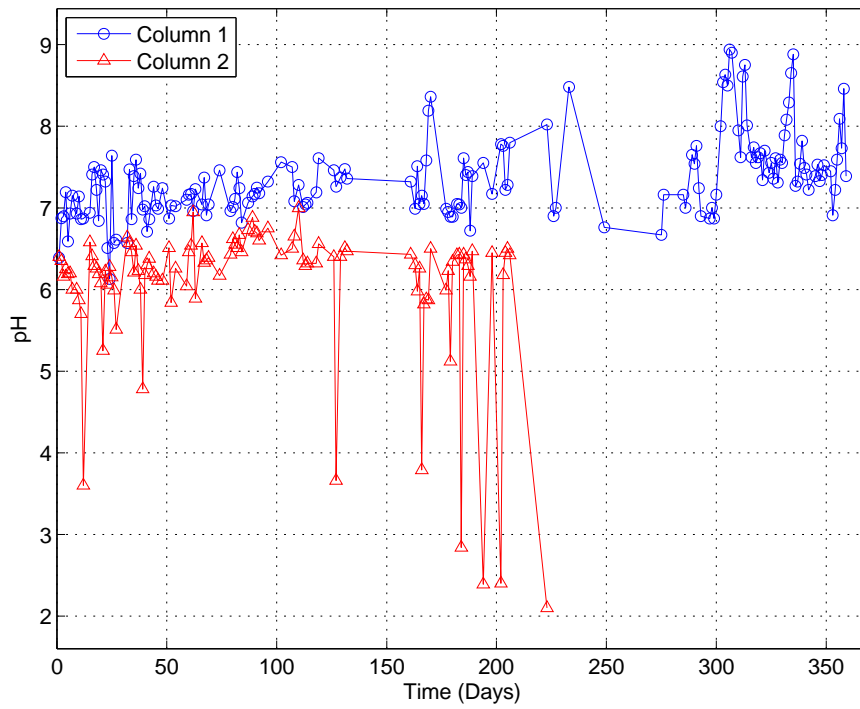


Figure 21: Solution pH in the effluent from the packed column reactors

Following the addition of the BESA, Column 1 entered a phase of relatively stable performance, maintaining a redox potential between -400 mV and -350 mV (Figure 20) which is indicative of efficient sulphate reduction. The average sulphide concentration was 5.13 mM (164 mg/l), with an average sulphate reduction efficiency of 79% (Figure 23), which equated to a volumetric removal rate of 9.40 mmol/l.day (902.86 mg/l.day).

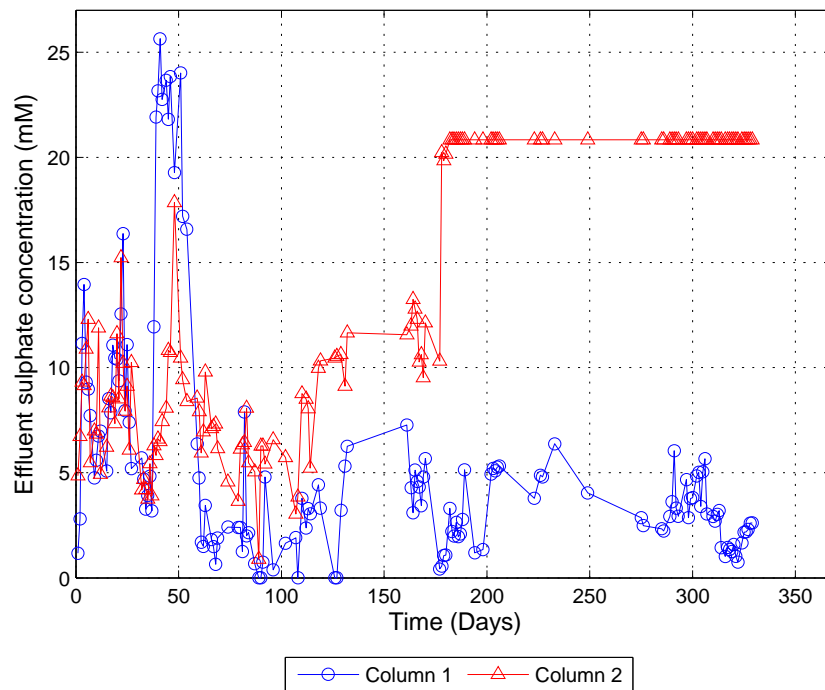


Figure 22: Sulphate concentration in the effluent from the packed column reactors

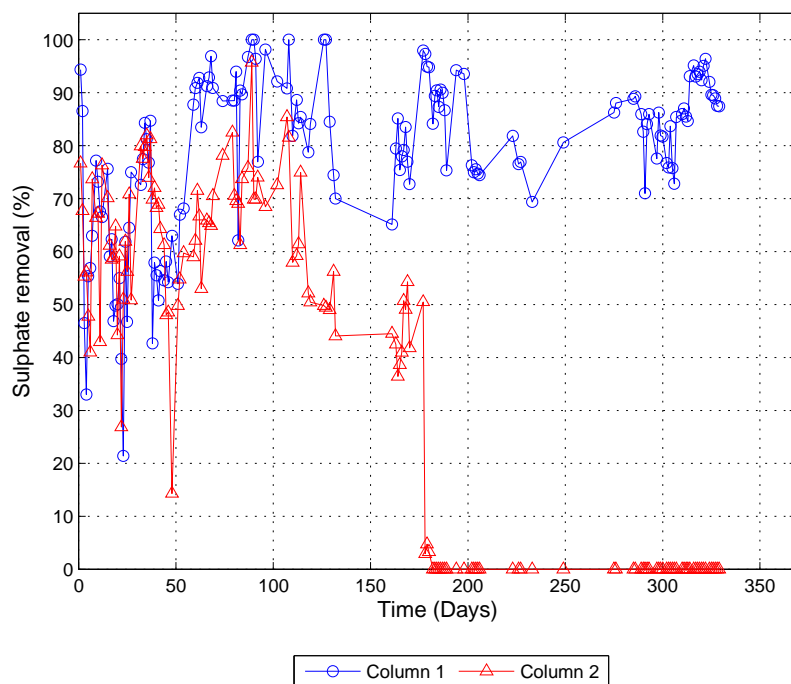


Figure 23: Sulphate removal efficiency, based on measurement of effluent sulphate concentration

The pH in the effluent from Column 1 stabilised within the range of pH 7.2-7.4. However, in April 2012 the pH increased to 7.5 (day 100), following a period of two weeks during which the column was not fed or sampled, after which it was less stable and increased to a maximum of pH 8.9 on day 306. Thereafter, the feed pH was decreased from pH 6.5 to between pH 5.0 and 5.1 to try and maintain a lower effluent pH. This was only partially successful, but did illustrate that the sulphate reduction process was efficient and stable and that the reactor was able to handle a more acidic ARD feed stream.

By contrast, Column 2 began generating sulphide much sooner with a sulphide concentration of 1.76 mM (56 mg/l) detected within the first week (Figure 24). However, Column 2 was only able to maintain a stable redox potential just below -300 mV until day 130 and the average effluent sulphide concentration was lower, at 1.71 mM (55 mg/l). Furthermore, Column 2 was unable to consistently maintain an effluent pH greater than pH 6.5 over the first two months of operation. The pH did occasionally drop below pH 6.0, indicating that the rate of acid generation was greater than the rate of alkalinity production by microbial sulphate reduction.

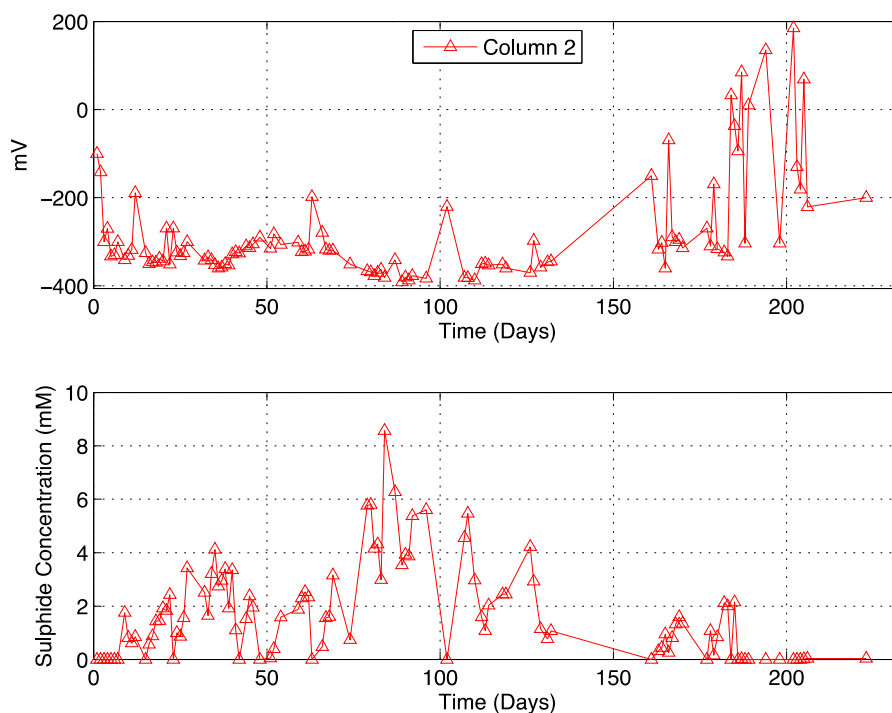


Figure 24: Redox potential and sulphide concentration measured in the effluent from Column 2

Acidity was most likely generated by the hydrolysis of the primary sewage sludge. Primary sewage sludge has a greater proportion of labile carbon than the dry activated sludge that was added to Column 1. This phenomenon is clearly illustrated in Figure 25 and Figure 26. There was a greater concentration ($> 200 \text{ mg/l}$) of VFAs in the effluent from Column 2 effluent. The feed to Column 1 was supplemented with sodium acetate at an acetate concentration of 1 g/l , so the residual acetate detected initially does not necessarily represent metabolism of the complex carbon. Similarly, as the acetate was already in the feed, rather than generated in the column, it would not further influence that pH.

Column 2 was not able to sustain a high sulphate removal efficiency, with an average removal efficiency of 63.7% after acclimatisation. This equated to a volumetric sulphate removal rate of 3.99 mmol/l.day (383 mg/l.day). The removal rate decreased further at the end of March 2012 (Day 109) to 50.6% (3.45 mmol/L.day). This decrease was probably due to the fact that the system became carbon limited. This was confirmed by the lack of VFAs in the effluent (Figure 26).

Column 2 was also not fed between days 123 and 139, in an effort to improve the sulphate reduction efficiency by allowing the SRP population to more completely colonise the packing material. However, Column 2 did not respond in the same manner as Column 1. After the recommencement of feeding the pH began to fluctuate significantly, in some cases dropping to below pH 3 (Figure 21). During previous studies this type of column failure was attributed to acidification caused by the accumulation of VFA products of molasses metabolism. However, in this case the molasses supplementation was insufficient and no residual VFAs were detected in the effluent.

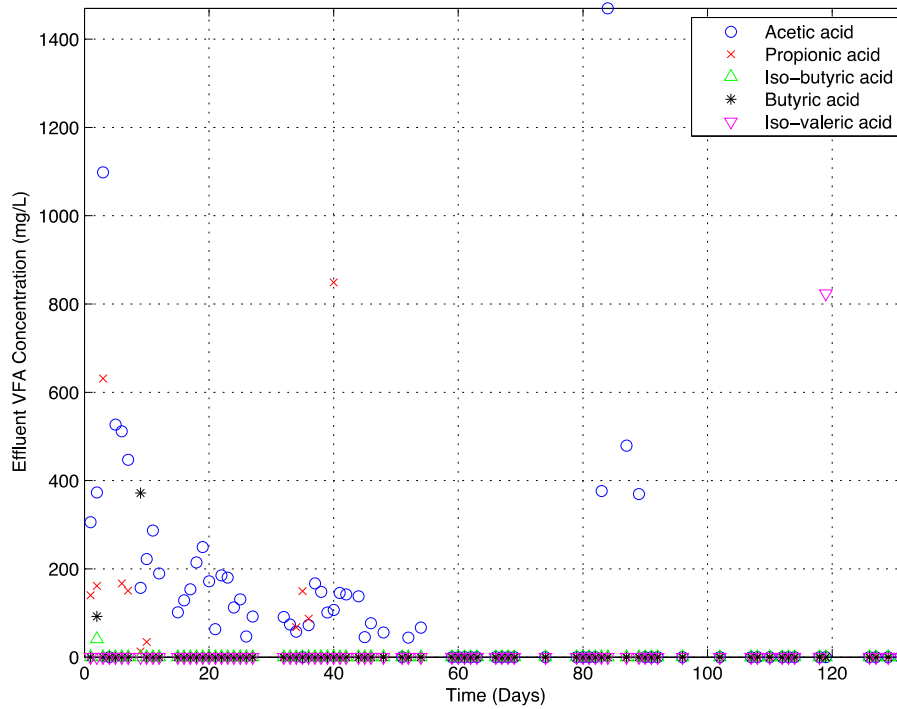


Figure 25: Volatile fatty acid concentrations detected in the effluent from Column 1. No VFAs were detected after day 129

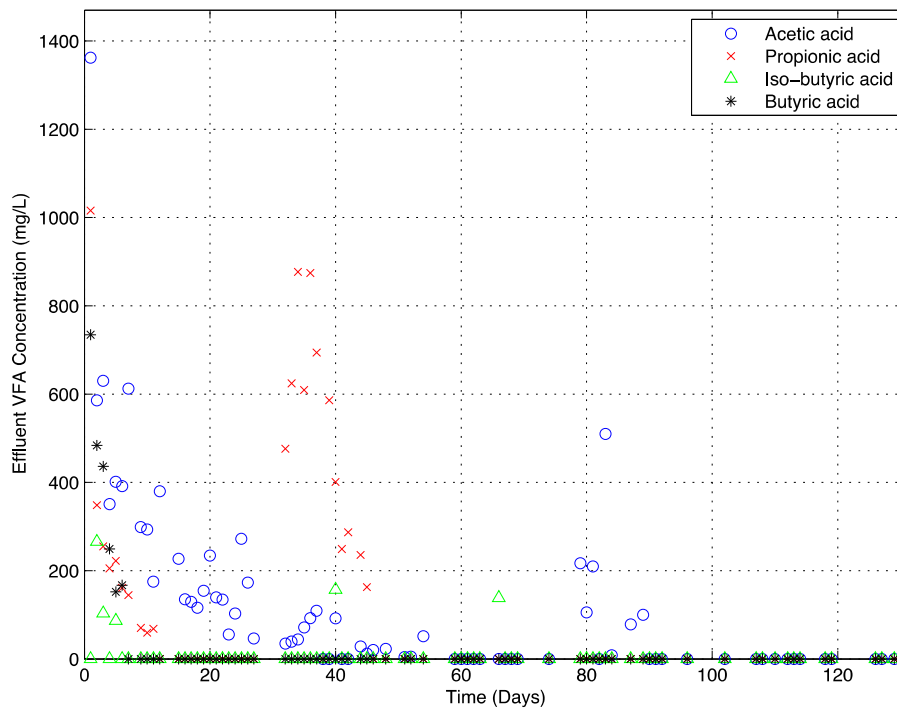


Figure 26: Volatile fatty acid concentrations detected in the effluent from Column 2. No VFAs were detected after day 111

The most likely explanation is that following the onset of organic carbon limitation, sulphate reduction rates decreased (Figure 23), thereby reducing the amount of sulphide and alkalinity generation. The presence of colloidal sulphur was detected, even in efficiently functioning reactors, indicating that sufficient oxygen was available for partial sulphide oxidation. As the sulphide concentration decreased the likelihood of complete sulphide oxidation to sulphate, with the associated proton generation, would increase. The significant increase in redox potential

observed (Figure 24) is consistent with this. Furthermore, as the pH decreased the speciation of aqueous sulphide would shift toward the more toxic $\text{H}_2\text{S}(\text{aq})$ species. Koschorreck (2008) reported 50% inhibition of sulphate reduction at H_2S concentrations as low as 1.8 mM (61 mg/l). Finally, as the redox potential became positive the ferrous iron in the feed could undergo oxidation, hydrolysis and ultimately precipitation as ferric hydroxide, with the release of three protons.

The column was re-inoculated with 50 ml of SRBR sludge on the 6th of June (day 176), but this failed to restart the sulphate reduction process. Furthermore, due to the poor performance over the preceding six months and low sulphide generation it was assumed that the sulphate reducing prokaryotes were unable to perform the BSR reaction due to a lack of freely available soluble organic carbon. Hence, the column was decommissioned in July 2012.

4.3.1.1 Relationship between pH and sulphur speciation

The fluctuations observed in the effluent sulphide concentration were more significant than expected, based on the sulphate reduction data. There was a dynamic relationship between measured sulphide concentration and the pH (Figure 27). When the pH increased to above pH 8 there was an associated decrease in measured sulphide on the same day or immediately thereafter. On day 288 the pH reached pH 8.5 and the sulphide concentration dropped to 1.3 mM (41.6 mg/l). Similarly on day 314 the pH reached a maximum of pH 8.9 and the sulphide concentration was reduced to 0 mM. However, the following day the pH fell to pH 7.65 and the sulphide concentration increased to 5 mM (160 mg/l). This was not due to analytical error or major fluctuations in performance, but rather the equilibrium reactions between the sulphur species generated and the protons. Due to the presence of a small amount of dissolved oxygen some of the sulphide was partially oxidised to elemental sulphur (Figure 28).

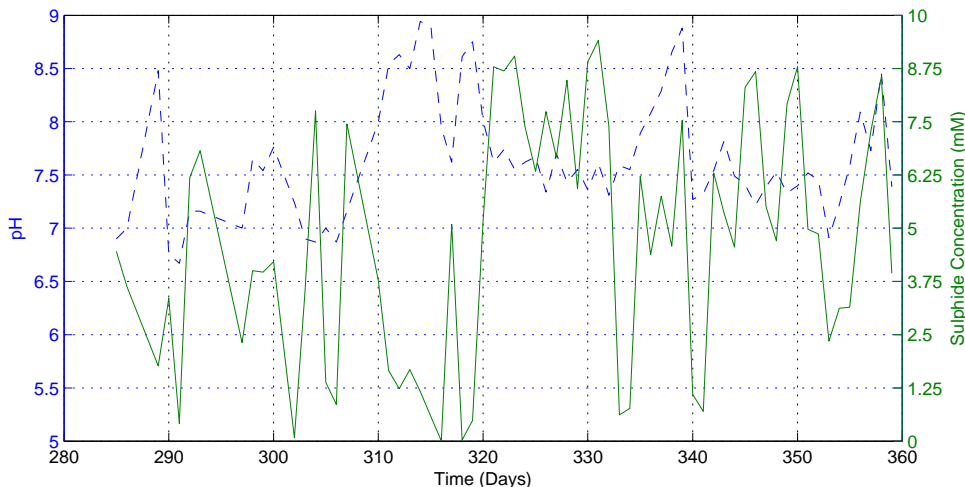


Figure 27: Relationship between the pH and sulphide concentration in the effluent from Column reactor 1. Dotted line represents pH and solid line sulphide concentration.

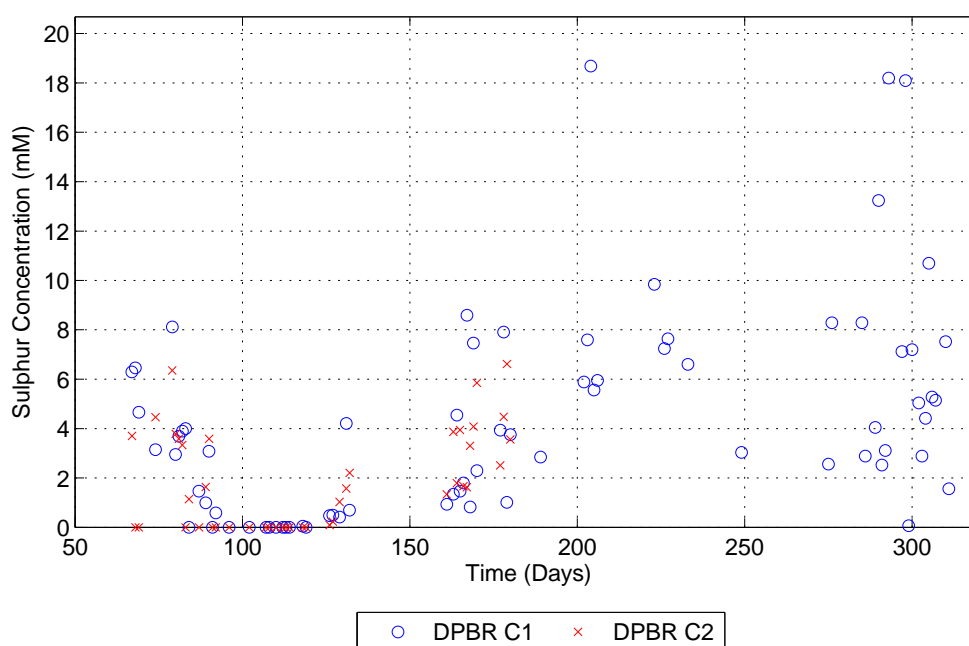


Figure 28: Colloidal sulphur concentration in the effluent from the column reactors. Circles represent Column 1 data and crosses Column 2

Under alkaline conditions ($\text{pH} > 8$) free bisulphide ions react with the colloidal sulphur to produce polysulphides of chain length (x) provided $x \geq 2$. In addition, bisulphide ions are also able to react with free hydroxyl ions to produce a polysulphide of chain length 2 (Kamyshny *et al.*, 2006). As a result of these reactions, the sulphide concentration appeared to be almost zero on days where the pH was particularly high, due to the majority of free bisulphide ions being converted to polysulphides. The polysulphide concentration was measured on day 311, yielding an S_2^{2-} concentration of 10.33 mM.

The effluent was also tested for the presence of colloidal sulphur over the (steady-state) period (day 60-310). Colloidal sulphur was present in varying concentrations from 0 to 18.3 mM (Figure 28). The colloidal sulphur concentration was significantly higher in Column 1 due to the higher solution pH. The mean colloidal sulphur concentrations were 6.85 and 2.13 mM for Columns 1 and 2 respectively. On day 203 the colloidal sulphur concentration increased to 18 mM following the decrease in pH, which caused majority of the polysulphides to decompose back to the constituents, bisulphide and colloidal sulphur. Therefore, there was an associated increase in the bisulphide concentration. The sulphur species formed as a result of the BSR process are therefore crucially dependent on the pH, colloidal sulphur concentration and hydroxyl ion concentration.



4.3.1.2 Liberation of volatile fatty acids from organic packing material

The reduction in sulphate removal efficiency in Column 2 coincided with the disappearance of VFAs from the column effluent (Figure 26), indicating the onset of carbon substrate limitation. In the column, the readily accessible, labile carbon lasted for approximately four months, releasing

acetic, propionic and iso-butyric acid. This was predominantly from the primary sewage sludge. A similar trend occurred in Column 1 (Figure 25) as there were no VFAs in the effluent stream after the first four months. However, Column 1 received sodium acetate in the feed, so there was a continuous supply of DOC to sustain some biological sulphate reduction.

In order to better understand the hydrolysis processes occurring within the packed columns, a reverse calculation was performed. The theoretical amount of acetic acid required to sustain the measured sulphate reduction was calculated. From Figure 29 it is clear that the amount of acetic acid supplied in the feed was significantly less than that required, while no acetic acid supplementation occurred in Column 2 (Figure 30). Hence, it can be concluded that break-down of the complex organic substrates did occur in both columns. Column 1 required an average concentration of 1100 mg/l (628.6 mg/l.day) of acetic acid to reduce the sulphate that was supplied at a rate of 1142.9 mg/l.day. Therefore, 291.2 mg/l.day of acetic acid was produced by hydrolysis of the organic packing material. On the other hand Column 2 required 216.7 mg/l.day of acetic acid which was obtained from hydrolysing the packing material.

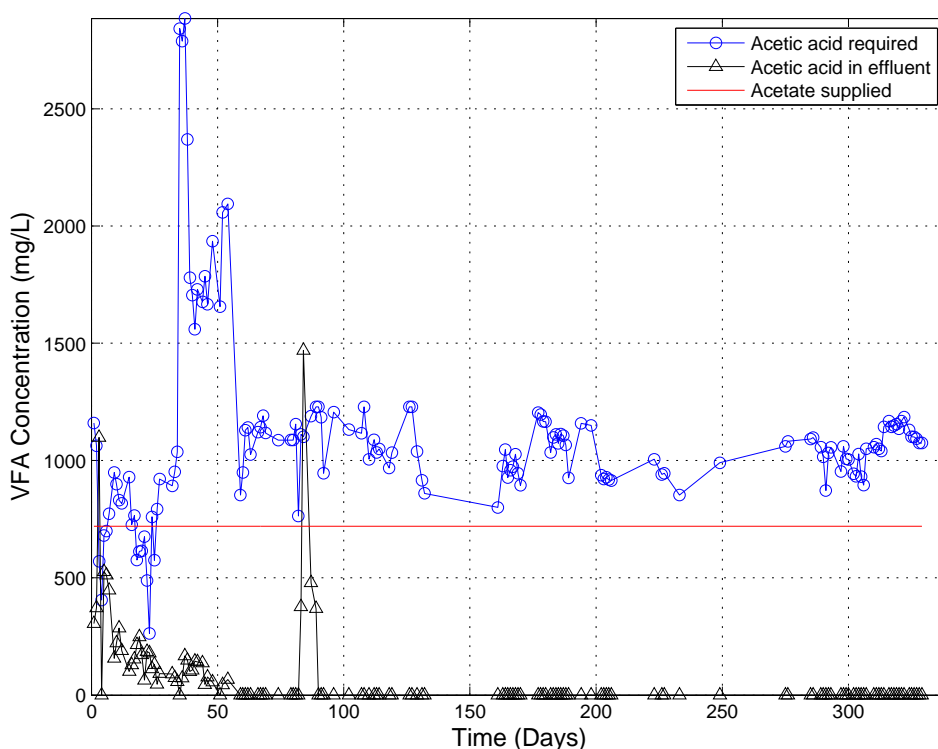


Figure 29: Acetic acid balance in Column 1. The discrepancy between the calculated acetic acid required to achieve the measured sulphate reduction and the acetate supplied in the feed represents acetate equivalents liberated from the packing material.

During the initial phase of operation the effluent from Column 2 contained an appreciable amount of VFAs, despite no supplementation of the feed. This suggests that the wet, primary sludge provided DOC more rapidly than the dry activated sewage sludge. Therefore, a column packed primarily with lignocellulosic material will not be ideal for a passive treatment BSR unit, due to the relatively slow hydrolysis. The composition of Column 1 packing material was 25% organic waste and 75% lignocellulosic material, whereas Column 2 had 1.89% organic waste and the remainder lignocellulosic materials.

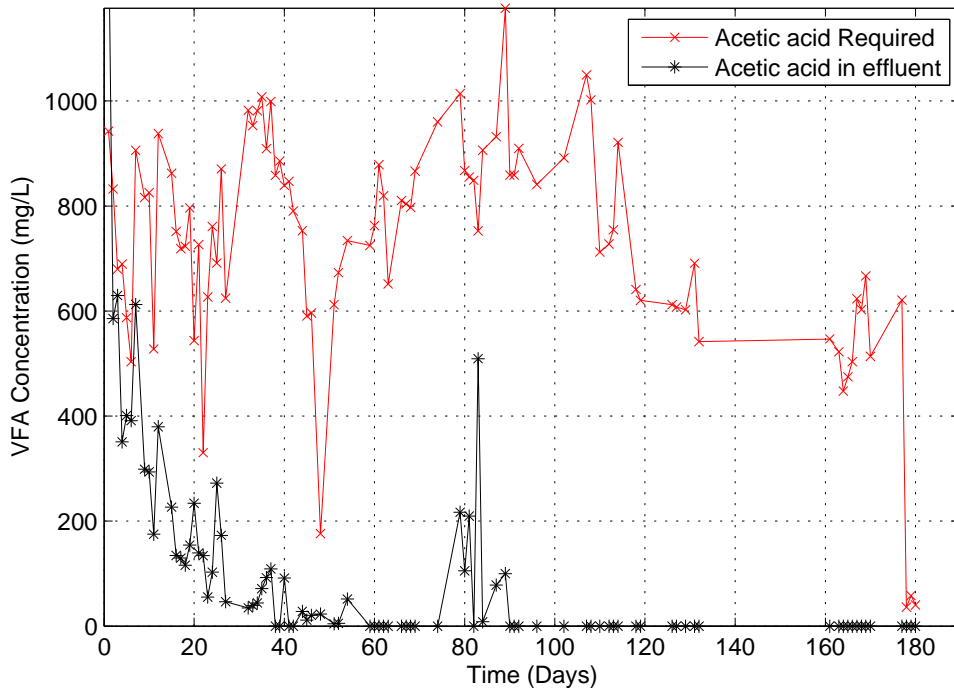


Figure 30: Acetic acid required to achieve the observed sulphate reduction in Column 2 and the measured concentration in the effluent. The sum represents the amount of acetic acid equivalents liberated from the packing material and molasses feed

Based on the amount of acetic acid required for the sulphate reduction, the corresponding amount of COD was calculated to be 1044 and 685 mg/l for Columns 1 and 2 respectively. The performance of the packed columns was ultimately dictated by the rate of VFA liberation. Based on the measured data, the mean COD:SO₄²⁻ was 0.52 and 0.34 for Columns 1 and 2 respectively. Given that the accepted theoretical ratio for optimum sulphate reduction is around 0.7, it is clear that complete sulphate removal from the packed columns was not possible. This analysis served as a motivation for the VFA liberation study that was conducted in parallel to the column work.

4.3.1.3 Relationship between organic carbon, colloidal sulphur and chemical oxygen demand

A COD analysis was conducted on the effluent from Column 1 and Column 2 (Figure 31). Filtered and unfiltered samples were tested. The data show often significant differences between the filtered and unfiltered samples, particularly in the effluent from Column 1. These data suggest the presence of particulate material contributing to the measured COD values. The cell densities, observed by light microscopy, were relatively similar in the effluent from each column, so could not account for the discrepancy observed in the Column 1 data. The data presented in Figure 29 and Figure 30 show the absence of soluble VFAs, so these could not contribute to the COD. The most likely explanation is the presence of colloidal sulphur in the effluent, which had been confirmed (Figure 28).

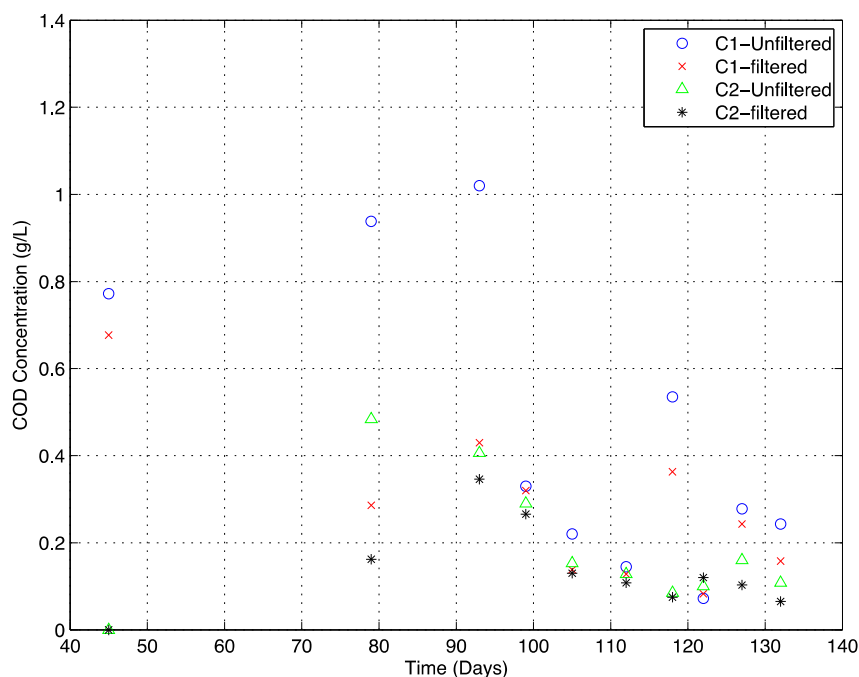


Figure 31: Chemical oxygen demand values of effluent samples from Column 1 and Column 2 over the period January to April 2012. Filtered and unfiltered samples were analysed

Sulphur can be oxidised to sulphate by the reagents used in the COD assay. Theoretically, one mole of sulphur would require two moles of oxygen to be fully oxidised. On a per mass basis, this would equate to 2 g COD per g sulphur oxidised. A control experiment was performed where an increasing mass of sulphur powder was added to successive COD reaction tubes and digested. The results showed conclusively that sulphur contributed to COD, with a linear relationship ($R^2 = 0.94$) between mass of sulphur and measured COD, however the COD values were significantly below the theoretical prediction, particularly when a higher mass was used. The sulphur powder is hydrophobic and it is likely that a portion of the sulphur floated on the liquid surface and was not digested. Evidence for this was visible in the tubes following digestion. Colloidal sulphur is fully suspended in the bulk liquid so would be more readily digested. In order to prove this conclusively a sample with a high colloidal sulphur concentration, quantified by HPLC, would have to be serially diluted and subject to a COD analysis, but this was not done during the current study. The likely relationship between colloidal sulphur and measured COD is best represented in Figure 32, which shows the analysis of effluent from Column 1 between day 198 and day 224. The data show that for most of the samples the colloidal sulphur could account for the majority of the measured COD. The remainder of the COD could be accounted for by cell biomass and organic molecules other than VFAs.

There is little comprehensive analysis of effluent from demonstration scale packed bed sulphate reducing reactors, with most confined to COD only. The potential contribution of colloidal sulphur, which should be present in most cases, has not been accounted for and may explain why relatively high COD values have been reported, despite a drop-off in sulphate reduction performance. The most common cause of the latter would be organic carbon deficiency, as demonstrated in this study.

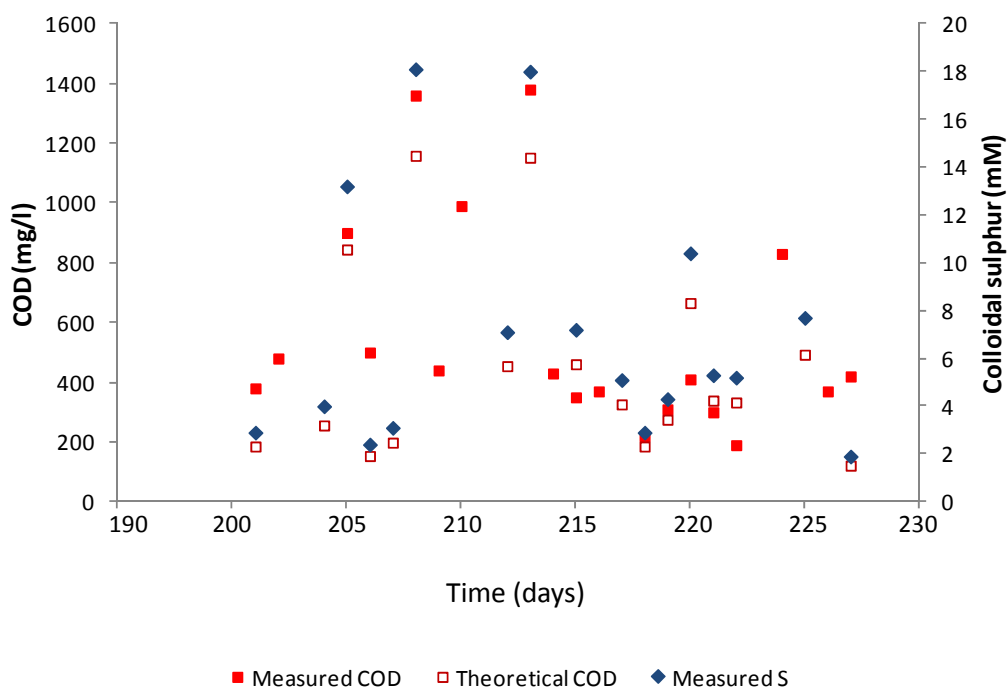


Figure 32: Relationship between measured colloidal sulphur, measured COD and theoretical contribution to total COD from colloidal sulphur for effluent from Column 1.

4.4 Linear flow channel studies

The performance data from selected linear flow channel studies will be summarised to highlight the potential of the system for sulphide oxidation. The focus of this study is on the kinetics of sulphide oxidation, specifically the importance of oxygen mass transfer into the reactive zone. The discussion will highlight the relationship between biofilm age and structure and sulphide oxidation rate and also between residence time and performance. Finally, a separate set of experiments, aimed at determining the oxygen mass transfer coefficient, will be described.

4.4.1 Definition of pseudo-steady-state

Steady-state is defined as a point in time when all process variables remain constant, except for minor fluctuations. Conventional ways of declaring steady-state within a chemical or biological system were not applicable, due to the unique characteristics of the LFCR. The primary reasons for not being able to use a conventional method of defining a steady-state are firstly, that the hydrodynamic regime within the reactor is extremely stratified, so process variables would vary with depth and length. Secondly, the flux of oxygen into the system is constantly changing due to the growth of the FSB, which acts as an impedance to the mass transport of oxygen. Therefore, pseudo-steady-state (PSS) is defined as the condition where the sulphide concentration increases with depth (y-direction) and a stable gradient is maintained. This implies that a stable hydrodynamic regime is in place and there is a constant steady flux of oxygen into the reaction (oxidation) zone.

4.4.2 Summary of the reactor hydrodynamics

The hydrodynamics of the linear flow channel reactor was studied in detail and has been reported previously (Van Hille *et al.*, 2012; Mooruth, 2013), but will be summarised below to assist with the interpretation of the data presented in this report.

The flow pattern was characterised in a series of tracer studies, using different concentrations of acid and base and a phenolphthalein indicator. The profile was confirmed using a sulphide solution.

The overall flow regime for the specific operating conditions could be characterised simply by the Reynolds number (Re). From the tracer experiments it was determined that there were two discrete flow regimes in the LFCR. The upper portion of the reactor was strictly laminar flow whilst, the lower portion had a laminar parabolic profile flow. The requirement for laminar flow in a circular tube is $Re < 2300$. From the tracer experiments it was determined that the Reynolds number range was, $0 < Re < 307$, hence the flow was extremely laminar. The lack of mixing exaggerated the effect of small differences in the density of the feed and bulk fluid.

The flow pattern was unconventional due to the heterogeneous nature of the fluid movement within the LFCR. The sulphide-laden fluid entered the reactor and caused some turbulent eddies in the bulk volume before sinking to the bottom of the channel due to the difference in density. There was some back mixing in the front corner of the reactor, thus confirming it as a dead-zone. The fluid then proceeded to move forward along the floor of the reactor with a laminar parabolic velocity profile. When it reached the back wall of the reactor, the fluid collided with the wall causing the laminar layer of feed to be displaced upwards. There was some mixing in the back corner resulting in a second dead-zone and movement of some of the feed back towards the entrance. This hydraulic regime is schematically represented by Figure 33 and Figure 34 shows an example of a typical tracer study. This particular flow pattern is governed by three factors, the first being laminar flow between 'two parallel plates', the second being density and lastly, advective and diffusive mass transport.

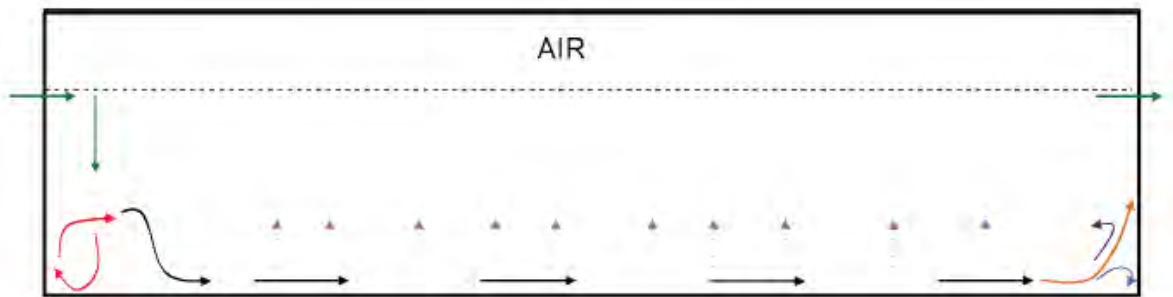


Figure 33: Schematic representation of fluid flow regime in the LFCR with various types of flow being displayed accordingly. The sinking influent (green arrows), entrance dead zone (red arrows), laminar parabolic flow (black arrows) and back corner dead zone (orange, maroon, blue arrows) are displayed. The smaller pink arrows represent the movement of fluid in the y-direction due to displacement from below

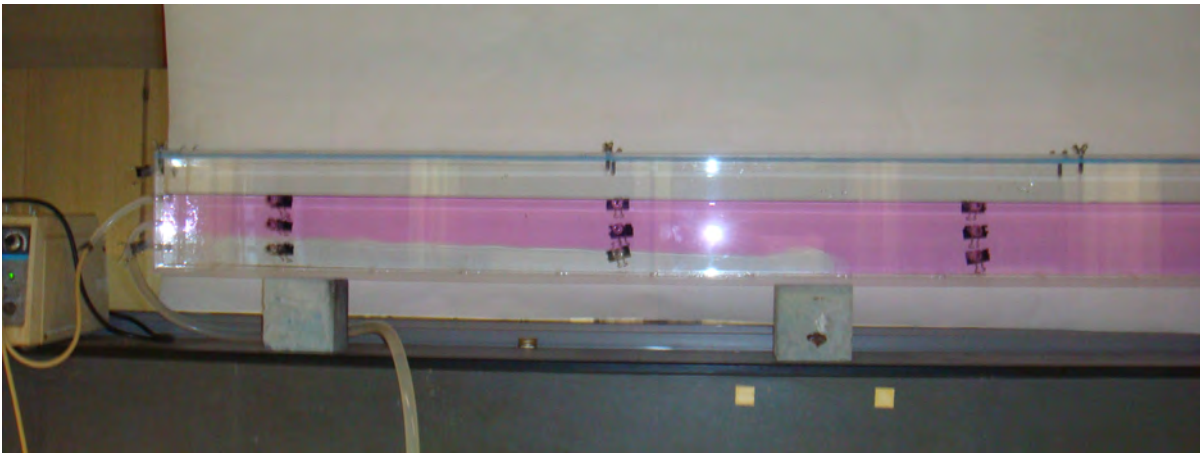


Figure 34: Example of a phenolphthalein tracer experiment showing discolouration of the indicator by the introduction of sulphuric acid into an alkaline solution. The relative density difference between the acid and alkaline solutions were similar to the sulphide feed and bulk liquid during LFCR operation

The consequence of the hydraulic regime is that the sulphide-laden feed entered the reactor, sank to the bottom and then displaced the overlying fluid by advective transport, with effluent leaving the reactor through the uppermost of the three exit ports. The reaction of sulphide with oxygen, penetrating the reactor from the surface, created the sulphide gradient that was used to determine pseudo-steady-state.

4.4.3 Overall performance and species balance

The initial experiments (runs 6 and 7) were performed with no acetate supplementation of either the initial reactor volume or the subsequent feed. The system relied entirely on organic carbon present in the packed bed reactor effluent, which was negligible. As a consequence the FSB formation was compromised. The biofilm was incomplete, not covering the entire surface of the reactor and while some sulphur was deposited the film was thin and brittle. The analysis of sulphur species showed that while essentially all the sulphide in the feed was converted, the primary product was sulphate. This was due to the formation of an incomplete biofilm, which did not present a sufficient barrier to oxygen mass transfer. This, coupled with the relatively low sulphide loading rate (6-10 mmol/day) resulted in a stoichiometric excess of oxygen and the complete oxidation, to sulphate, of a significant proportion of the sulphide. This highlighted the importance of organic carbon flux through the entire process. A microbial ecology study (Mooruth, 2013), using 16S ribosomal RNA gene sequence as the basis for identification of microbial species, revealed that the biofilm was dominated by autotrophic species. This was consistent with absence of soluble organic carbon and illustrated the importance of heterotrophic species in the development of a complete, structurally sound biofilm. Subsequent experiments were supplemented with acetate to support the heterotrophic community.

A summary of the results, specifically detailing the overall performance and sulphur species material balance for experimental runs 8 to 16-(2) is presented in Table 8. The performance of the LFCR was influenced by a number of factors, including how quickly a complete biofilm was established and PSS achieved, the sulphide oxidation rate and removal efficiency and finally, the quantity of sulphur that reported to the FSB.

Table 8: Summary of overall performance and distribution of sulphur species for the biological LFCR experiments

Experiment	HS ⁻ converted		HS ⁻ conversion (%)	Sulphur species (mmol)						Unaccounted for (%)
	HS ⁻ loading (mmol/d)	HS ⁻ converted (mmol)		Sulphate	Colloidal S	Biofilm S	Collapsed S	Polysulphide		
8	33.6	580.7	96.1	191.0	44.9	144.1	202.8	0	0.36	
9	29.7	498.3	93.3	317.7	(79.3) ¹	178.0	83.8	0	0.38	
10	60.5	572.7	82.2	33.0	6.7	527.0	0	4.0	0.36	
11	69.5	754.2	91.0	151.7	46.0 ²	501.8	0	16.2	5.2	
12	52.8	617.4	84.7	109.9	(60.5) ¹ 40.3 ²	480.7	0	0	7.9	
13	122.8	1023.7	85.0	269.8	(4.95) ¹	698.6	0	0	6.1	
14	111.5	879.0	80.7	113.9	27.8	660.1	0	0	9.2	
15 ³	56.8	378.8	93.5	299.8	(145.3) ¹	225.8	0	0	0.4	
16-(1)	98.9	452.6	65.2	71.7	119.4	122.1	0	0	36.4	
16-(2)	111.9	572.1	82.0	56.8	185.4	435.2	0	0	16.8	

¹ Values in parentheses must be considered negative with respect to the sulphur balance as this sulphur was further oxidised to sulphate

² Colloidal sulphur reacted with sulphide to form polysulphide, rather than being oxidised to sulphate

³ Experimental run 15 was conducted with an operating volume of 12.5 l in order to achieve a 12 hour residence time

Experimental run 8 was conducted at a four day residence time and PSS was established on the fourth day. A floating sulphur biofilm began developing on day one, and a sulphide removal efficiency of 96.1% was attained. However, the LFCR exhibited 'poor performance' due to the collapse of the FSB and loss of the sulphur deposits.

On the other hand experimental run 10 was conducted at a two day residence time and PSS was established on the fourth day. A lower sulphide removal efficiency (82.2%) was achieved as compared to experimental run 8. However, the FSB remained structurally intact over the duration of the experiment and a greater quantity of sulphur reported to the biofilm, representing a more efficient overall performance. Lastly, experimental run 15 was conducted at a half day residence time and PSS was established on day one. A floating sulphur biofilm was formed within the first day and a high sulphide removal efficiency of 93.5% was achieved. However, a significant proportion of the deposited sulphur fell into the bulk liquid due to delamination of the lower layers of the FSB. A portion of this sulphur was oxidised fully to sulphate and a large proportion of sulphide was oxidised completely to sulphate. The sulphur material balance was closed to within 0.18% percent difference (S%) between the measured sulphide converted and sum of the sulphur species products. This experiment clearly exhibited numerous phenomena associated with of a 'poor performing' LFCR.

In an effort to close the sulphur species material balance, the headspace gas exiting the reactor was passed through a sodium hydroxide (3 M) scrubber to trap any H₂S gas that may have been liberated. The sulphide concentration in the solution was measured several times during and at the end of each experimental run. However, no sulphide was detected in the scrubbing solution, confirming that there was negligible liberation of H₂S gas from the LFCR surface.

The highest sulphide conversion efficiency was achieved in experimental run 8 (96.1%), although a significant portion of the oxidised sulphide was converted to undesirable products. The lowest sulphide conversion was 65.2% in experimental run 16-(1). There was no definitive relationship between sulphide conversion and sulphide loading or residence time, due to numerous factors influencing the overall performance of the LFCR. Nevertheless, the sulphur recovery in the LFCR was consistently higher than that achieved in the GARL study (Van Hille *et al.*, 2012), confirming that the original reactor configuration was inefficient. Furthermore, these results clearly illustrate the fact that the LFCR reactor becomes oxygen limited and is unable to achieve a 100% sulphide removal efficiency. However, sulphide conversion to elemental sulphur in the FSB is the true measure of the performance of the LFCR, as it is more beneficial to harvest the sulphur than for it to remain as colloidal sulphur.

4.4.4 Sulphide oxidation rate

The sulphide oxidation rate was measured for all experimental runs. Experimental runs 8 and 9 were conducted at a four day residence time, with acetate addition to the initial volume in the reactor, but no further supplementation in the feed. Both experiments were at unsteady-state from day one to three, during which time the sulphide oxidation rate increased steadily to reach a maximum of approximately 1.7 and 2.0 mmol/ℓ.day (56 and 66 mg/ℓ.day) respectively (Figure 35).

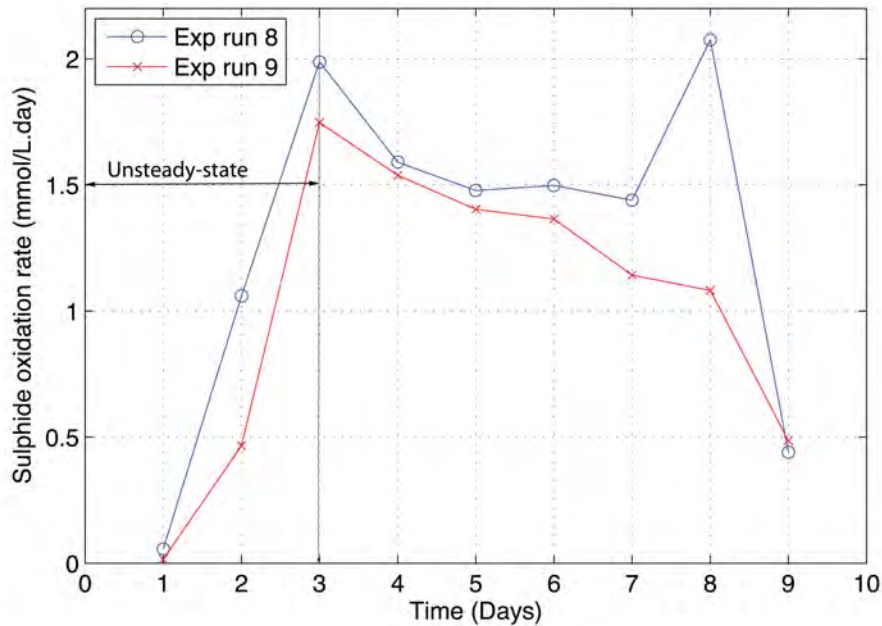


Figure 35: Mean daily sulphide oxidation rates across the LFCR for experimental runs 8 and 9. Experiments run at a 4 day HRT and sulphide loadings of 33.6 and 29.7 mmol/d respectively

Once pseudo-steady-state had been achieved, on day four, the sulphide oxidation rate decreased steadily over the subsequent six days. This clearly shows that once a floating sulphur biofilm is established the oxygen mass transport is impeded, resulting in a decrease in the sulphide oxidation rate. The impedance of oxygen mass transfer is necessary to ensure that sulphur is the primary product. During unsteady state, while the biofilm is still developing, oxygen mass transfer is not significantly impeded and a greater proportion of the sulphide is completely oxidised to sulphate. The data highlight the need to optimise the harvesting frequency in order to maintain sulphide conversion at an optimal level.

A similar trend was observed for the two day residence time studies. The trends for experimental runs conducted at one and a half (run 16-(1) and 16-(2)) and one day residence time (runs 13 and 14) differed slightly from the trends observed previously. The biofilm formed more rapidly, so the unsteady state period was shorter. The rate of sulphide oxidation appeared to increase during the first few days of PSS, which would contrast with the model of increasing oxygen impedance as the biofilm developed. However, the observed trend was primarily a function of fluctuation in the feed sulphide concentration. An example of this, for run 14, is presented in Figure 37.

The phenomenon of decreasing oxidation rate with biofilm age does still hold. The performance peaks on day 7, where 97% of the sulphide in the feed (6 mM) is oxidised. On day 8 this decreases to 86% (feed concentration 5.8 mM) and by day 9 to only 68%, despite a reduction in feed concentration to 2.6 mM.

These data sets summarise the overall performance of the LFCR under different conditions. The sulphide oxidation rate fluctuates significantly during an operational cycle, increasing during the unsteady-state phase, where the relatively unimpeded oxygen mass transfer results in the formation of a significant amount of undesired products and steadily decreasing once pseudo-steady-state is established. The decline in the rate was primarily due to the deposition of sulphur in the biofilm, increasing the resistance to oxygen mass transfer and decreasing the overall oxygen mass flux. The sulphide oxidation rate, in most cases, declined to a minimum within four residence times after PSS was reached. Therefore, it would be advantageous to harvest the FSB after

approximately three to four residence times to maintain a high sulphide oxidation rate and high sulphur recovery, as was demonstrated in experiment 16.

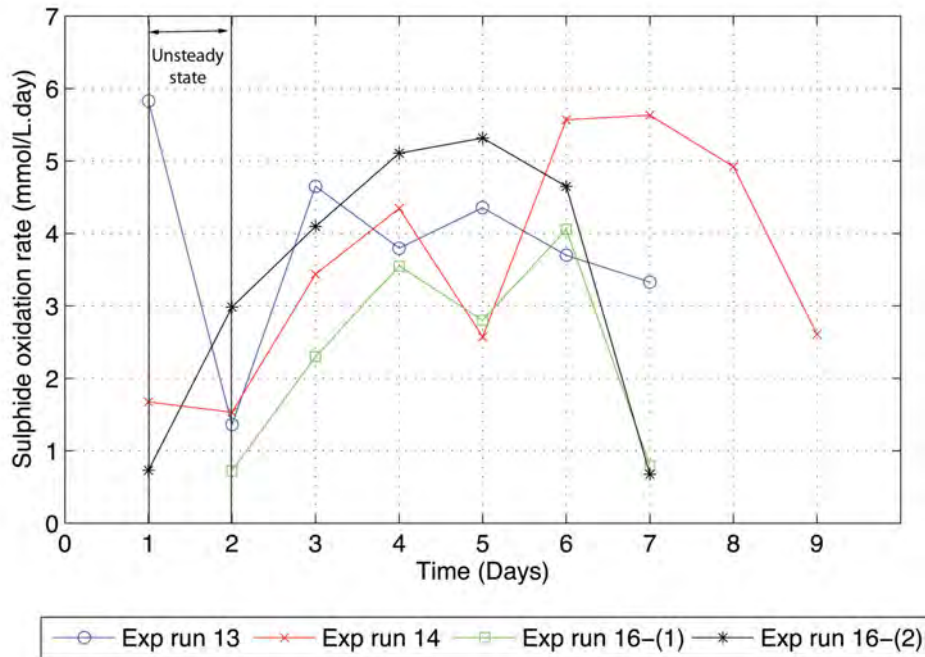


Figure 36: Mean daily sulphide oxidation rates across the LFCR for experimental runs 13, 14 and 16. Runs 13 and 14 were performed at a 1 day HRT and sulphide loadings of 122.8 and 111.5 mmol/d respectively, while runs 16-(1) and 16-(2) were consecutive, separated by a biofilm harvest. Sulphide loading rates were 98.9 and 111.9 mmol/day respectively

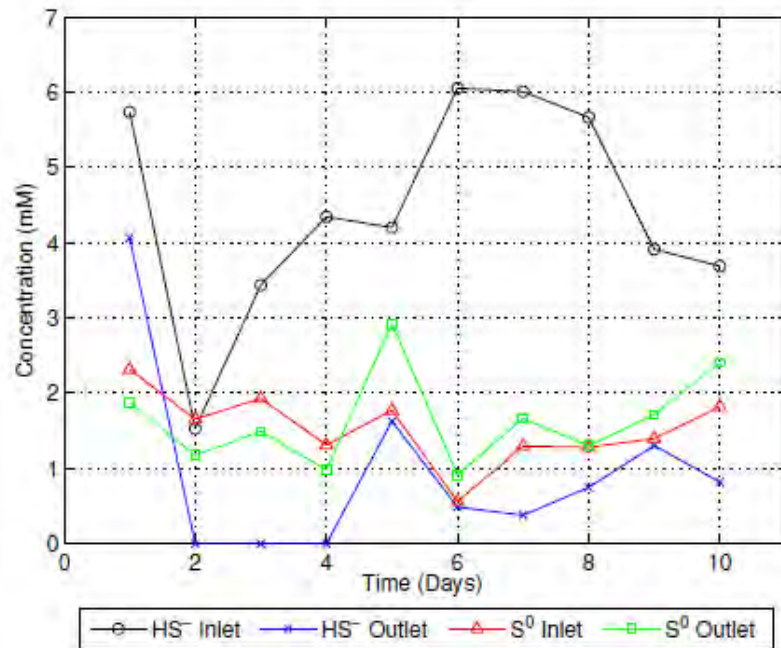


Figure 37: Feed and effluent sulphide and colloidal sulphur concentrations (mM) for the duration of experimental run 14

4.4.5 Relationship between residence time and sulphur yield

The sulphur yield is the primary measure of system performance. The two best performing experimental runs were 10 and 14, which showed the highest sulphur yield, while at the same time minimising the amount of sulphide completely oxidised to sulphate. Optimum performance was associated with a relatively consistent feed composition and rapid establishment of a complete biofilm.

Experimental run 10 was run at a two day residence time and achieved an 82.2% sulphide conversion, with 92% of the converted sulphide reporting as solid sulphur in the FSB. The average sulphide loading rate was 60.5 mmol/day (Table 8). While the average sulphide conversion was approximately 10% lower than runs 8 and 9, the overall efficiency of the LFCR was increased three fold, due to the rapid formation of a fully developed FSB, facilitating greater sulphur accumulation and minimising the conversion of sulphide to sulphate. In addition, less colloidal sulphur was formed (1.2% of converted sulphide) due to the more compact FSB structure, which prevented the penetration of sufficient oxygen to support sulphide oxidation in the bulk fluid. The impact of residence time on FSB structure will be explained in more detail in a subsequent section. The contour plots revealed that a steady sulphide gradient was maintained within the reactor throughout the duration of the experiment. This was achieved by maintaining a relatively consistent volumetric sulphide loading rate. The sulphate concentration in the feed was consistently below 9 mM (860 mg/l) due to the efficient operation of the upstream packed bed at the time of the experiment (Figure 38). The mean sulphide concentration in the feed was approximately 5.03 mM (166 mg/l) and sank to the reactor floor, even though the bulk fluid had a greater proportion of dissolved sulphate. This was due to the fact that the (mass) ratio of sulphide to sulphate was 1:4, hence the relative density difference (RDD) was 0.00019 g/cm³. By comparison, during run 9 the (mass) ratio of sulphide to sulphate was 1:28, with a RDD of -0.0006113 g/cm³.

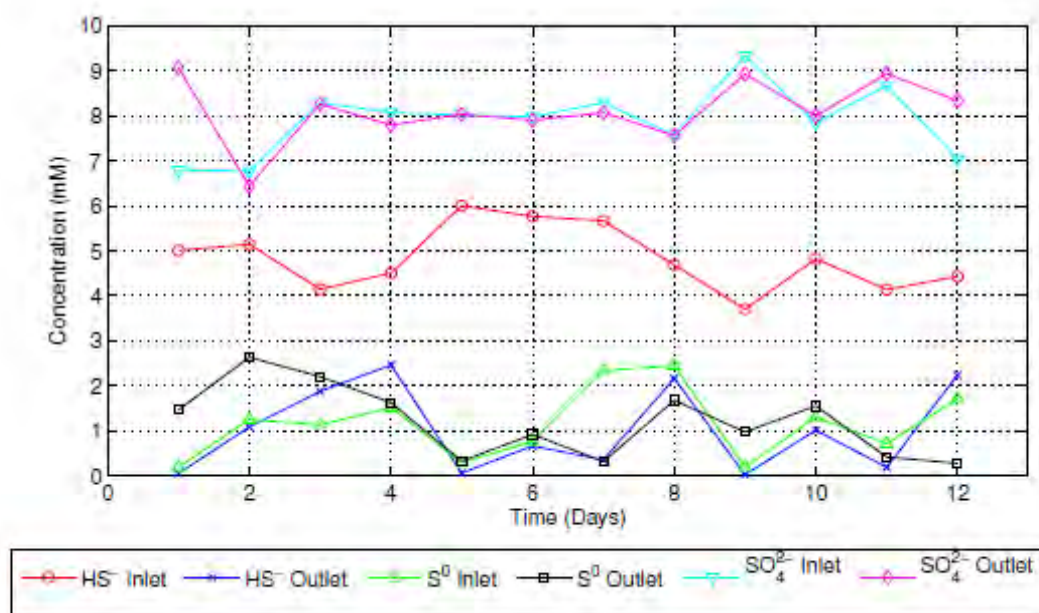


Figure 38: Feed and effluent sulphide and colloidal sulphur concentrations (mM) for the duration of experimental run 10

In summary, during experimental run 10 the floating sulphur biofilm was able to retain 527 mmoles (67.5 g/m²) of sulphur, which was substantially higher than previous experiments, whilst minimising unwanted by-product formation.

Similarly, in experimental run 14 pseudo-steady-state was attained on day two and the mean sulphide concentration in the feed was 4.46 mM at a loading rate of 111.5 mmol/day (Figure 37). The feed composition was less consistent, with a greater degree of fluctuation in sulphide concentration. The overall sulphide conversion was 80.7% with 75.1% of the converted sulphide reporting to the FSB as sulphur. The amount of sulphate formed (113.9 mmol) was relatively low, accounting for just under 13% of the converted sulphide. A small amount (3.2%) of the sulphide was converted to colloidal sulphur. A total of 9.2% (77.2 mmol) of the converted sulphide could not be accounted for. This was most likely converted to thiosulphate and polysulphides, as the bulk fluid had a green-yellowish colour just below the surface of the FSB on day one and four. The influent pH was high (pH 9.14 and pH 8.79) on the respective days, which favoured the production of polysulphides. Colloidal sulphur was consistently present in the feed (0.8-2.3 mM) and could be converted to polysulphides when the pH was sufficiently high. However, the formation of a robust FSB ensured sulphur was the primary product. The biofilm was able to accumulate 660.1 mmol (84.5 g/m²) of sulphur. This was significantly greater than experimental run 10, due to the lower residence time and consequently greater volumetric sulphide loading rate.

A linear relationship between sulphur yield and residence time was determined, which showed that a decrease in residence time, down to one day, led to an increase in sulphur recovery (Figure 39).

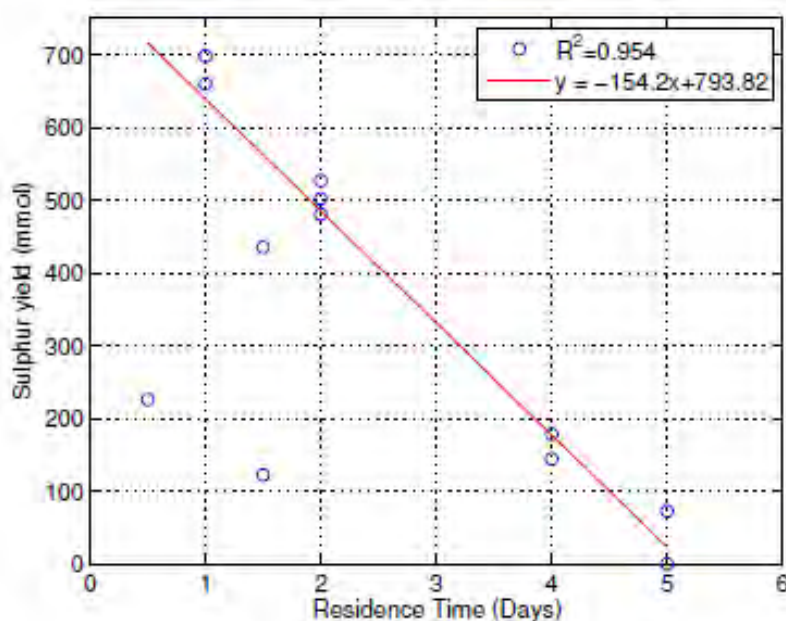


Figure 39: Relationship between sulphur yield and residence time for the series of LFCR experiments. The two points in the bottom left quadrant were omitted when determining the relationship

The data from the study at a 0.5 day residence time (run 15) and the first part of run 16 were excluded when determining the mathematical relationship. During run 15 the biofilm delaminated due to lack of structural integrity, while the harvesting of the biofilm at the end of the first part of run 16 was ineffective and a substantial portion collapsed and sank to the reactor floor, so could not be quantified. The constant (m) is essentially represented by Equation 14.

$$m = \dot{V}_{S_2} \times V_{\text{reactor}} = -154.2 \text{ mmol/day} \quad \text{Equation 14}$$

Dividing the constant by the reactor volume showed that the sulphur yield decreased by 6.2 mmol/l for each one day increase in residence time. Hence, there is an inverse relationship between residence time and sulphur recovery, assuming relatively similar sulphide concentrations in the feed. There was a decrease of approximately 10% in sulphide removal at the lower residence times (1-1.5 days), due to insufficient oxygen provision. The sulphide exited the channel as unreacted HS^- , rather than an undesirable by-product. The associated benefit of increased sulphur recovery is significantly more desirable and the sulphide conversion efficiency could be improved by a small increase in reactor surface area. The linear relationship did not hold below a one day residence time, due to the reduced sulphur recovery at a shorter residence time. The primary reason was that sulphur was deposited in the biofilm faster than the organic backbone could be laid down, resulting in decreased structural integrity and delamination of the biofilm layers, with the lower layers sinking to the reactor floor.

4.4.6 Relationship between residence time and complete oxidation of sulphide

The optimisation of the LFCR operating conditions to maximise the conversion of sulphide to sulphur should minimise the complete oxidation of sulphide and elemental sulphur to sulphate. This is achieved by ensuring the rapid formation of a compact biofilm, such that the mass transfer of oxygen into the reactive zone is regulated. The relationship between residence time and sulphate production is presented in Figure 40. The data represent the complete oxidation of sulphide to sulphate, as well as the oxidation of sulphur from the FSB to sulphate. It does not include the oxidation of colloidal sulphur in the feed to sulphate, primarily due to the fact that colloidal sulphur in the feed could not be controlled, so there was no consistent relationship.

It was demonstrated that the optimum residence time in the LFCR was approximately two days (2.18 days), at which less than 8% of the sulphide was fully oxidised. Sulphate production was highest at the higher residence times (4-5 days) and to a large extent was due to the complete oxidation of sulphide to sulphate. The 'poor performance' could be attributed to slow or incomplete biofilm formation and also the production of an overly porous biofilm. In addition, if the biofilm does not have the structural integrity to support the mass of deposited sulphur and collapses, partially or completely, oxygen penetration would increase.

The early runs (8 and 9), at the longer residence time, did not receive acetate supplemented feed, so when the acetate in the original reactor volume was consumed the system became carbon limited. This affected the structure of the biofilm. In addition, the lower sulphide loading resulted in slower deposition of sulphur in the biofilm and so the impedance of oxygen mass transfer was initially less efficient, resulting in the high overall sulphide oxidation efficiency, but also the increased incidence of complete oxidation. At the low end of the residence time scale, the sulphur was deposited into the biofilm faster than the organic backbone could be generated, resulting in loss of structural integrity, delamination and biofilm collapse.

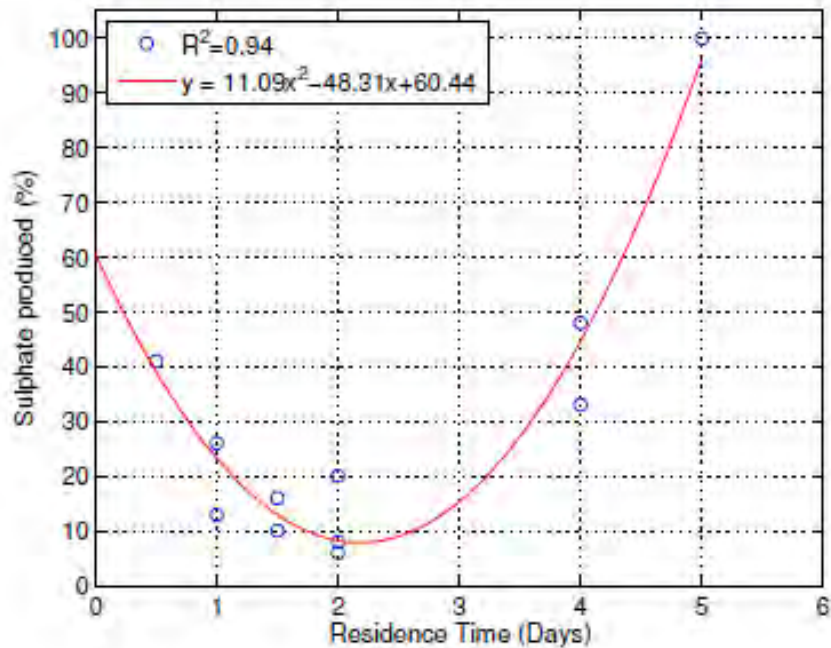


Figure 40: Relationship between residence time and complete oxidation of sulphide to sulphate. The sulphate produced value excludes the oxidation of colloidal sulphur in the reactor feed

4.4.7 Carbon species material balance

The preceding sections have focused on the overall performance of the system and the relationship between residence time and process parameters. The discussion has highlighted the importance of biofilm formation and structural integrity and how these were compromised under organic carbon deficient conditions. For experimental runs 8-10 acetate was added to the initial reactor volume to promote biofilm formation, but was not supplemented in the feed continuously. This had an impact on the structure of the biofilm that formed and will be discussed in greater detail in a subsequent section. The feed to experimental runs 11-16 were supplemented with acetate and these data will be used to determine the minimum amount of acetate equivalents to sustain optimal LFCR performance.

The data from the experimental runs are summarised in Table 9. The data show a general trend of increasing acetate utilisation rate with decreasing residence time. However, when the utilisation was recalculated to make consumption independent of residence time the majority of the experiments showed the consumption of between 0.1 and 0.2 g acetate/l feed. The values were higher for experimental runs 12 and 14, possibly in response to the increased loading. The data suggest that the feed to the LFCR needs to have a minimum organic carbon load equivalent to 0.1 g/l acetate. This is substantially higher than the measured acetate concentrations in the effluent from the packed bed reactors after the first month of operation (Figure 29 and Figure 30).

Analysis of the acetate data on a daily basis revealed that acetate utilisation was not constant as a function of time, but followed a relatively cyclical pattern with an increase around the establishment of PSS and then a decrease over subsequent days, followed by a second increase. For experimental run 12 the pattern was repeated three times. This suggests that organic carbon is required in greater amounts at certain times during biofilm development. The detailed analysis of biofilm structure suggested that the biofilm was laid down in layers, which would be consistent with a cyclical increase in carbon assimilation.

Table 9: Acetate material balance for the LFCR experimental runs 11-16

Run	RT (days)	Feed concentration (g/l)	Mean utilisation (%)	Acetate used (g)	Utilisation rate (g/l.day)
11	2	0.99	15.9	15.7	0.053
12	2	2.26	15.3	99.1	0.283
13	1	1.17	9.0	26.5	0.106
14	1	2.24	17.0	115.3	0.461
15	0.5	0.86	7.4	12.38	0.141
16 (1)	1.5	1.24	10.3	24.18	0.123
16 (2)	1.5	1.77	10.5	31.5	0.160

4.4.8 Floating sulphur biofilm analysis

At the end of each experimental run small sections of the biofilm were sampled and prepared for analysis by SEM. The remainder of the biofilm was harvested and used to determine the composition.

4.4.8.1 Chemical composition of the biofilm

A decrease in residence time led to an increase in the relative proportion of sulphur in the FSB. However, an increase in the organic loading rate did not lead to a proportional increase in the organic content of the FSB. At a four day residence time the average sulphur content was 52.6%, while at a two day residence time it increased to 88% and reached a maximum of 94% at 12 hours (Figure 41). Therefore, as residence time decreased there was an increase in the amount of sulphur deposited in the FSB. As a result the FSB became mainly inorganic. The organic carbon content of the biofilm decreased with a decrease in residence time, despite the acetate utilisation data showing a slight increase, suggesting that the rate at which the organisms can lay down the organic carbon backbone of the biofilm is significantly slower than the rate at which sulphide can be oxidised. This is consistent with the observation at the 12 hour residence time, where the biofilm collapsed due to insufficient structural integrity.

For the experiments where the feed was supplemented with acetate only a small fraction of the acetate that was utilised could be accounted for as organic carbon in the biofilm. For example, for experimental run 12, 99 g of acetate (40.3 g carbon) was utilised, but the organic carbon content of the FSB was only 2.1 g of carbon. Therefore, the vast majority of the acetate was consumed for cell metabolism and proliferation of cells not associated with the biofilm. Heterotrophic organisms are capable of acetate assimilation via the glyoxylate or tricarboxylic acid cycle, thus forming CO₂ as a by-product. Therefore, a more comprehensive carbon balance would be necessary to determine the evolution of CO₂ to the atmosphere. Under alkaline conditions much of the evolved CO₂ would dissolve and speciate to bicarbonate (HCO₃⁻). This too could be quantified in future studies. Similar trends were observed in the other experimental runs (Table 10). This confirmed that a relatively pure sulphur product could be recovered when the reactor was run optimally. The values for run 15 and 16 (1) are represent only that portion of the biofilm that was successfully harvested, so are not representative of how much sulphur was actually formed. For run 15 the biofilm delaminated and the lower layers collapsed and could not be recovered, while for run 16 (1) the attempt to harvest the biofilm by skimming it off the surface was not successful and caused the majority of the biofilm to crumble and sink.

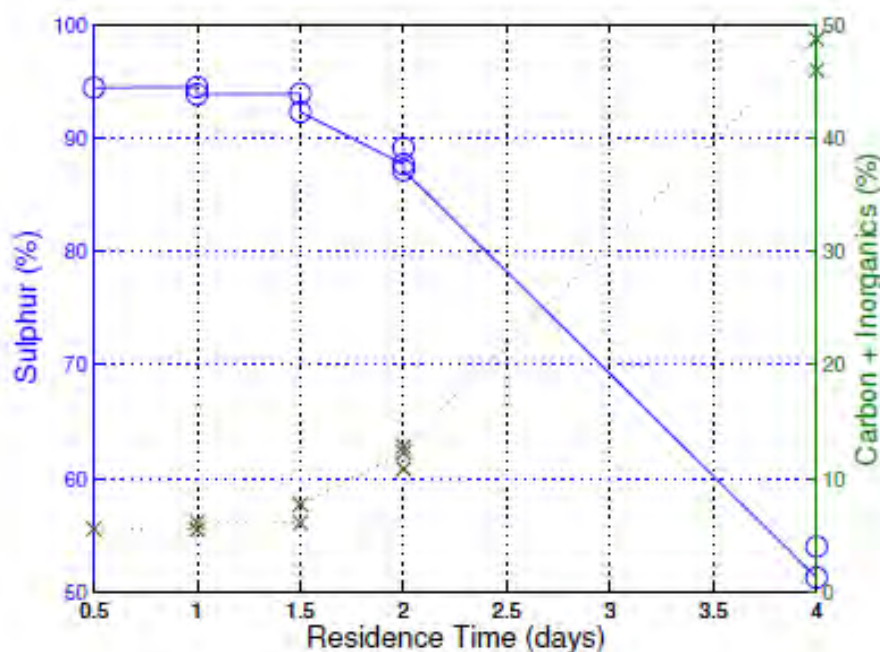


Figure 41: Relative proportion of elemental sulphur (○) versus organic carbon (×) and inorganic salts in the FSBs harvested at the end of each experimental run

Table 10: Elemental composition of the FSB from experiments 8 to 16 (2). The sulphur content represents elemental sulphur and excludes sulphate salts

Experimental run	Sulphur (g)	Carbon (g)	Inorganic salts (g)
8	4.61	4.38	0
9	5.70	4.63	0.22
10	16.86	2.24	0.13
11	16.06	1.64	0.32
12	15.38	2.14	0.12
13	22.36	0.80	0.34
14	21.12	1.09	0.29
15	7.23	0.16	0.26
16 (1)	3.91	0.42	0.05
16 (2)	13.93	1.11	0.05

4.4.9 Analysis of biofilm structure

Visual observations, confirmed by SEM analyses, showed that the floating sulphur biofilms were extremely heterogeneous structures, made up of extracellular polymeric substances (EPS), sulphur, inorganic precipitates, water, cells and cell clusters. Flemming and Wingender (2010) described the EPS matrix as a network providing sufficient mechanical stability to maintain a spatial arrangement for micro-consortia over a prolonged period. This stability is provided by the hydrophobic interactions, cross-linking by multivalent cations and entanglement of the biopolymers. Furthermore, they showed that the presence of Ca^{2+} ions increased the mechanical stability of mucoid *Pseudomonas aeruginosa* biofilms. This effect was explained by the Ca^{2+} ions cross-linking polyanionic alginate molecules, thereby increasing the mechanical strength of the EPS matrix. Hydrogen bonding and Van der Waals interactions between the biopolymers also increase the structural integrity of biofilms. Furthermore, it has been shown that Ca^{2+} ions influence the

hydraulic conductivity of biofilms, and cause increased retention of colloids with an increase in biofilm growth (Morales *et al.*, 2007).

Sulphur was formed by biological sulphide oxidation as well as chemical sulphide oxidation. Evidence of chemical sulphide oxidation is shown in Figure 42, where large rhombic sulphur crystals (98 μm) were identified on the underside of the FSB.

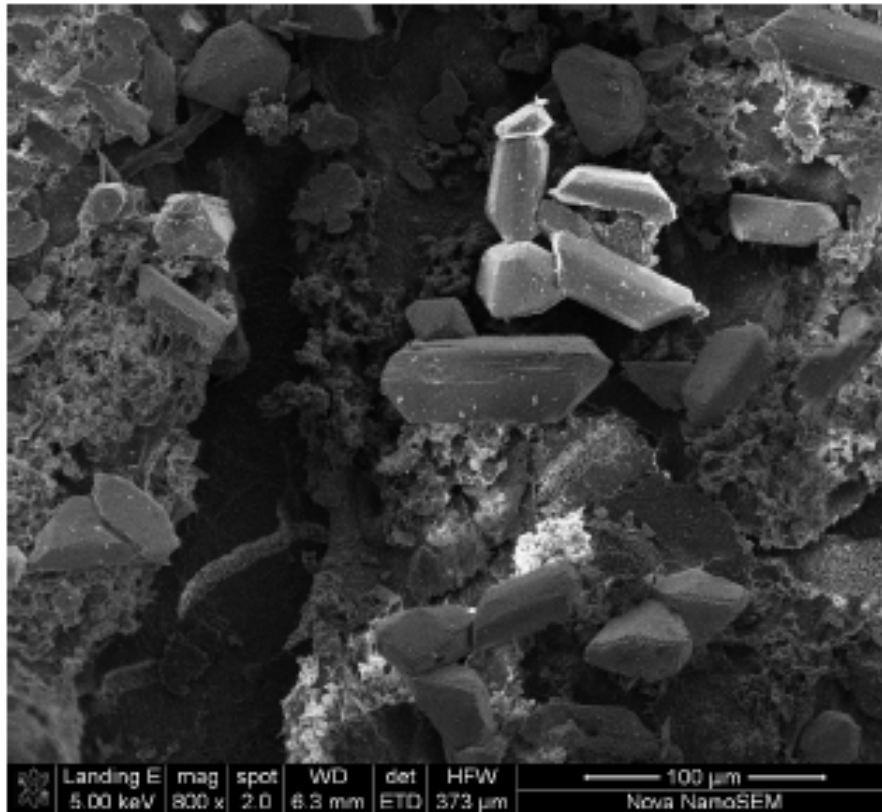


Figure 42: Rhombic sulphur crystals attached to the underside of the biofilm showing evidence of chemical sulphide oxidation

The relationship between residence time and floating sulphur biofilm thickness was investigated. The thickness of the FSB was determined by SEM analyses. The thickest FSB (407 μm) was generated at a two day residence time, whilst the thinnest FSB (134 μm) was generated at a 6.5 day residence time. At a two day residence time the FSB formed in layers, and had well defined boundary edges. Furthermore, layers where sulphur deposition was particularly dense could be clearly seen in the SEM images (Figure 43).

A similar trend was observed in the 1 and 1.5 and 0.5 day residence time biofilms (Figure 44), they were extremely dense and rich in sulphur, with a clear defined structure.

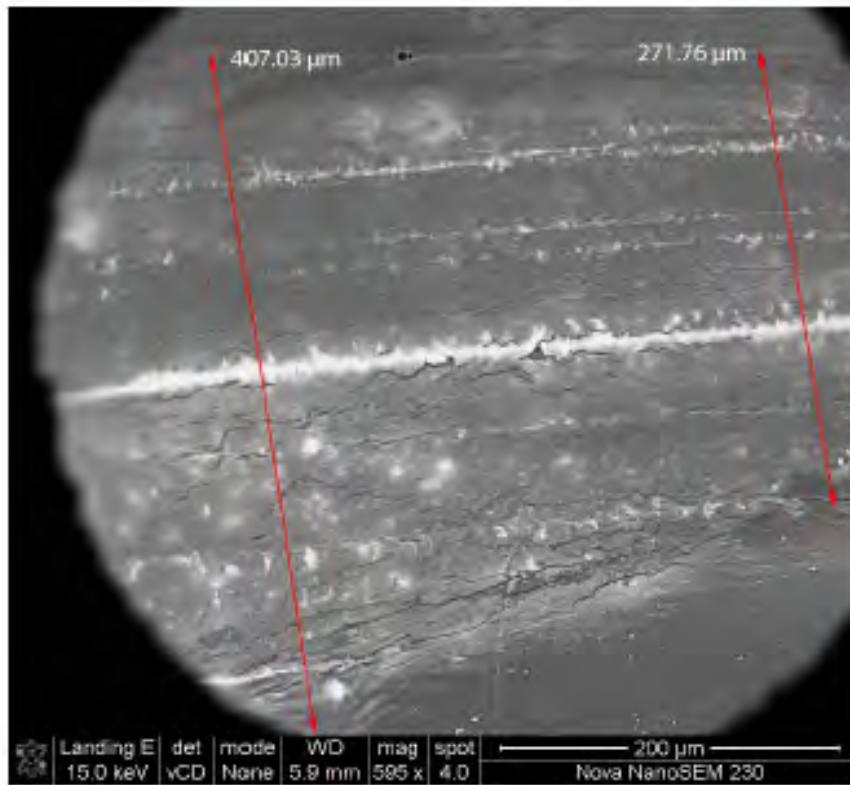


Figure 43: Cross-sectional SEM of part of the biofilm sampled from experimental run 12 (two day residence time). The biofilm thickness is annotated on the image. Discrete layers are clearly visible, as are areas of dense sulphur deposition (bright white)

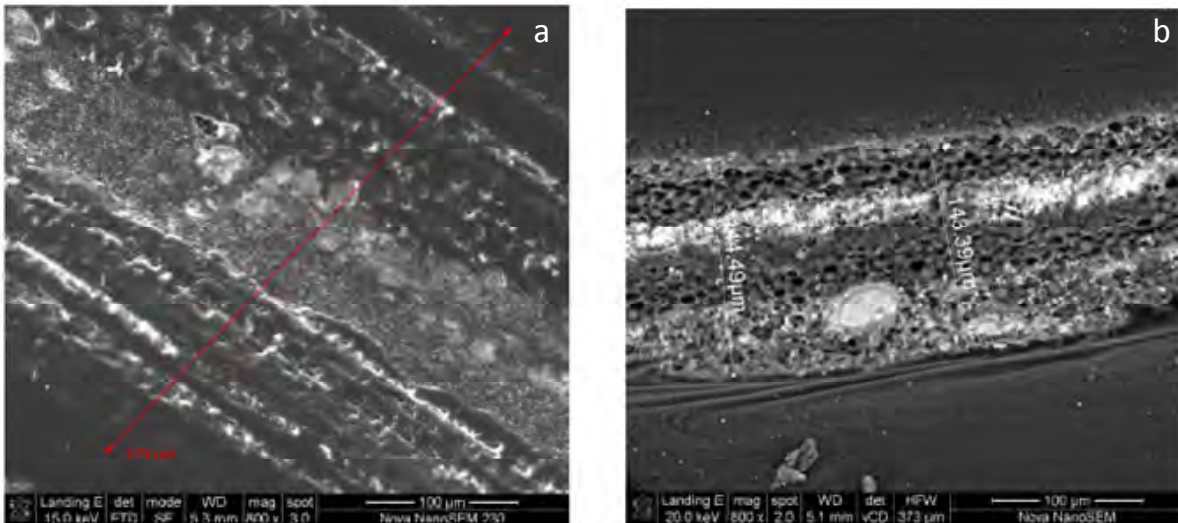


Figure 44: Cross-sectional SEM images of biofilm sampled from experimental runs 14 (a) and 16 (2) (b) showing discrete layers and areas of dense sulphur deposition

Evidence from the operation of the reactors suggested that the biofilm had relatively high structural integrity in the axial direction, but less so in the vertical direction, with delamination observed in a number of cases. Evidence from the cross-sectional SEM images suggests that the parallel layers are held together by strands of EPS. An example of this is presented in Figure 45.

By contrast, the structure of the biofilms formed when the reactor was run at longer residence times was very different. A complete biofilm was observed on the reactor surface and the upper

layer was relatively well defined. However, the lower part of the FSB was poorly defined, with no clear visible edge (Figure 46).

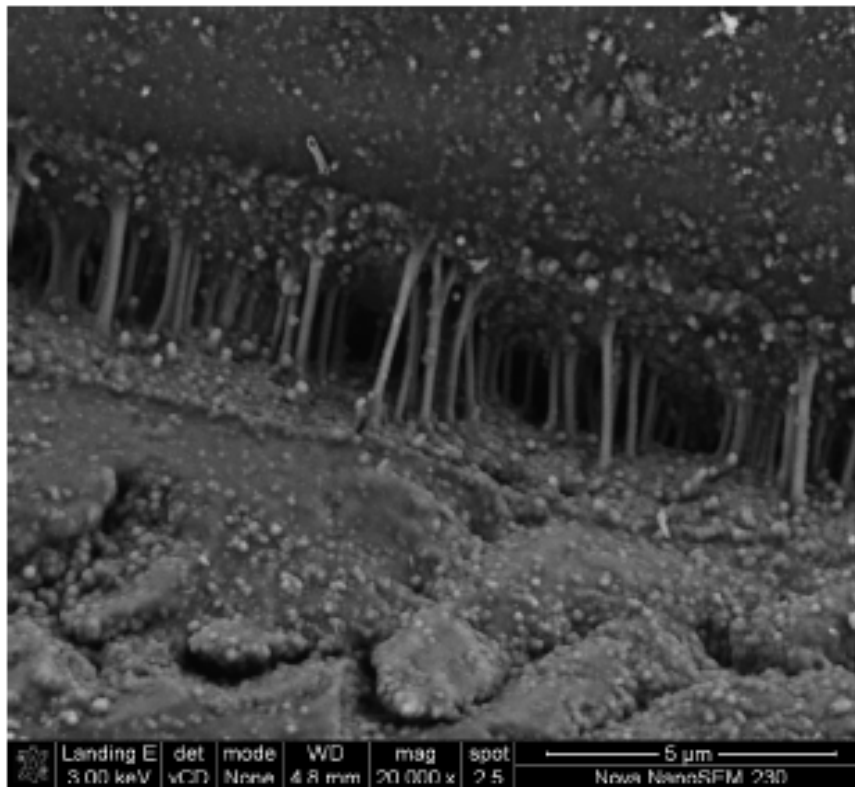


Figure 45: Cross-sectional SEM illustrating how parallel layers within the biofilm could be held together by EPS strands. The strands are between 1-2 μm long

In addition, the biofilm was significantly more porous and contained significantly less sulphur. Furthermore, there were no distinct layers or regions where sulphur deposition was particularly dense. A number of separate samples were prepared for SEM and all had a similar appearance, suggesting an accurate representation of the structure, rather than an artefact of sample preparation. The observations are consistent with the performance data and elemental composition of the biofilm.

The relationship between residence time and biofilm thickness is shown in and a relatively linear trend (Figure 47), with thickness decreasing with increasing residence time. A linear relationship is best represented by Equation 15, where (x) is residence time (days) and (F) FSB thickness (μm). This equation is only valid for residence times over the range of one to seven days. Due to delamination and tearing of the FSB in experiment 15, the biofilm was significantly thinner.

$$F_{thickness} = -49.27x + 443.5$$

Equation 15

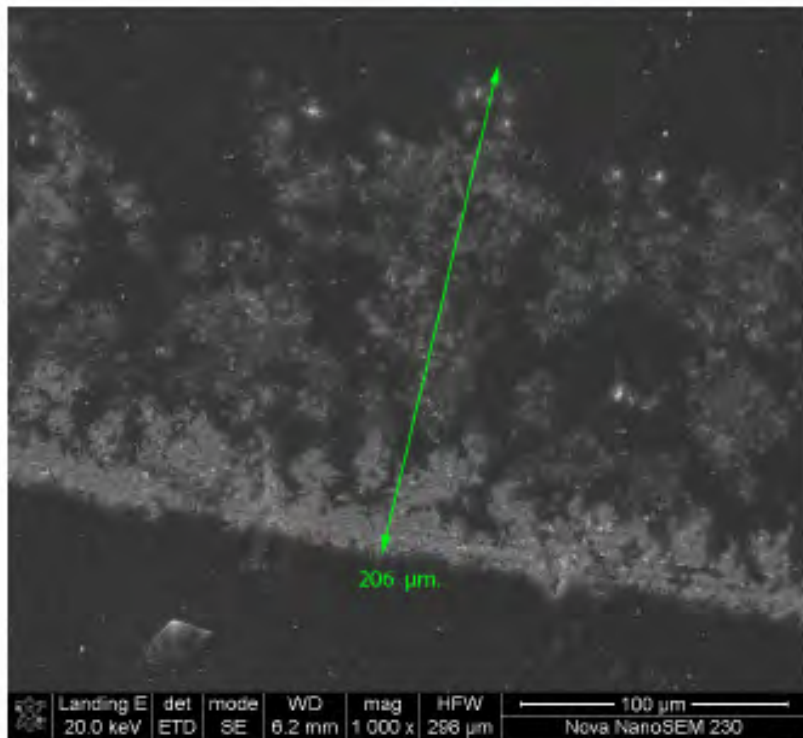


Figure 46: Cross-sectional SEM image of biofilm sampled from experimental run 8 (four day residence time) showing porous structure. The biofilm is inverted with the lower edge representing the upper surface

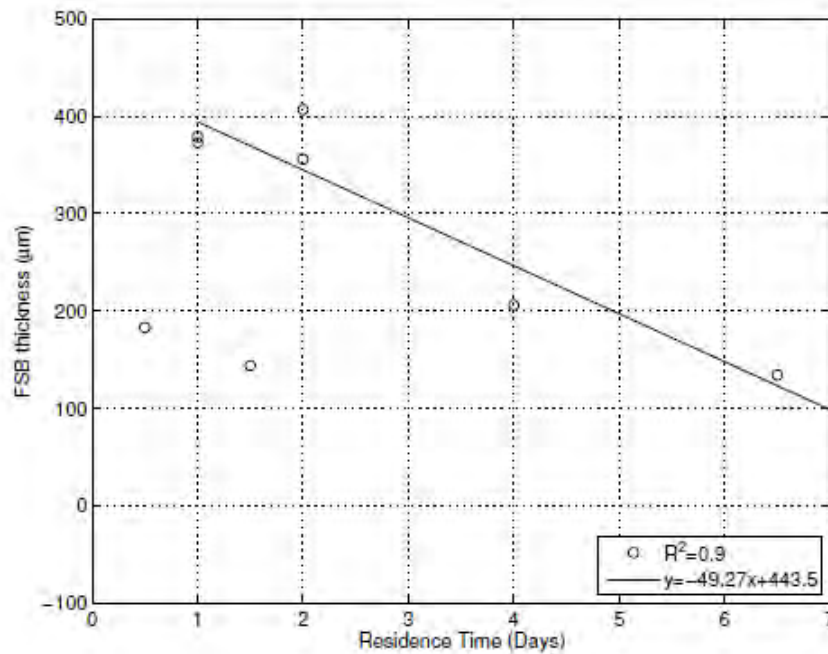


Figure 47: Relationship between FSB thickness and residence time, with the maximum thickness achieved at residence times between one and two days

4.4.9.1 Arrangement of microbial community

The SEM images of the underside and cross-section of the biofilms revealed interesting information on the structure of the microbial community and how the cells are associated with the biofilm matrix. An indication of the microbial diversity is clear from the different cell morphologies (Figure 48a). This was confirmed by the microbial ecology study (Mooruth, 2013). The immobilisation of cells within the EPS matrix was also clearly visible (Figure 48b).

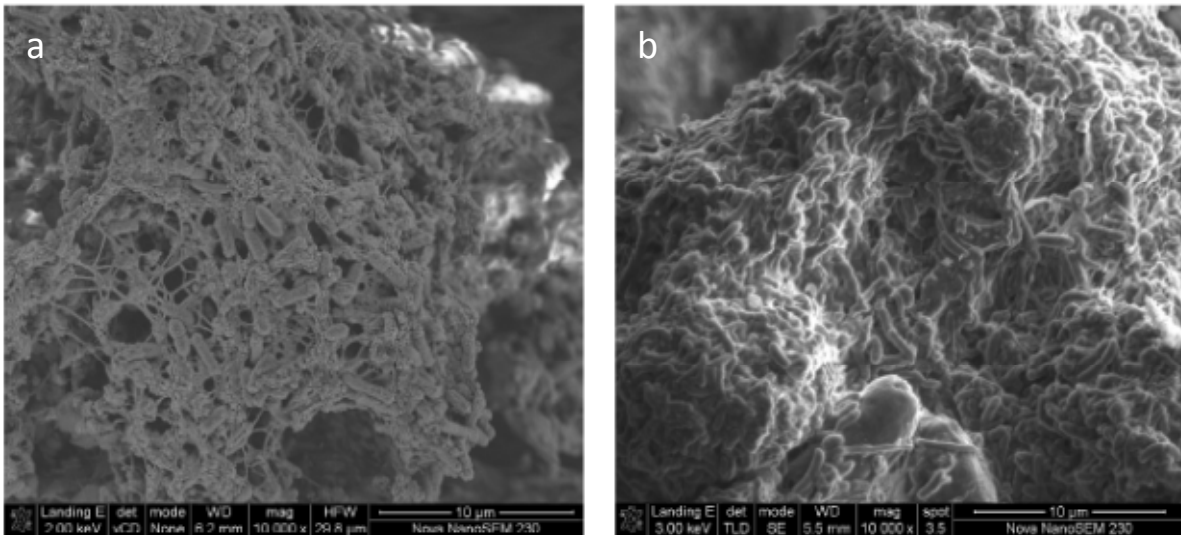


Figure 48: Scanning electron micrographs of the underside of the biofilm showing (a) the immobilisation of cells within the EPS matrix and (b) morphological diversity

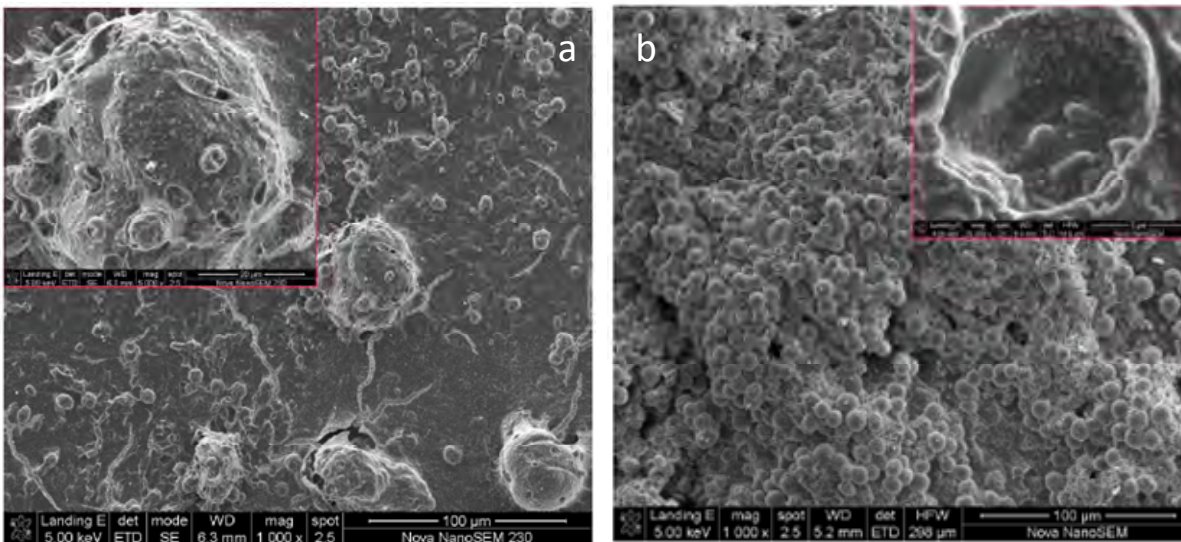


Figure 49: Scanning electron micrographs of the biofilm from (a) run 12 and (b) run 13, showing the presence of pod-shaped macrostructures

An interesting feature of the FSB was the observation of spherical balls and oval-shaped pods. These structures were covered in EPS and had pores/holes on the outer surface, possibly for the movement of necessary substrate and by-products in and out of the pods. The structures varied in size from 8-56 µm in diameter (Figure 49). Numerous smaller structures, possibly cell clusters, were attached to the outer surface of the pod, which was covered in a layer of EPS. Similar pods were observed on the top-surface of the FSB, while smaller, spherical shaped pods occurred in the FSB matrix.

The pore-like structures on the surface of the pod are clearly visible in Figure 50. The density scatter image in the insert confirms the presence of sulphur particles within the pod, suggesting that the structures may be involved in creating a favourable microenvironment for particular microbial species.

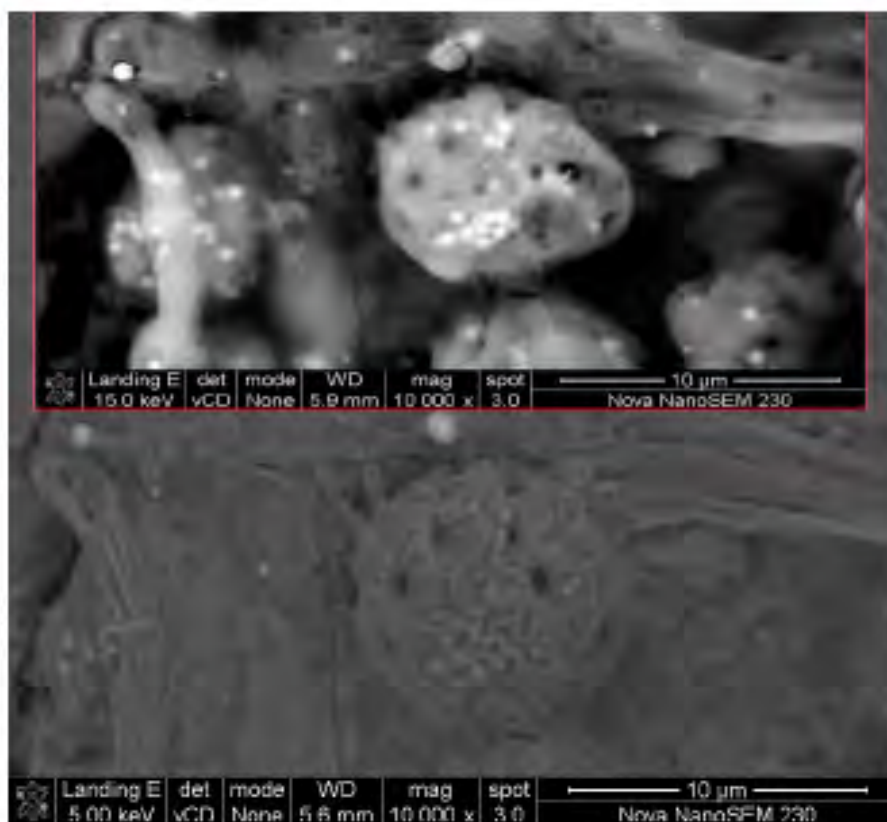


Figure 50: Scanning electron micrograph showing the topography of an individual pod (main image). The insert is a density scatter image of the same pod clearly showing the presence of sulphur granules within the pod

Pod-like structures were initially observed in *Escherichia coli* urinary tract infections and were believed to protect the bacteria from antibiotics, as well as host inflammatory responses (Anderson *et al.*, 2003). A similar occurrence of pods was observed in a study conducted by Norlund and co-workers (2009), in which two species (*Acidiphilium sp.* DBS4-1 and *Acidithiobacillus ferrooxidans*) coexisted within a pod. They proposed that formation of the pod was linked to the co-ordination of their sulphur metabolisms for mutual benefit as *Acidiphilium sp.* DBS4-1 reduced sulphur to sulphide, which was then oxidised by *At. ferrooxidans* back to colloidal sulphur. Therefore, the pod was necessary to create the correct redox conditions for sulphur cycling. However, in their study the pods were planktonic and not attached to a biofilm.

4.4.10 Conceptual model for biofilm formation and maturation

From the samples and analyses conducted on the FSB samples harvested from experimental runs 8-16-(2), it was evident that the FSB formed in a particular manner. The proposed mechanistic model is summarised in Figure 51. At the start of the experiment, during the unsteady-state phase, a layer of colloidal sulphur aqueous, approximately 0.5 cm deep, forms below the surface where oxygen reacts with the dissolved sulphide being displaced upwards from the base of the reactor. This process was observed in the abiotic controls and in the absence of any barrier to further oxygen penetration is rapidly oxidised further. The laminar flow in the reactor allows the air-water interface to act as an “attachment surface” for heterotrophic bacteria. In the presence of sufficient

dissolved organic carbon these organisms lay down a thin scaffold of EPS to initiate biofilm formation. The EPS framework retains some of the colloidal sulphur and is colonised by sulphide oxidising organisms. Consequently, a thin layer of white semi-solid sulphur and EPS forms on the liquid surface. As the biofilm develops it impedes oxygen mass transfer and creates a microenvironment suitable for partial oxidation of sulphide. As the concentration of EPS increases, the biofilm matrix of the FSB is formed under the thin layer. This provides the required surface area for the deposition of chemically and biologically produced sulphur on the underside of the FSB. As the underside becomes heavily-laden with sulphur a new biological layer of EPS and cells is formed, encapsulating the sulphur deposits. This new layer is initially attached to the previous layer by EPS strands, thereafter additional EPS is deposited to increase the mechanical strength of the FSB and its ability to hold a greater quantity of sulphur. The structure of the biofilm is heterogeneous and interlaced with pores and conduits, which facilitate the movement of dissolved species. As the FSB becomes thicker and more heavily laden with sulphur, the barrier to oxygen transfer to the reactive zone at the biofilm-bulk liquid interface increases, resulting in a decrease in the overall sulphide oxidation rate. The conceptual model is supported by the performance data and the cross-sectional SEM images.

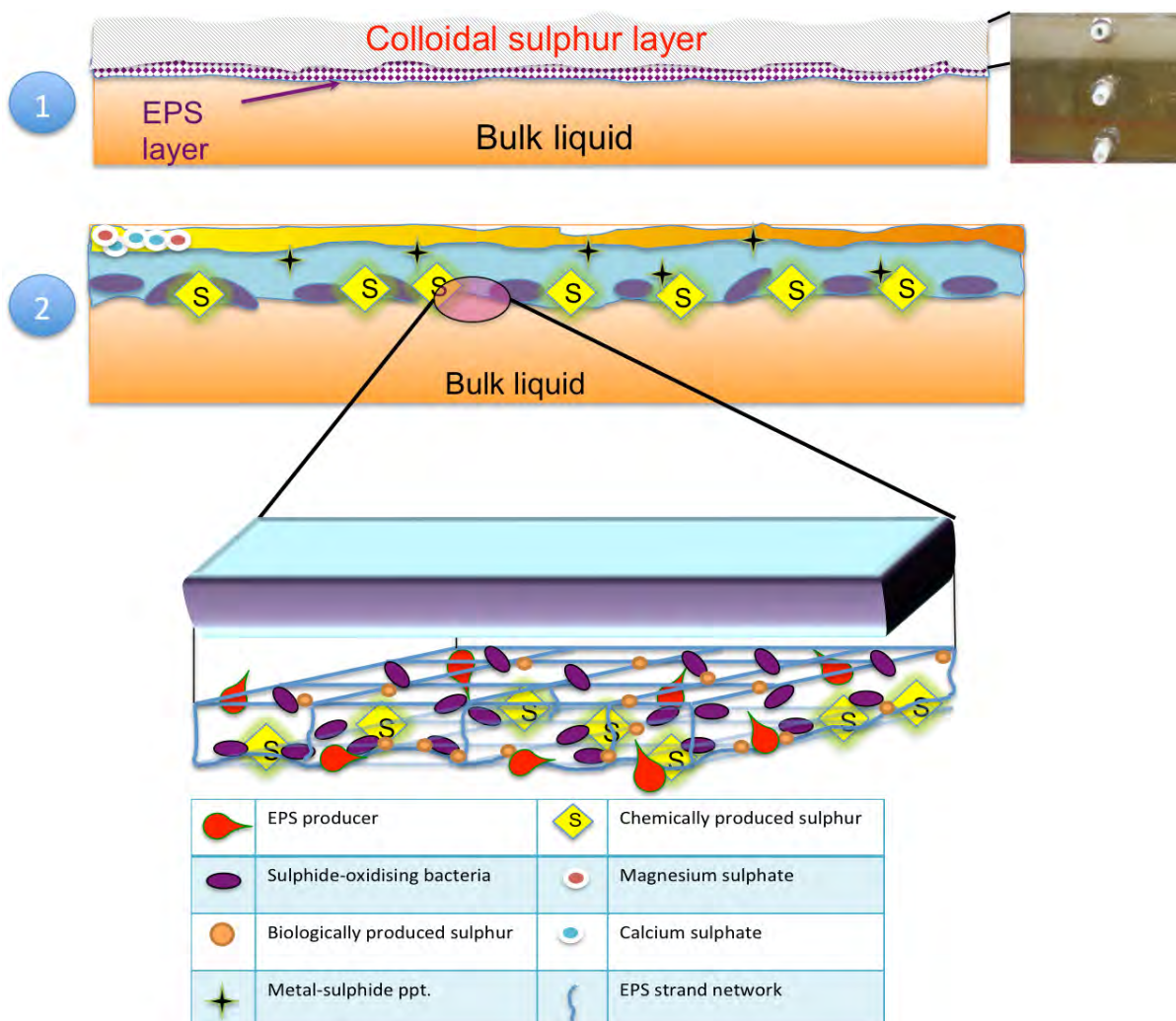


Figure 51: Conceptual model of floating sulphur biofilm formation. The upper image (1) describes the first 12 hours. The inset image at the top right illustrates the colloidal sulphur layer. The middle image (2) depicts the processes occurring during the establishment of pseudo-steady-state, while the lower image depicts the process occurring during the formation of a new layer

The most appropriate analogy to describe the floating sulphur biofilm is one which was proposed by Watnick and Kolter (2000) and Flemming and associates (2007). They described a biofilm as a

house containing many rooms with bacteria/cell clusters and these houses form a city. The floating sulphur biofilm can be likened to that of a high rise apartment building, which consists of many floors, with each floor represents a new layer added to the FSB. Each floor is separated and supported by reinforced pillars, similar to those provided by the EPS strands and deposits providing mechanical stability. Bacteria and cell clusters live in between the layers in the different apartments. Movement along the corridors of each floor and in between the floors is possible, via the pores and conduits in the structural matrix of the FSB. Sulphur deposits and inorganic precipitates are stored in between the layers in the apartment rooms. This analogy best represents the method and manner in which the various bacteria work together in a symbiotic and cohesive manner. The FSB infrastructure is further supported by the Van der Waals forces, hydrogen bonding and physiochemical interactions that improve the mechanical strength of the biofilm.

4.4.11 Dissolved oxygen profiles through the floating biofilms

The dissolved oxygen (DO) profile through the FSB was measured as a function of depth, position and time. This was performed to determine the mass flux of oxygen through the FSB. These analyses were conducted during experimental runs 8-16-(2), however only selected data will be presented to highlight the relevant phenomena. Additionally, the SEM analyses were conducted in order to characterise the biofilm structure, porosity and composition.

4.4.11.1 Effect of structural heterogeneity of the biofilm

An example of the type of DO profile data obtained is described below, for a reactor operated at a one day residence time. The profile was measured at the inlet port, above the first sample port (1.1) and three quarters of the distance along the LFCR (Figure 52). The profiles were measured on day 5 and day 10. However, a portion of the biofilm near the entrance of the reactor was harvested on day 4, so that a profile could be obtained through a one day old biofilm. The profiles (Figure 53) show that the decrease in oxygen concentration is not linear with increasing depth and is clearly affected by biofilm age. The profile through the one day old biofilm (green triangles in Figure 53) shows a relatively high DO for the 30 μm of depth. This drops off rapidly between 30 and 35 μm , where sulphide oxidation occurs most rapidly. As the biofilm is still very thin the sulphide oxidising bacteria are immobilised over a small depth. Below that depth the oxygen consumption is due to abiotic reactions and the action of more dispersed, planktonic organisms, resulting in a slower decrease in DO.

As the biofilm becomes older (day 5 profile) the DO drops off closer to the surface and more rapidly. The specific profile shows a number of spikes in DO and these most likely represent the tip of the probe penetrating a conduit within the biofilm, where the liquid has a higher DO content. While a complete biofilm is present at this stage it is not yet densely packed. From a performance perspective this represents the period where the sulphide oxidation in the reactor is highest.

The profiles at day 10 show a very rapid decrease in DO, with the concentration decreasing to zero between 40 and 60 μm below the surface. At this point the biofilm is densely packed with sulphur and the overall sulphide oxidation rate across the reactor had decreased to almost zero, as very little oxygen reached the reaction zone.

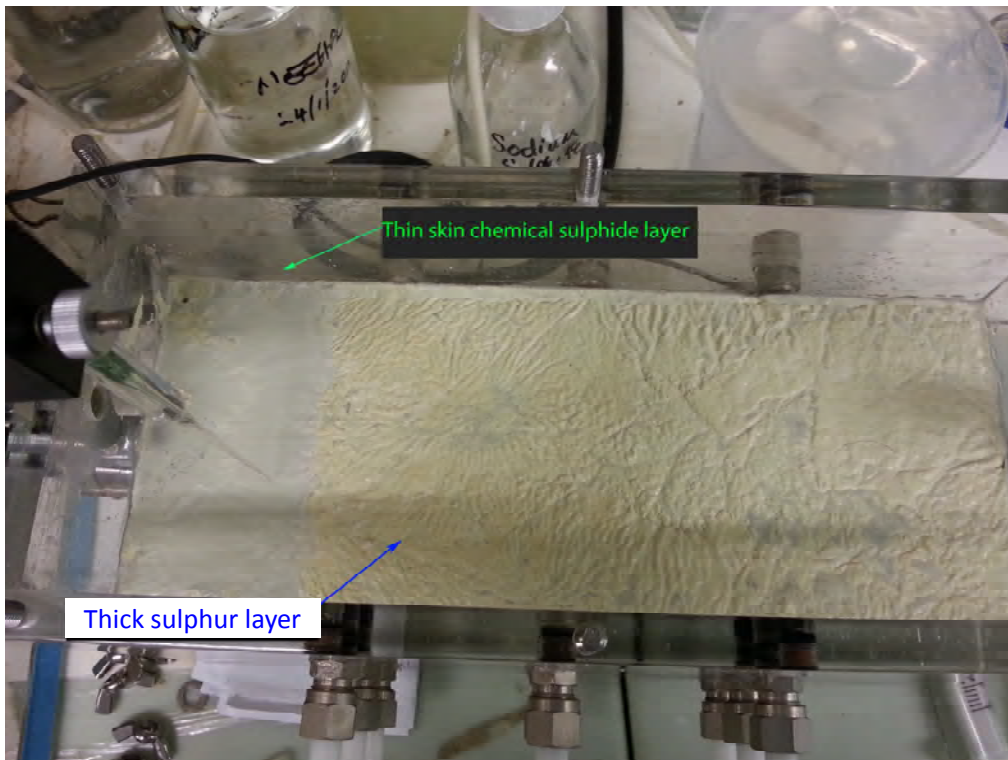


Figure 52: Photograph illustrating the apparatus used to determine the DO profile through the biofilm. The newly formed and mature biofilm (five day old) sections are clearly visible

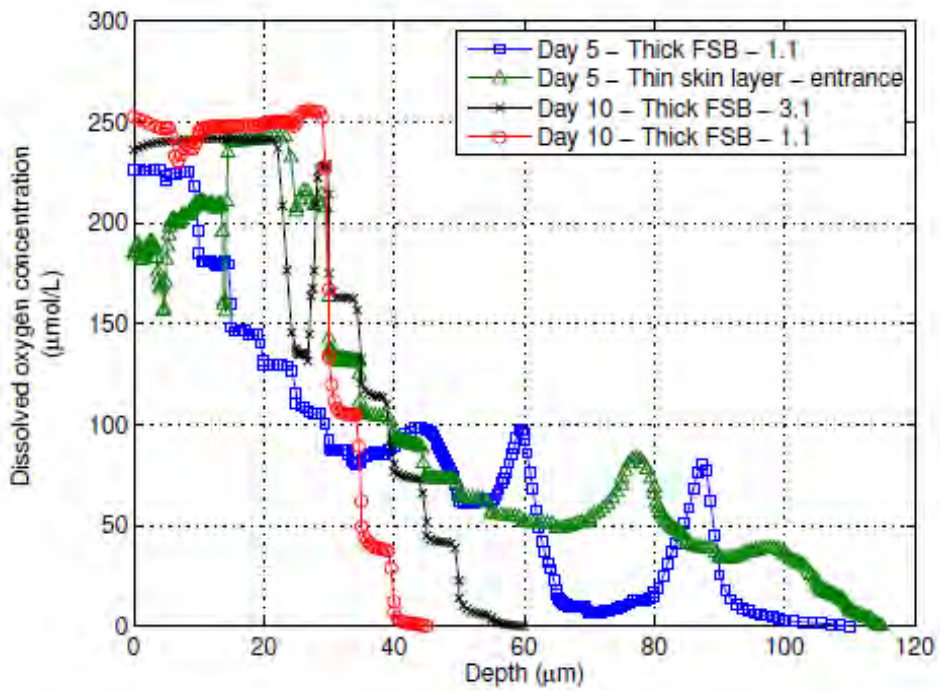


Figure 53: Dissolved oxygen profile through the FSB, as a function of position and time. Data from experimental run 13 (one day RT)

4.4.12 Measurement of oxygen mass transfer coefficient

One of the primary aims of this project was to amend the existing oxygen requirement model to account for impeded diffusion of oxygen through the developing biofilm. In order to generate data to achieve this, experiments were conducted in a smaller unit in an attempt to determine the oxygen mass transfer coefficient.

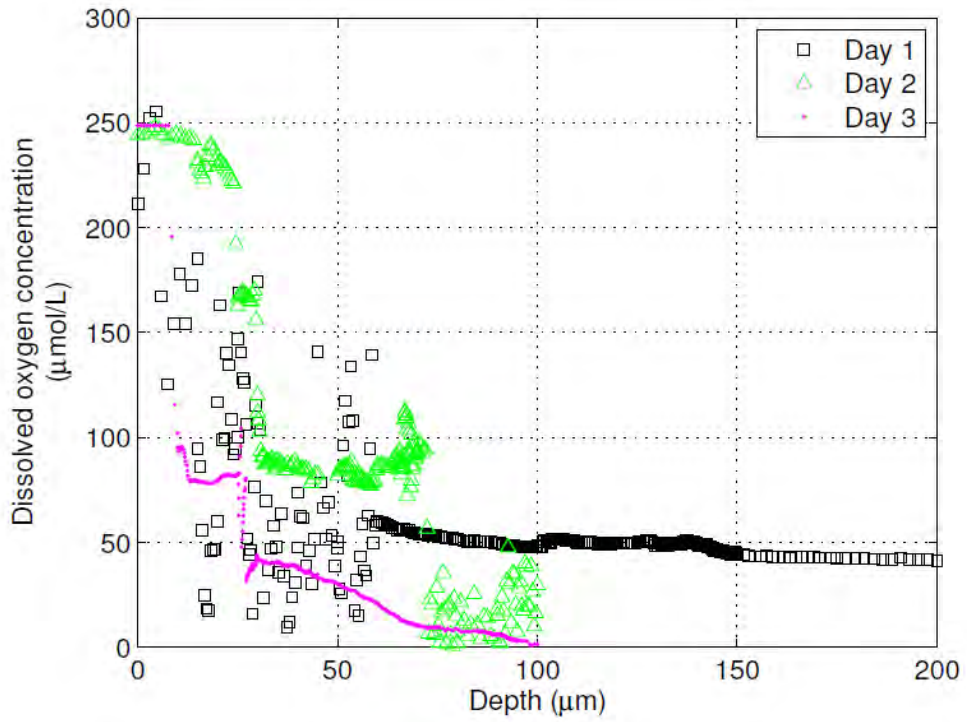
The floating sulphur biofilm was thin and incomplete at the start of the experiment (0-16 hours) and became much thicker and heavily laden with sulphur as time progressed. On day one, the dissolved oxygen concentration was 'scattered' with no discernible profile, due to the FSB being extremely thin, incomplete and the reaction zone most likely occurring within the first 60 μm . As the experiment progressed the DO profile became more defined and the DO concentration decreased much sooner due to increased oxygen consumption (sulphide oxidation) and impedance of diffusion.

The DO concentration on day one has a maximum value of 250 $\mu\text{mol}/\ell$ and subsequently decreased to 40 $\mu\text{mol}/\ell$ at a depth of 200 μm (Figure 54). On day two the rate at which DO decreased was similar and reached 0 $\mu\text{mol}/\ell$ at a depth of 100 μm . A similar trend was observed on day three, however the initial decrease in concentration was significantly steeper. By day four the average DO concentration was 40 $\mu\text{mol}/\ell$ up to a depth of 75 μm , whilst on day five the concentration reached zero much sooner at a shallow depth of 55 μm . Therefore, as time progressed the FSB became thicker and the depth to which oxygen could penetrate became smaller. This was due to the upper inorganic and biofilm layers which increased the resistance of the FSB, hence significantly less oxygen was able to penetrate the lower layers. The oxygen that was able to penetrate was consumed rapidly due to the high concentration of sulphide within the reaction zone and the proliferation of sulphide oxidising bacteria.

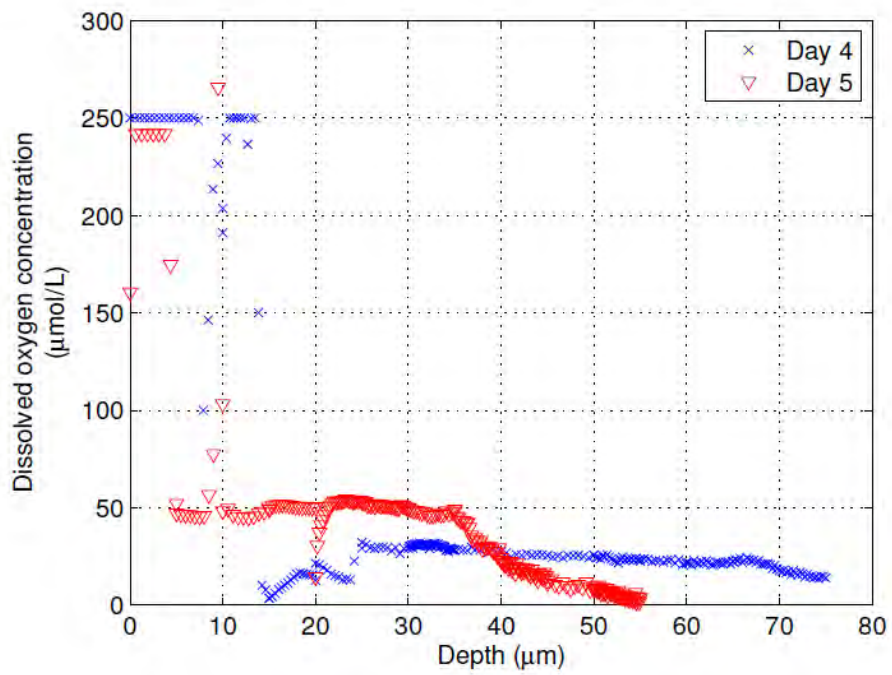
Each dissolved oxygen concentration profile was fitted with an exponential curve ($C(y) = ae^{by}$) in order to determine the rate at which the concentration was decreasing with depth (y) (Table 11). The coefficients 'a' and 'b' increased as time progressed, indicating an increase in the steepness of the curve. The calculated derivatives showed that the rate of change of DO concentration with depth increased greatly within the first 50 μm but then became less severe up to a depth of 200 μm . Likewise, the rate of change of concentration with depth increased greatly with time.

Table 11: Exponential functions fitted to the dissolved oxygen concentration data for days 1-5. In addition, the goodness of fit and respective functions' derivatives are presented, as well as the calculate diffusion and local mass transfer coefficients

Day	Function	Max depth (μm)	R^2	Derivative ($C'(y)$)	D_f (m^2/s)	k_f (m/s)
1	$C_1(y) = 109e^{-0.0070y}$	200	0.32	$C_1'(y) = -0.76e^{-0.0070y}$	4.13×10^{-8}	1.65×10^{-4}
2	$C_1(y) = 296e^{-0.0236y}$	100	0.81	$C_1'(y) = -6.97e^{-0.0236y}$	3.94×10^{-10}	2.35×10^{-6}
3	$C_1(y) = 241e^{-0.0541y}$	100	0.86	$C_1'(y) = -13.04e^{-0.0541y}$	9.34×10^{-11}	1.87×10^{-6}
4	$C_1(y) = 220e^{-0.0700y}$	75	0.87	$C_1'(y) = -15.40e^{-0.0700y}$	1.51×10^{-11}	2.15×10^{-7}
5	$C_1(y) = 350e^{-0.0703y}$	55	0.95	$C_1'(y) = -24.61e^{-0.0703y}$	1.09×10^{-11}	3.63×10^{-7}



(a) Day 1, 2 and 3



(b) Day 4 and day 5

Figure 54: Dissolved oxygen profiles through the FSB operated at a one day residence time, measured on days 1-5

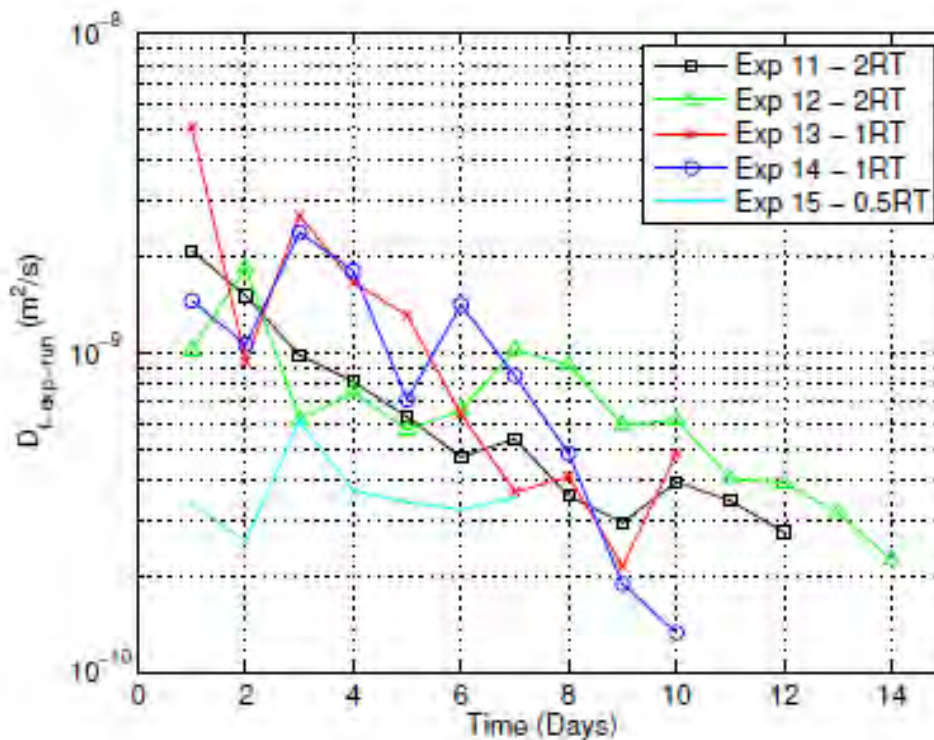


Figure 55: Calculated oxygen diffusion coefficients in the FSB as a function of biofilm age for experimental runs 11-15

The data in Figure 55 clearly show that the (theoretically calculated) oxygen diffusion coefficient in the FSB decreased by an order of magnitude over the duration of experiments 11-15. This is similar to the trend observed in the oxygen mass transport coefficient study, and the DO profiles did become steeper due to less oxygen penetration into the FSB. However, the diffusion coefficients (D_f) were an order of magnitude smaller than those calculated for experimental runs 11-15 ($D_{f-exp-run}$). The most likely explanation for the discrepancy between the DO profiling data and the calculated diffusion coefficients relates to the porosity of the biofilm. The FSB has a certain amount of porosity, that is determined by the manner in which the FSB is formed, in addition to arrangement of the sulphur and inorganic deposits. Moreover, the FSB is extremely heterogeneous, resulting in varying resistances to oxygen penetration in the FSB. For these reasons further study would be necessary to determine the porosity factor.

Biofilms typically have a high water content. Therefore, one could assume that the diffusion coefficient of oxygen in a biofilm is similar to that in water. Picioreanu and co-workers (2000a, b) proposed that the oxygen substrate diffusion coefficient was $2.3 \times 10^{-9} \text{ m}^2/\text{s}$, when modelling mass transport phenomena within a biofilm. On the other hand Fu and associates (1994) showed that the effective diffusivity of oxygen in different biofilm layers was 25-90% lower than the diffusivity of oxygen in water. The discrepancy illustrates that the concepts and assumptions generally applied to the calculation and modelling of mass transport coefficients in attached biofilms, may not necessarily hold for floating biofilms (Picioreanu *et al.*, 2000a, b; Wanner *et al.*, 2006; Zhang and Bishop, 1994).

5 CONCLUSIONS

The experimental programme illustrated that organic carbon liberation from packed bed reactors is unlikely to be sufficient to sustain efficient levels of sulphate reduction beyond the short term, once the readily labile organic carbon has been liberated. Supplementation with relatively significant (1 g/l) concentrations of readily usable organic carbon, such as acetate, was needed to sustain sulphate reduction. While the majority of the sulphate reduction ($\pm 75\%$) was reliant on the acetate, continued hydrolysis of the lignocellulose was observed. Despite this, the VFA concentration in the effluent from the packed bed reactors was negligible after the first four months. Therefore, further organic carbon supplementation ($> 100 \text{ mg/l}$ acetate) of the feed to the LFCR was necessary for biofilm development and efficient sulphide oxidation.

Under optimal conditions the biofilm formed within 12 hours, following which the oxygen mass transfer into the liquid was significantly reduced (k_f from $1.65 \times 10^{-4} \text{ m/s}$ to $2.35 \times 10^{-6} \text{ m/s}$ between 24 and 48 hours). The reduced mass transfer prevented complete sulphide oxidation, so the majority of the sulphide was oxidised to sulphur within the biofilm. The HRT and sulphide loading affected the rate of formation and structure of the biofilm, influencing performance. Optimal performance was achieved at an HRT between one and two days. Harvesting of the biofilm would be required every two to three residence times to maintain optimum sulphide oxidation rates.

The outcomes of the research clearly show the potential of the floating sulphur biofilm concept and the optimised LFCR reactor system. A summary of overall performance, under optimised operating conditions, is presented in Figure 56, showing a conservative sulphur yield of $13.5 \text{ g/m}^2/\text{day}$ for the system. For a moderately sized system (100 m x 100 m) this represents a daily yield of 135 kg or close to 50 tons per year. If the relative sizes of the individual units were maintained the feed to the SRB reactor would be $173 \text{ m}^3/\text{d}$.

The greatest inefficiency in the process is the performance of the sulphate reduction step, with the persistence of sulphate and colloidal sulphur in the effluent contributing to the relatively low (42-66%) total sulphur species removal. A more efficient sulphate removal step could enhance the overall efficiency of the integrated process. In addition, the effect of temperature fluctuations on the rate of sulphide oxidation in the LFCR needs to be quantified.

6 RECOMMENDATIONS

The current research illustrated that floating sulphur biofilm could achieve efficient sulphide oxidation and sulphur recover, using the linear flow channel reactor. However, the current packed bed sulphate reducing reactor could not provide the necessary organic carbon to sustain biofilm regeneration in the long term. Therefore, the design of the integrated process will need to be reconsidered, in order to ensure the required carbon flux. In addition, an effective method for biofilm harvesting and sulphur recovery needs to be developed.

For the operation of existing units, the most important recommendations are the reconfiguration of the inlet and outlet ports to the LFCR channels, to ensure the correct hydrodynamic profile, and the supplementation of the feed to the LFCR with soluble organic carbon, to sustain the necessary heterotrophic community members. In addition, the restriction of light to channels is recommended to reduce the prevalence of photosynthetic species, particularly cyanobacteria. These have been shown to have a detrimental effect during the current research and have been detected in significant numbers in the channels at the demonstration scale plant.

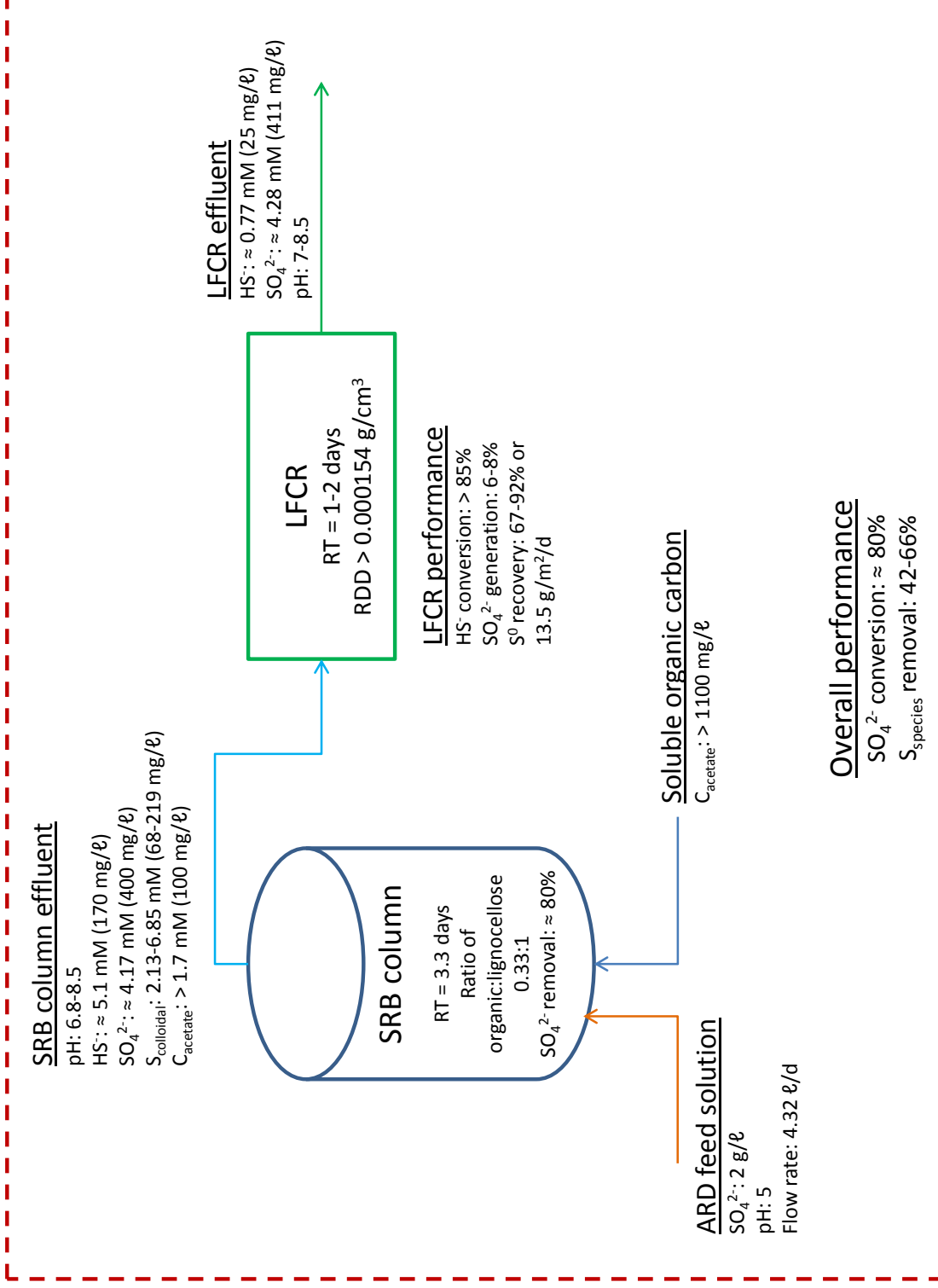


Figure 56: Summary of operating conditions and overall performance of the integrated system under optimised conditions. The relatively low total sulphur species removal is due to the persistence of colloidal sulphur and sulphate in the effluent from the SRB column

7 LIST OF REFERENCES

- ABSOLOM D, LAMBERTI F, POLICOVA Z, ZINGG W, VAN OSS C and NEUMANN A (1983) Surface thermodynamics of bacterial adhesion. *Applied and Environmental Microbiology* **46** 90-97.
- ANDERSON G, PALERMO J, SCHILLING J, ROTH R, HEUSER J and HULTGREN S (2003) Intracellular bacterial biofilm-like pods in urinary tract infections. *Science* **301** 105-107.
- ANDREASEN K, PETERSEN G, THOMSEN H and STRUBE R. (1997) Reduction of nutrient emission by sludge hydrolysis. *Water Science and Technology* **35** (10) 79-85.
- ANNACHHATRE A and SUKTRAKOOLVAIT S (2001) Biological sulfate reduction using molasses as a carbon source. *Water Environment Research* **73** 118-125.
- APPELS L, BAEYENS J, DEGREVE J and DEWIL R (2008) Principles and potential of the anaerobic digestion of waste-activated sludge. *Progress in Energy and Combustion Science* **34** 755-781.
- BEYENAL H and LEWANDOWSKI Z (2002) Internal and external mass transfer in biofilms grown at various flow velocities. *Biotechnology Progress* **18** 55-61.
- BHAT T, SINGH B and SHARMA O (1998) Microbial degradation of tannins - a current perspective. *Biodegradation* **9** 343-357.
- BOSHOF G, DUNCAN J and ROSE P (2004) Tannery effluent as a carbon source for biological sulphate reduction. *Water Research* **38** 2651-2658.
- BOWKER M (2002) *The biology and molecular ecology of floating sulphur biofilms*. MSc thesis, Rhodes University, Grahamstown, South Africa.
- BLUM D and SPEECE R (1991) A database of chemical toxicity to environmental bacteria and its use in interspecies comparisons and correlations. *Research Journal of the Water Pollution Control Federation* **63** 198-207.
- CHANG I, SHIN P and KIM B (2000) Biological treatment of acid mine drainage under sulphate reducing conditions with solid waste materials as substrate. *Water Research* **34** 1269-1277.
- CHEN Y, JIANG S, YUAN H, ZHOU Q. and GU G (2007) Hydrolysis and acidification of waste activated sludge at different pHs. *Water Research* **41** 683-689.
- CHRISTENSEN B, LAAKE M and LIEN T (1996) Treatment of acid mine water by sulphate-reducing bacteria; Results from a bench scale experiment. *Water Research* **30** 1617-1624.
- CLINE JH, HERSHBERGER TV and BENTLY OG (1958) Utilization and/or Synthesis of Valeric Acid during the Digestion of Glucose, Starch and Cellulose by Rumen Micro-Organisms *in vitro*. *Journal of Animal Science* **17** 284-292.
- COCOS I, ZAGURY GJ, CLEMENT B and SAMSON R (2002) Multiple factor design for reactive mixture selection for use in reactive walls in mine drainage treatment. *Water Research* **32** 167-177.
- COETSER S, HEATH R, MOLWANTWA J, ROSE P and PULLES W (2005) Implementing the degrading packed bed reactor technology and verifying the longterm performance of passive treatment plants at Vryheid Coronation Colliery. Research report no. 1348/1/05, Water Research Commission, Pretoria, South Africa.
- COSTERTON J (2000) Biofilms in the new millennium: musings from a peak in Xanadu. In: *Community structure and cooperation in biofilms*, ALLISON DG, GILBERT P, LAPPIN-SCOTT HM and WILSON M. Cambridge University Press, Cambridge, UK.
- COSTERTON J (2007) *The biofilm primer*. Springer-Verlag, Berlin, Germany.
- COSTERTON J, LEWANDOWSKI Z, CALDWELL D, KORBER D and LAPPIN-SCOTT H (1995) Microbial biofilms. *Annual Review of Microbiology* **47** 711-745.
- DE BEER D, STOODLEY P and LEWANDOWSKI Z (1996) Liquid flow and mass transport in heterogeneous biofilms. *Water Research* **30** 2761-2765.

- DE BEER D, STOODLEY P, ROE F and LEWANDOWSKI Z (1994) Effects of biofilm structures on oxygen distribution and mass transport. *Biotechnology and Bioengineering* **43** 1131-1138.
- DOPSON M and JOHNSON DB (2012) Biodiversity, metabolism and applications of acidophilic sulfur-metabolizing microorganisms. *Environmental Microbiology* **14** 2620-2631.
- DVORAK D, HEDIN R, EDENBORN H and MCINTIRE P (1992) Treatment of metal-contaminated water using bacterial sulphate reduction: results from pilot-scale reactors. *Biotechnology and Bioengineering* **40**:609.
- DWORKIN M, FALKOW S, ROSENBERG E, SCHLEIFER K and STACKEBRANDT E (2006) *The Prokaryotes*, vol. 2. Springer Science+Business Media, New York, USA.
- ELLIOT P, RAGUSA S and CATCHESIDE D (1998) Growth of sulphate reducing bacteria under acidic conditions in an upflow anaerobic bioreactor as a treatment system for acid mine drainage. *Water Resources* **32** 3724-3730.
- FLEMMING H-C, NEU T and WOZNIAK D (2007) The EPS matrix: The "House of biofilm cells". *Journal of Bacteriology* **189** 7945-7947.
- FLEMMING H-C and WINGENDER J (2010) The biofilm matrix. *Nature Reviews Microbiology* **8** 623-633.
- FU Y, ZHANG T and BISHOP P (1994) Determination of effective oxygen diffusivity in biofilm grown in a completely mixed bioreactor. *Water Science and Technology* **29(10-11)** 455-462.
- GIBERT O, DE PABLO J, CORTINA J and AYORA C (2004) Chemical characterisation of natural organic substrates for biological mitigation of acid mine drainage. *Water Research* **38** 4186-4196.
- GREBEN H, BALOYI J, SIGAMA J and VENTER S (2009) Bioremediation of sulphate rich mine effluents using grass cuttings and rumen fluid microorganisms. *Journal of Geochemical Exploration* **100** 163-168.
- HARMS G, ZENGLER K, RABUS R, AECKERSBERG F, MINZ D, MORA R and WIDDEL F (1999) Anaerobic oxidation of o-xylene, m-xylene and homologous alkylbenzenes by new types of sulfate-reducing bacteria. *Applied and Environmental Microbiology* **65** 999-1004.
- HULSHOFF POL L, LENS P, STAMS A and LETTINGA G (1998) Anaerobic treatment of sulphate-rich wastewaters. *Biodegradation* **9** 213-224.
- JEFFERSON K (2004) What drives bacteria to produce a biofilm? *FEMS Microbiology Letters* **236** 163-173.
- JEFFRIES T (1994) Biodegradation of lignin and hemicelluloses. In: *Biochemistry of Microbial Degradation*, RATLEDGE C. Kluwer Academic Publishers, Dordrecht, Netherlands.
- JOHNSON DB and HALLBERG KB (2003) The microbiology of acidic mine waters. *Research in Microbiology* **154** 466-473.
- JONG T and PARRY D (2003) Removal of sulfate and heavy metals by sulfate reducing bacteria in short-term bench scale upflow anaerobic packed bed reactor runs. *Water Research* **37** 3379-3389.
- KAMYSHNY JR A, EKELTCHIK I, GUN J and LEV O (2006) Method for the determination of inorganic polysulfide distribution in aquatic systems. *Analytical Chemistry* **78** 2631-2639.
- KOSCHORRECK M (2008) Microbial sulphate reduction at a low pH. *FEMS Microbiology Ecology* **64** 329-342.
- LAPPIN-SCOTT H and COSTERTON J (1995) *Microbial Biofilms*. Cambridge University Press, Cambridge, UK.
- LAWRENCE J, KORBER D, HOYLE B and COSTERTON J (1991) Optical sectioning of microbial biofilms. *Journal of Bacteriology* **173** 6558-6567.
- LAZAROVA V and MANEM J (1995) Review Paper: Biofilm characterization and activity analysis in water and wastewater treatment. *Water Research* **29** 2227-2245.

- LIAMLEAM W and ANNACHHATRE A (2007) Electron donors for biological sulfate reduction. *Biotechnology Advances* **25** 452-463.
- LEE K (2010) *Anaerobic digestion of brewer's spend grain in a novel plug flow reactor system*. MSc thesis, University of Georgia, Atlanta, US.
- LEE S, HA J and CHENG K-J (2000) Relative contributions of bacteria, protozoa and fungi to in vitro degradation of Orchard grass cell walls and their interactions. *Applied and Environmental Microbiology* **66** 3807-3813.
- LYND L, WEIMER P, VAN ZYL W and ISAK S (2002) Microbial cellulose utilization: Fundamentals and biotechnology. *Microbiology and Molecular Biology Reviews* **66** 506-577.
- MOLWANTWA J (2007) *Floating sulphur biofilms: Structure, function and biotechnology*. PhD. thesis, Rhodes University, Grahamstown, South Africa.
- MOLWANTWA J, COETSER S, HEATH R, PULLES W and BOWKER M (2010) Monitoring, evaluation and verification of long-term performance of the passive water treatment plant at Vryheid Coronation Colliery. Research report no. 1623/1/10, Water Research Commission, Pretoria, South Africa.
- MOORUTH N (2013) *An investigation towards passive treatment solutions for the oxidation of sulphide and subsequent removal of sulphur from acid mine water*. PhD thesis, University of Cape Town, Cape Town, South Africa.
- MOOSA S, NEMATI M and HARRISON S (2002) A kinetic study of anaerobic reduction of sulphate, Part I: Effect of sulphate concentration. *Chemical Engineering Science* **57** 2773-2780.
- MORALES C, STRATHMANN M and FLEMMING H-C (2007) Influence of biofilms on the movement of colloids in porous media. Implications for colloid facilitated transport in subsurface environments. *Water Research* **41** 2059-2068.
- MUYZER G and STAMS A (2008) The ecology and biotechnology of sulphate-reducing bacteria. *Nature Reviews Microbiology* **6** 441-454.
- NAGPAL S, CHUICHULCHERM S, LIVINGSTON A and PEEVA L (2000) Ethanol utilization by sulfate-reducing bacteria: An experimental and modeling study. *Biotechnology and Bioengineering* **70** 533-543.
- NORLUND K, SOUTHAN G, TYLISZCZAK T, HU Y, KARUNAKARAN C, OBST M, HITCHCOCK AP and WARREN LA (2009). 'Microbial architecture of environmental sulfur processes: A novel syntrophic sulfur-metabolizing consortia'. *Environmental Science and Technology* **43**:8781-8786.
- OMIL F, LENS P, HULSHOFF POL L. and LETTINGA G (1996) Effect of upward velocity and sulphide concentration on volatile fatty acid degradation in a sulphidogenic granular sludge reactor. *Process Biochemistry* **31** 699-710.
- OYEKOLA OO (2008) *An investigation into the relationship between process kinetics and microbial community dynamics in a lactate-fed sulphidogenic CSTR as a function of residence time and sulphate loading*. PhD thesis, University of Cape Town.
- PAREEK S, KIM S, MATSUI S and SHIMIZU Y (1998) Hydrolysis of (ligno)cellulosic materials under sulfidogenic and methanogenic conditions. *Water Science and Technology* **38(2)** 193-200.
- PARK S, KO Y and KIM C (2001) Toxic effects of catechol and 4-chlorobenzoate stresses on bacterial cells. *The Journal of Microbiology* **39** 206-212.
- PERRY R and GREEN D (2008) *Perry's Chemical Engineers' Handbook*. 8th ed., McGraw-Hill, New York, USA.
- PICIOREANU C, VAN LOOSDRECHT M and HEIJNEN J (2000a) Effect of diffusive and convective substrate transport on biofilm structure formation: A two-dimensional modeling study. *Biotechnology and Bioengineering* **69** 504-515.
- PICIOREANU C, VAN LOOSDRECHT M and HEIJNEN J (2000b) A Theoretical study on the effect of surface roughness on mass transport and transformation in biofilms. *Biotechnology and Bioengineering* **68** 355-369.

- POINAPEN J, EKAMA G and WENTZEL M (2009) Biological sulphate reduction with primary sewage sludge in an upflow anaerobic sludge (UASB) reactor - Part 3: Performance at 20°C and 35°C. *Water SA* **35** 543-552.
- PUREVDORJ-GAGE B (2004) *Pseudomonas Areuginosa biofilm structure, behaviour and hydrodynamics*. PhD thesis, Montana State University, CITY?, USA.
- PUREVDORJ-GAGE B and STOODLEY P (2004) *Microbial Biofilms*, ASM Press, chapter 9, pp. 160-173.
- RASMUSSEN K and LEWANDOWSKI Z (1998a) The accuracy of oxygen flux measurements using microelectrodes. *Water Research* **32** 3747-3755.
- RASMUSSEN K and LEWANDOWSKI Z (1998b) Microelectrode Measurements of Local Mass Transport Rates in Heterogeneous Biofilms. *Biotechnology and Bioengineering* **59** 302-309.
- ROMAN H (2004) *The degradation of lignocellulose in a biologically-generated sulphidic environment*. PhD thesis, Rhodes University, Grahamstown, South Africa.
- ROMAN H, MADIKANE M, PLETSCHKE B and ROSE P (2008) The degradation of lignocellulose in a chemically and biologically generated sulphidic environment. *Bioresource Technology* **99** 2333-2339.
- SAND W and GEHRKE T (2006) Extracellular polymeric substances mediate bioleaching/biocorrosion via interfacial processes involving iron(III) ions and acidophilic bacteria. *Research in Microbiology* **157** 49-56.
- SCHINK B, PHILIPP B and MULLER J (2000) Anaerobic degradation of phenolic compounds. *Naturwissenschaften* **87** 12-23.
- SHEORAN A, SHEORAN V and CHOUDHARY R (2010) Bioremediation of acid-rock drainage by sulphate-reducing prokaryotes: A review. *Minerals Engineering* **23** 1073-1100.
- SPIERS A, BOHANNON J, GEHRIG S and RAINEY P (2003) Biofilm formation at the air-liquid interface by the *Pseudomonas fluorescens* SBW25 wrinkly spreader requires an acetylated form of cellulose. *Molecular Microbiology* **50** 15-27.
- STOODLEY P, STOODLEY L, BOYLE J, JORGENSEN F and LAPPIN-SCOTT H (2000) Environmental and genetic factors influencing biofilm structure. In: *Community structure and cooperation in biofilms*, ALLISON DG, GILBERT P, LAPPIN-SCOTT HM and WILSON M. Cambridge University Press, Cambridge, UK.
- TSUKAMOTO T and MILLER G (1999) Methanol as a carbon source for microbiological treatment for acid mine drainage. *Water Research* **33** 1365-1370.
- UCISIK A and HENZE M (2008) Biological hydrolysis and acidification of sludge under anaerobic conditions: The effect of sludge type and origin on the production and composition of volatile fatty acids. *Water Research* **42** 3729-3738.
- VAN DYK J and PLETSCHKE B (2012) A review of lignocellulose bioconversion using enzymatic hydrolysis and synergistic cooperation between enzymes-Factors affecting enzymes, conversion and synergy. *Biotechnology Advances* **30** 1458-1480.
- VAN HILLE R, MOORUTH N, RAJA S and HEATH R (2012) Towards passive treatment solutions for the oxidation of sulphide and subsequent sulphur removal from acid mine water. Research report no. 1834/1/12, Water Research Commission, Pretoria, South Africa.
- VAVILIN V, FERNANDEZ B, PALATSI J and FLOTATS X (2008) Hydrolysis kinetics in anaerobic degradation of particulate organic material: An overview. *Waste Management* **28** 939-951.
- WAN C and LI Y (2012) Fungal pretreatment of lignocellulosic biomass. *Biotechnology Advances* **30** 1447-1457.
- WANNER O, EBERL H, NOGUERA D, PICIOREANU C and VAN LOOSDRECHT M (2006) *Mathematical modeling of biofilms*. Report of the IWA Biofilm Modeling Task Group, Scientific and Technical Report No. 18, IWA Publishing, London, UK.

- WATNICK P and KOLTER R (2000) Biofilm, city of microbes. *Journal of Bacteriology* **182** 2675-2679.
- WAYBRANT K, PTACEK C and BLOWES D (2002) Treatment of mine drainage using permeable reactive barriers: Column experiments. *Environmental Science and Technology* **36** 1349-1356.
- WEIMER P, RUSSELL J and MUCK R (2009) Lessons from the cow: What the ruminant animal can teach us about consolidated bioprocessing of cellulosic biomass. *Bioresource Technology* **100** 5323-5331.
- WEISSENBORN P and PUGH R (1996) Surface tension of aqueous solutions of electrolytes: Relationship with ion hydration, oxygen solubility, and bubble coalescence. *Journal of Colloid and Interface Science* **184** 550-563.
- WHITTINGTON-JONES K, MOLWANTWA J and ROSE P (2006) Enhanced hydrolysis of carbohydrates in primary sludge under biosulfidogenic conditions. *Water Research* **40** 1577-1582.
- WIDDEL F (1988) Microbiology and ecology of sulfate- and sulfur-reducing bacteria. In: JB ZEHNDER (ed.) *Biology of anaerobic microorganisms*. Wiley and Sons. New York. pp. 469-526.
- YAMASHITA T, YAMAMOTO-ILKEMOTO R and ZHU J (2011) Sulfate-reducing bacteria in a denitrification reactor packed with wood as a carbon source. *Bioresource Technology* **102** 2235-2241.
- ZAGURY GJ, KULNIEKS V and NECULITA C (2006) Characterization and reactivity assessment of organic substrates for sulphate-reducing bacteria in acid mine drainage treatment. *Chemosphere* **64** 944-954.
- ZEYAUULLAH M, ABDELKAFE A, ZABYA W and ALI A (2009) Biodegradation of catechols by micro-organisms - A short review. *African Journal of Biotechnology* **8** 2916-2922.
- ZHANG T and BISHOP P (1994) Density, porosity and pore structure of biofilms. *Water Research* **28** 2267-2277.